University of Alberta

Stability of Water-in-Diluted Bitumen Emulsion Droplets

by

Song Gao

A thesis submitted to the Faculty of Graduate Studies and Research
in partial fulfillment of the requirements for the degree of

Doctor of Philosophy
in
Chemical Engineering

Department of Chemical and Materials Engineering

Spring 2010
Edmonton, Alberta

Examining Committee

Zhenghe Xu, Department of Chemical and Materials Engineering

Jacob Masliyah, Department of Chemical and Materials Engineering

Tony Yeung, Department of Chemical and Materials Engineering

Kevin Moran, Department of Chemical and Materials Engineering

Subir Bhattacharjee, Department of Mechanical Engineering

Suzanne Giasson, University of Montreal

Abstract

There are several technical challenges in large scale heavy oil processing. In the oil sand industry, for example, the existence of water-in-oil emulsion in diluted bitumen produced from froth treatment presents a great challenge to the industry. In this work, the effect of different bitumen components, including asphaltenes, maltenes (deasphalted bitumen) and indigenous naphthenic acids (NAs), on the stability of water-in-diluted model oil emulsion was systematically investigated. A biodegradable polymer was developed and introduced to break the water-in-oil emulsions.

The stability of water-in-oil emulsions depends on the mechanical barrier between two approaching water droplets in model oil with bitumen components. The micron-scale techniques are used in this study to study the mechanical behavior of emulsion drops due to its priority to maintain the surface area to volume ratio which is representative of the commercially observed emulsions.

Several parameters, including interfacial tension isotherm, crumpling ratio and probability of coalescence, were measured to understand the interfacial reheology. Based on these experiments, the mechanical properties of emulsion drops can be evaluated in situ.

A non-toxic and biodegradable polymer, ethylcellulose, was used to break up the water-in-diluted bitumen emulsion. The demulsification mechanism was studied in this work.

The knowledge from this work provides improved insights on molecular mechanism of emulsion stability/demulsification and contributes to the design of demulsification systems in industrial oil sands extraction processes.

Acknowledgement

I would like to take this opportunity to thank my supervisors, Drs. Zhenghe Xu, Jacob Masliyah and Kevin Moran for their encouragement and support throughout this work. They taught me to welcome challenges and to question preconceptions.

Thanks to Dr. Xianhua Feng for his collaboration in the demulsifier investigation. I appreciate Dr. Paolo Mussone for sharing the results of Brewster angle microscopy. My gratitude also goes to Dr. Mike Mackinnon, of Syncrude Canada, for the helpful discussions on the analysis of naphthenic acids. I acknowledge Mr. Jim Skwarok, Ms. Shaiu-yin Wu, Ms. Leanne Swekla and Ms. Lisa Carreiro for being accommodating and resourceful on every occasion. I would also like to thank my peers and colleagues at the University of Alberta and the Syncrude Research Centre; they helped to make my research experience most enjoyable. I would like to extend my gratitude to all administrative and support staff at the Chemical and Materials Engineering Department and Syncrude Research Centre for being friendly and helpful.

The financial support from the Natural Sciences and Engineering Research Council (NSERC) of Canada through NSERC Industrial Research Chair in Oil Sands Engineering is acknowledged. I also want to thank Syncrude Research Centre for providing a unique and wonderful experience by allowing me to conduct my research in their lab.

Finally, my deepest gratitude goes to my family and friends. I am forever grateful to my parents and my husband for their love and support and for being part of my life.

Table of Contents

List of Tables

List of Figures

List of Symbols

μ	Chemical potential, partial molar Gibbs energy
γ	Interfacial / surface tension (N/m)
π	Interfacial / surface pressure
θ	Contact angle
α β σ	three phases in a system
Γ	Surface coverage of surface active species (molecule / nm^2)
a	Activity
c	Concentration
k	Boltzmann constant
n	Mole
x y z	Coordinate for an arbitrarily curved surface
K	Spring constant
R	Universal gas constant
G	Surface excess free energy
T	Temperature
ΔA	Small area displacement
P	Pressure
R_1 R_2 R_d	Radii of curvature
F	Applied force
U	Internal energy
V	Volume
S	Entropy

List of Acronyms

AFM	Atomic Force Microscope
ASA	Additional Setting Areas
BAM	Brewster Angle Microscope
CSS	Cyclic Steam Simulation
CHWE	Clark Hot Water Extraction
CT	Composite / Consolidated Tailings
FTIR	Fourier Transform Infrared Spectroscope
LB	Langmuir-Blodgett
MFT	Mature Fine Tailings
NAs	Naphthenic Acids
NaN	Sodium Naphthenates
PSV	Primary Separation Vessel
SAGD	Steam Assisted Gravity Drainage
TOR	Tailing Oil Recovery

Chapter 1

Introduction

1.1 Oil sands

With an estimated volume in-place of approximately 1.7 trillion barrels, or 270 billion m^3 (ERCB ST98-2008) of crude bitumen, Canada's oil sands, located in the Province of Alberta, are one of the world's largest hydrocarbon accumulations. Oil sands are unconsolidated sand deposits impregnated with bitumen, a high molar mass viscous petroleum. Oil sands contain roughly 80-85 wt% mineral solids and what remains is distributed between bitumen and water (Liu et al., 2004). A bitumen content of 6 to 8 wt% is considered a low grade (poor) oil sands, a content of 8 to 10 wt% is considered an average grade (medium) oil sands, while above 10 wt% is considered to be a high-grade (rich) oil sands (Takamura, 1985). Bitumen can be fractionated to produce gasoline, heating oils and diesel fuels. Surface (in-pit) mining is used for shallow oil sands deposits, typically less than 100 meters deep. If the reserves are too deep to be economical for surface mining operations, alternative operations such as steam assisted gravity drainage (SAGD) or cyclic steam simulation (CSS) can be applied (Canada's Oil Sands Heavy Oil, 2000). The Clark Hot Water Extraction (CHWE) process is widely used to extract bitumen from mined oil sands. A schematic view of a typical bitumen extraction process is given in Figure 1.1.

The oil sands ore is mined using a truck and shovel approach and then transported to the extraction plant. After being crushed, the ore is mixed with water and introduced to a hydrotransport pipeline system. The digestion of oil sands lumps takes place in the hydrotransport pipeline to liberate and aerate bitumen. The temperature of the system is set at approximately 40-50 ^{o}C to allow the digestion and liberation of bitumen. Within the hydrotransport pipelines, the bitumen is first liberated from the sand grains as droplets, then they coalesce with each other with eventually aeration. A low dosage of air can be fed into the pipeline to help the aeration of bitumen.

The conditioned slurry from the hydrotransport pipeline is then fed into a super-pot type of distributor, where it is distributed into primary gravity separation vessels (or cell) (PSV, PSC). The stream, referred as middlings, is retrieved from the middle of the PSV to avoid the building up of solids. At Syncrude, the bottom stream from the gravity separation vessels, known as tailings, is combined with the middlings stream and sent to a tailing oil recovery unit (TOR) for further treatment. The bitumen froth is produced at the top of the PSV. This bitumen-rich froth contains typically 60 wt% bitumen, 30 wt% water and 10 wt% of solids. It is heated in the deaerator to remove the air before being sent to the froth treatment plant where it is mixed with a light solvent, naphtha.

The addition of a light hydrocarbon (diluent) will reduce the density and viscosity of the froth to facilitate the removal of water and solids. After removing the water and solids in a series of centrifuges and inclined plate settlers, the diluted bitumen still contains about 2 wt% water and 0.4 wt% solids. The diluent is then stripped off in the diluent recovery unit (DRU) and recycled to the froth treatment. The resulting bitumen is directed to the upgrading plant for further treatment.

The residue bitumen in the tailings and middlings streams is separated in cyclo-separators. The resulting streams containing rejected solids are combined and directed to the tailings ponds. The coarse fraction of the solids will rapidly segregate from the fines and settle down. However, it will take two to three years for the fines to form a stable suspension called mature fine tailings (MFT). Further consolidation and complete settling of the MFT could take more than a century (Eckert et al., 1996). Gypsum ($CaSO_4 \cdot 2H_2O$) can be added to MFT to consolidate the fines together with the coarse solids. The process is called consolidated or composite tailings (CT). By this way, the water in tailings will be released rapidly and recycled to the extraction plant.

1.2 Bitumen

Bitumen is a crude oil containing thousands of different hydrocarbon components. UNITAR defines crude oils according to their density and viscosity. The American Petroleum Institute relates crude oil density in terms of API gravity (equation 1.1).

$$ {}^{O}API = \frac{145}{specific\ gravity\ at\ 15.6^{o}C} - 131.5 \qquad [1.1] $$

Bitumen can be defined as an extra heavy crude oil with typical API value less than 10 (Table 1.1).

Table 1.1. Definition of oils and bitumen (Gray, 1994)

Type	Viscosity (mPa.s)	Density (g/cm^3)	API Gravity
Conventional Oil	$< 10^2$	< 0.934	> 20
Heavy Oil	$10^2 \sim 10^5$	0.934 ~ 1.0	20 ~ 10
Bitumen	$> 10^5$	> 1.0	< 10

Properties in the table are reported at a standard temperature of 15.6°C.

Based on solubility and adsorption characteristics, bitumen can be separated into several classes. This classification is very important in the froth treatment processes of bitumen production. A separation protocol, SARA (Saturates, Aromatic, Resins, Asphaltenes) (Bulmer and Starr, 1979) is well established and accepted (Figure 1.2) to describe bitumen in terms of solubility classes. When dissolved in paraffinic solvents (i.e., heptane, pentane or hexane), an insoluble fraction of bitumen precipitates and it is called asphaltenes. Maltenes, also called deasphalted bitumen, contain all the soluble fractions in a paraffinic solvent. These components can be further separated by chromatography. After being fed into a column, the maltenes are separated into saturates, aromatics and resins based on their adsorption characteristics. It should be noted that the amount and properties of precipitated asphaltenes depend on the choice of solvents and exact procedure used to perform the separation (Mitchell and Speight, 1973). Bitumen used in this study is extracted from the Athabasca region of Alberta. The typical SARA composition of Alberta bitumen is summarized in Table 1.2.

Table 1.2 Fractional composition of Alberta Bitumen (Strausz, 1989)

Bitumen fraction	Composition (wt%)
Asphaltenes	13 ~ 22
Resins	29 ~ 49
Aromatics	18 ~ 32
Saturates	15 ~ 21

Extensive research has been focused on the structure and chemical nature of asphaltenes. The asphaltene groups have some common features even though their structure can vary widely. Asphaltenes are polyaromatics with heteroatom functional groups and contain hydrophilic and hydrophobic structure (Yarranton et al., 2000). Compared with other fractions of bitumen, asphaltenes have a higher molar mass, higher heteroatom concentration and lower H/C ratio than the resin compounds (Strausz, 1989; Yarranton, 1997). Recent research indicates that the lower limit of molecular weight of asphaltene molecules may be as low as 500 Da (Groenzin and Mullins, 2001; Badre et al., 2006).

Deasphalted bitumen (maltenes) is typically composed of saturates, aromatics and resins. It is reported that Athabasca bitumen contains about 2 wt% low molecular weight natural surfactants. They are primarily carboxylic salts of naphthenic acids with the possibility of sulfonic salts (Bowman, 1967; Baptista and Bowman, 1969; Leja et al., 1968). These surfactants can be partitioned by the addition of alkaline solution (i.e. NaOH). The molecular weight of these surfactants ranges from about 166 to 450 g/mol (Schramm et al., 2000). Recent research has shown that naphthenic acids will not co-precipitate with asphaltenes and likely report to the maltene fraction (Yang and Czarnecki, 2005).

1.3 Emulsions

Emulsions are colloidal systems in which at least one liquid is dispersed as drops throughout an immiscible liquid. The dispersed droplets can have diameters ranging on the order of one to ten microns (Hunter, 1986; Davis, 1988). The understanding of emulsions has significantly contributed to the development of construction materials, biological, pharmaceutical, food, petrochemical, petroleum, and environmental and health industries (Hunter, 1986). It is very important to control the stability of emulsions for commercial products and processes. For example, cosmetics and dairy products must be stable emulsions to ensure its quality and shelve life. Microencapsulated drug delivery systems need to be stable everywhere except at the target organ where the micoemulsion is designed to become unstable and release the drug. However, the stability of the emulsions in petroleum production needs to be low to allow successful phase separation.

The two common types of emulsions are oil-in-water (O/W) and water-in-oil (W/O) emulsions, where oil refers to the water-immiscible fluid (Figure 1.3). Since free energy is associated with the interface, emulsions are thermodynamically unstable due to the extra energy cost caused by large interfacial areas. Consequently, the dispersed phase tends to coalesce to minimize the interfacial area, which eventually leads to phase separation (demulsification). Stable emulsions will only result if the reverse process of phase separation is sufficiently slower. Generally, an emulsifying agent is needed to ensure a stable or meta-stable emulsion. These components may stabilize the emulsion by preventing direct contact of emulsified droplets and/or resisting drainage of thin continuous phase films between emulsion drops (Hunter, 1986; Everett, 1988). The most common emulsifying agents are macromolecular stabilizers (like proteins, polysaccharides, and other types of polymers), surfactants and solids. Surfactants are substances with two well-defined regions: hydrophobic (oil soluble) and hydrophilic (water soluble). A very significant property of a surfactant is its tendency to adsorb at surfaces and interfaces due to this amphiphilic nature (Figure 1.4; Masliyah, 2000). The hydrophilic part of the surfactant (a dipole or charged polar group) tends to remain in the polar phase, while the hydrophobic part (a hydrocarbon chain) resides in the hydrocarbon phase (Hunter, 2001). Adsorption of the surfactants will influence the surface properties of the emulsified droplets; eventually altering the overall stability of the emulsion.

1.4 Theoretical background

1.4.1 Surface/interfacial tension

The most fundamental surface property of any liquid surfaces is the surface free energy or surface tension. The origin of surface tension is from the energy difference between molecules at the surface and molecules in the bulk. It is defined as the reversible work required to create a unit area of surface at constant temperature and pressure (equation 1.2),

$$\gamma = \left(\frac{\partial G}{\partial A}\right)_{T,P,n_i} \text{ in } \frac{mJ}{m^2} \qquad (1.2)$$

Alternatively, it refers to a force per unit length resisting such an increase in surface area, (equation 1.3; Hunter, 1986),

$$\gamma = \frac{F}{L} \quad \text{in} \quad \frac{mN}{m} \qquad (1.3)$$

The term surface free energy emphasizes the work required to bring molecules from the interior of the phase to the surface. Surface tension denotes the surface of a liquid has some kind of contractile “skin” (Adamson and Gast, 1997). It is instructive to describe surface tension in terms of macroscopic properties. An appropriate constitutive relation may be derived as follows. For a small section of an arbitrarily curved surface (Figure 1.5), the selected surface must be small enough to ensure that the radii of curvature, R_1 and R_2, are constant. With a slight increase in the curvature, the change in the area will be

$$\Delta A = (x+dx)(y+dy) - xy = x\,dx + y\,dy + dx\,dy \approx x\,dx + y\,dy \qquad (1.4)$$

The required work to create this additional surface is

$$W = \gamma(x\,dx + y\,dy) \qquad (1.5)$$

Suppose the pressure difference across the surface is ΔP, this pressure will act on the area *xy* and through a distance *dz*. The required work can be expressed as

$$W = \Delta P\; xy\; dz \qquad (1.6)$$

For the same angle, θ (Figure 1.5),

$$\frac{x+dx}{R_1+dz} = \frac{x}{R_1} \qquad or \qquad dx = \frac{x\,dz}{R_1} \qquad (1.7)$$

and

$$\frac{y+dy}{R_2+dz} = \frac{y}{R_2} \qquad or \qquad dy = \frac{y\,dz}{R_2} \qquad (1.8)$$

At an equilibrium state, equation (1.5) is equivalent to equation (1.6), substituting equations (1.7) and (1.8) into equation (1.5), the pressure difference can be obtained

$$\Delta p = \gamma(\frac{1}{R_1} + \frac{1}{R_2}) \qquad (1.9)$$

This equation was given by Young (1805) and Laplace (1806). It shows the equilibrium mechanical relationship between two immiscible liquids. Δp is the pressure difference across an arbitrary curved interface, γ is the surface/interfacial tension, the term in brackets is the mean curvature, where R_1 and R_2 are the principal radii of curvature (Adamson, 1976). For a plane surface, the radii are infinite, which means no pressure difference across a planar surface. For a spherical drop of radius R, the mean curvature is simplified to 2/R; equation (1.9) can be rewritten as follows:

$$\Delta P = \frac{2\gamma}{R} \qquad (1.10)$$

Several convenient methods, including maximum bubble pressure method, Du Noüy ring method and Wilhelmy plate method, are widely used to measure surface/interfacial tension.

1.4.1.1 Maximum bubble pressure method

In this technique, a bubble of a gas is slowly produced from a capillary immersed in a liquid (Figure 1.6). The growth of the bubble can be divided into three stages: a flat surface (stage 1), a hemispherical shape when its radius equals to that of the capillary (stage 2) and a section of sphere (stage 3). Since the radius of the bubble is minimum at the point of hemispherical shape, the pressure difference ΔP across the curvature is maximum based on equation (1.10).

According to the force balance,

$$P^O = P_O + P_h + \Delta P \qquad (1.11)$$

$$P^O = P_O + P \qquad (1.12)$$

where P_o is the atmosphere pressure, P_h is the pressure corresponding to the hydrostatic head h, P^o is the applied pressure to blow the bubble from the tip of the capillary, ΔP is the pressure difference across the bubble surface and P is the pressure difference caused by the liquids in the U-tube (Figure 1.6). By equating (1.11) and (1.12),

$$P = P_h + \Delta P = P_h + \frac{2\gamma}{R} \qquad (1.13)$$

Since ΔP_{max} is given at the point that the radius of the bubble is the same as that of the capillary ($R = r$), equation (1.13) can be expressed as follows,

$$\Delta P_{\max} = \frac{2\gamma}{r} = P_{\max} - P_h \qquad (1.14)$$

By this way, the surface/interfacial tension can be calculated from the measurable parameters P_{max}, P_h and r at designed condition.

1.4.1.2 Du Noüy ring method

The Du Noüy ring method (1919) can involve the detachment of a ring from a liquid surface (Figure 1.7). At first, an immersed ring is gradually directed towards the liquid surface. The ring is then detached from the liquid by applying external force. At the point when the liquid surface is vertical (as shown by the dotted lines in Figure 1.7), the largest detachment force can be related to the surface tension of the liquid.

$$F_{tot} = G_{ring} + F \qquad (1.15)$$

where F_{tot} is the total force that can be measured using an electronic balance, G_{ring} is the gravity force of the ring and F is the surface tension force of the liquid. By definition,

$$dW = F\ dx = \gamma\ dA = \gamma\ \partial L\ dx \qquad or \qquad F = \gamma\ L \qquad (1.16)$$

In this case,

$$L = 2\pi\ (R + r) + 2\pi\ (R - r) = 4\pi R \qquad (1.17)$$

where r is the radius of the ring and R is the middle radius of the ring. Substitute equation (1.16) and (1.17) into equation (1.15),

$$\gamma = \frac{F_{tot} - G_{ring}}{4\pi R} \qquad (1.18)$$

1.4.1.3 Wilhelmy plate method

A thin vertical plate is suspended at a liquid surface from the arm of a sensitive torsion balance, such as the Roller-Smith balance, with an elevating device to either lower the plate to the liquid or raise the liquid surface to the plate. Figure 1.8 shows the schematic view of surface tension measurement using Wilhelmy plate method (Wilhelmy, 1863). At equilibrium state of surface I (Figure 1.8),

$$F_{tot} = G_{plate} + F \qquad (1.19)$$

$$F = F_{tot} - G_{plate} = \gamma\ P\cos\theta \qquad (1.20)$$

where F_{tot} is the total force that can be measured using a balance, G_{plate} is the gravity force of the plate, F is the surface force of the liquid, γ is the surface tension, P is the perimeter of the plate and θ is the contact angle.

Assuming a zero contact angle (surface II), equation (1.20) can be simplified,

$$F = F_{tot} - G_{plate} = \gamma\ P = \gamma\ 2(L + d)$$

$$\gamma = \frac{F_{tot} - G_{plate}}{2(L + d)} \qquad (1.21)$$

If the width of the plate is very small, with respect to the length, the equation can be simplified to,

$$\gamma = \frac{F_{tot} - G_{plate}}{2L} \qquad (1.22)$$

1.4.2 Gibbs adsorption equation

The thermodynamic parameters of a two-phase system are partially determined by the presence of an interface. A “Gibbs dividing plane” (Gibbs, 1874-1878) is introduced to understand the variation of surface tension with composition. Assume that a system is composed of three parts: two bulk phases, α and β, and an arbitrary dividing plane (Gibbs dividing plane) (Figure 1.9). It is the imaginary surface at which excess of solvent molecules is zero.

For a general infinitesimal reversible process in a two-phase system (Hunter, 1986),

$$\begin{array}{ll} U \rightarrow U + dU & V^{\alpha} \rightarrow V^{\alpha} + dV^{\alpha} \\ S \rightarrow S + dS & V^{\beta} \rightarrow V^{\beta} + dV^{\beta} \\ n_i = n_i + dn_i & A \rightarrow A + dA \end{array} \qquad (1.23)$$

At fixed temperature and in a constant volume,

$$\mu_i^{\alpha} = \mu_i^{\beta} = \mu_i^{\sigma} = \mu_i \qquad (1.24)$$

Since

$$\begin{array}{l} U = U^{\alpha} + U^{\beta} + U^{\sigma} \\ S = S^{\alpha} + S^{\beta} + S^{\sigma} \end{array} \qquad (1.25)$$

A governing equation for the system becomes,

$$\begin{aligned} dU &= dU^{\alpha} + dU^{\beta} + dU^{\sigma} \\ &= T\ dS^{\alpha} + \sum_i \mu_i^{\alpha}\ dn_i^{\alpha} - P^{\alpha}\ dV^{\alpha} + T\ dS^{\beta} \\ &\quad + \sum_i \mu_i^{\beta}\ dn_i^{\beta} - P^{\beta}\ dV^{\beta} + T\ dS^{\sigma} + \sum_i \mu_i^{\sigma}\ dn_i^{\sigma} + \gamma\ dA \qquad (1.27) \\ &= T\ dS^{\alpha} + \sum_i \mu_i\ dn_i^{\alpha} - P^{\alpha}\ dV^{\alpha} + T\ dS^{\beta} \\ &\quad + \sum_i \mu_i\ dn_i^{\beta} - P^{\beta}\ dV^{\beta} + T\ dS^{\sigma} + \sum_i \mu_i\ dn_i^{\sigma} + \gamma\ dA \end{aligned}$$

For the bulk phase,

$$dU^{\alpha} = T\ dS^{\alpha} - P\ dV^{\alpha} + \sum_i \mu_i\ dn_i^{\alpha} \qquad (1.28)$$

$$dU^{\beta} = T\ dS^{\beta} - P\ dV^{\beta} + \sum_i \mu_i\ dn_i^{\beta} \qquad (1.29)$$

Then, for the Gibbs surface,

$$dU^{\sigma} = T\ dS^{\sigma} + \gamma\ dA + \sum_i \mu_i\ dn_i^{\sigma} \qquad (1.30)$$

Integration of equation (1.30), it can be obtained,

$$U^{\sigma} = T\,S^{\sigma} + \gamma\,A + \sum_i \mu_i\, n_i^{\sigma} \qquad (1.31)$$

Differentiation of equation (1.31), leads to,

$$dU^{\sigma} = T\ dS^{\sigma} + S^{\sigma}\ dT + \gamma\ dA + A\ d\gamma + \sum_i \mu_i\ dn_i^{\sigma} + \sum_i n_i^{\sigma}\ d\mu_i \qquad (1.32)$$

Comparison of equations (1.30) and (1.32) results in,

$$S^{\sigma}\ dT + A\ d\gamma + \sum_i n_i^{\sigma}\ d\mu_i = 0 \qquad (1.33)$$

Since temperature is constant, equation (1.33) becomes,

$$-\,d\gamma = \sum_i \frac{n_i^{\sigma}}{A}\ d\mu_i = \sum_i \Gamma_i\ d\mu_i \qquad (1.34)$$

For a two component system,

$$-d\gamma = \Gamma_1 \; d\mu_1 + \Gamma_2 \; d\mu_2 \tag{1.35}$$

Suppose the Gibbs dividing surface is an arbitrarily chosen surface so that

$\Gamma_1 = 0$ and $\Gamma_2 = \Gamma_2^{\sigma} = \Gamma_{2,1}$,

Equation (1.35) can be rewritten in the form,

$$-d\gamma = \Gamma_{2,1} \; d\mu_2 \tag{1.36}$$

Since

$$\mu_2 = \mu_2^o + RT \; \ln a_2 \tag{1.37-1}$$

$$d\mu_2 = RT \; \ln a_2 \tag{1.37-2}$$

Substitute equation (1.37-2) into (1.36),

$$\Gamma_{2,1} = -\frac{1}{RT} \frac{d\gamma}{d \ln a_2} \tag{1.38}$$

For a highly dilute solution, $c_2 \propto a_2$, then,

$$\Gamma_{2,1} = -\frac{1}{RT} \frac{d\gamma}{d \ln c_2} \tag{1.39}$$

This adsorption isotherm equation (Hunter, 1986) describes a relationship between the amount of species adsorbed and its solution concentration in terms of the surface tension. Generally, the adsorption of surfactant films at the interface decreases the interfacial tension by reducing the molecular interaction energy across the interface.

1.5 Stability of emulsions

In most cases, emulsification occurs in the presence of a surface active agent (also called surfactants) in two immiscible liquids. The interfacial film formed by the adsorption of the surfactants on the emulsified droplets is of great importance to the emulsion stability (Figure 1.10). There are two stages in the destabilization of an emulsion: flocculation and coalescence. Flocculation depends on the relative magnitude of the attractive and repulsive forces among the droplets. It involves the clustering of emulsified droplets. However, it is reversible, and the convective forces can break up the flocculation or flocs. If the droplets collide and flocculate, the continuous phase between the drops drains out until a thin layer of film forms between the droplets (Tadros and Vincent, 1983). The dampening of flocculation will keep the droplets intact, while the growing of flocculation will result in the film rupture and merging of droplets, which is called coalescence. The occurrence of coalescence will increase droplet size, decrease droplet numbers and eventually destabilize the emulsion (Vold and Groot, 1963; Rehfeld, 1962; Reddy and Fogler, 1981).

1.6 Thesis outlines

This research aims to understand the influence of bitumen components on the stability of water-in-diluted bitumen emulsions using an array of techniques, including micropipette technique, Langmuir trough (Langmuir-Blodgett films), Brewster angle microscopy, atomic force microscopy and Fourier transform infrared spectroscopy. The role of indigenous naphthenic acids is also investigated. The results will provide insights into the behavior of emulsified water droplets and theoretical basis to emulsion destabilization. A biodegradable polymer is introduced to destabilize the water-in-diluted bitumen emulsion and the corresponding destabilizing mechanisms are carefully described. All the experiments are carried out under the conditions that are representative of industrial oil sands extraction operations. The theme of this research is developed in the following chapters.

Chapter 2 gives a detailed introduction for the related techniques used in this work and the corresponding experimental protocols. The interfacial properties of the emulsified water droplets, including interfacial tension, crumpling ratio and coalescence probability, are evaluated using micropipette technique. The interfacial films of different systems (such as bitumen and asphaltenes) are characterized using a Langmuir trough. Brewster angle microscope and atomic force microscope provide a straightforward description of the sample surface. Chapter 2 is intended to provide background information and context for the chapters that follow.

Chapter 3 focuses on the role of bitumen components, asphaltenes and maltenes, in stabilizing water-in-diluted model oil emulsions. Results show that asphaltene is the main stabilizer for the emulsions. However, it is shown that certain species contained in maltenes might also contribute to the stabilization of the emulsion even without obvious formation of steric layer.

In Chapter 4, we investigate the influence of indigenous naphthenic acids on the emulsion stability. It has been shown that the level of naphthenic acids in the bitumen changes the interfacial properties, and eventually changes the emulsion stability. This study provides valuable information of identifying a predictor based on pH control by a process aid for optimizing recovery.

Chapter 5 describes the use of a biodegradable polymer to destabilize the water-in-diluted bitumen emulsions based on the understanding of stabilization mechanism described in Chapters 3 and 4. The demulsification performance was compared with a commercial demulsifier currently used by industry. The destabilization mechanism of this product is carefully investigated to support implementation in industrial process.

Finally, Chapter 6 provides a discussion on the contribution of the thesis and summarizes recommendations for future work.

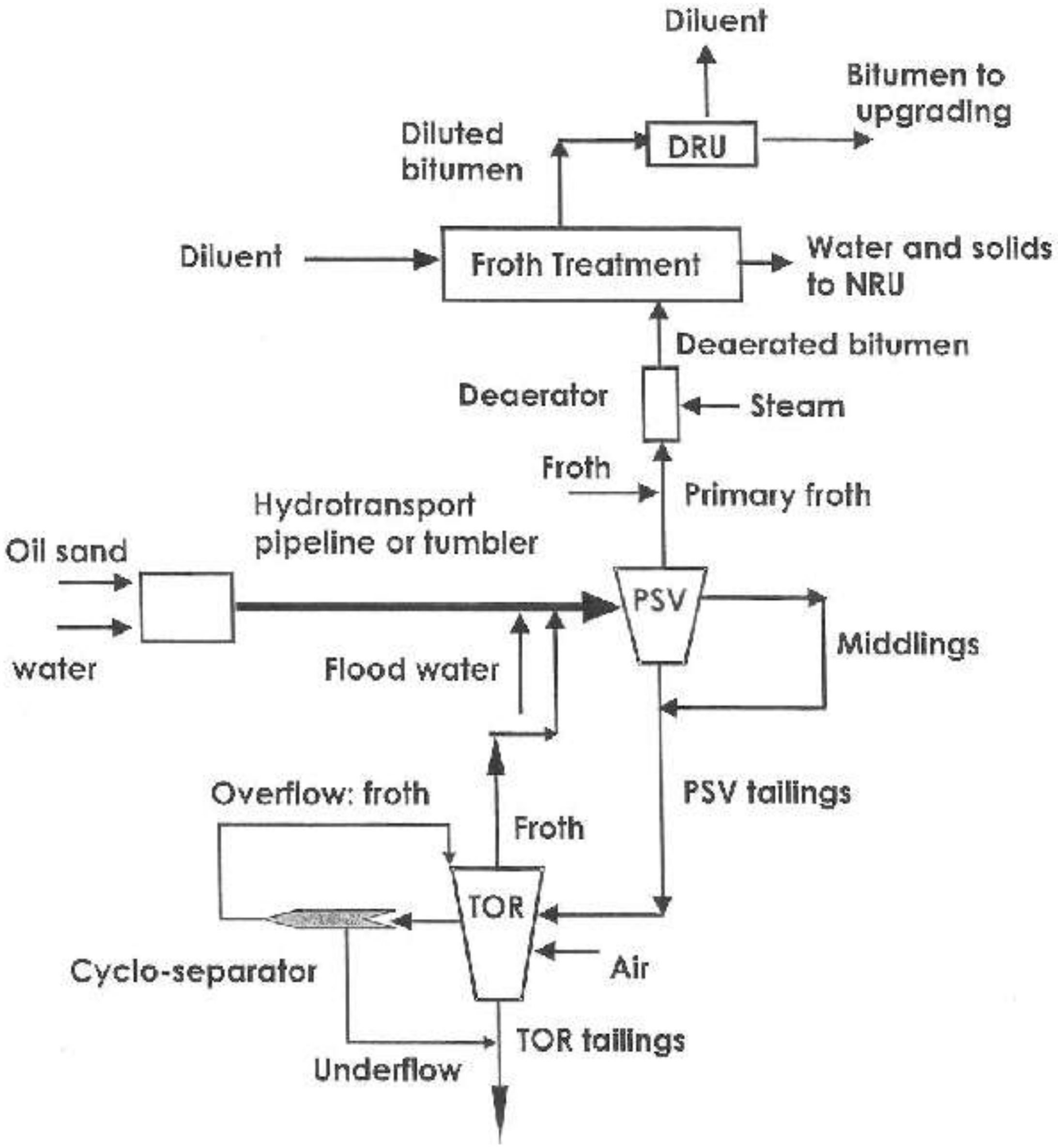

Figure 1.1. Schematic view of typical bitumen extraction process

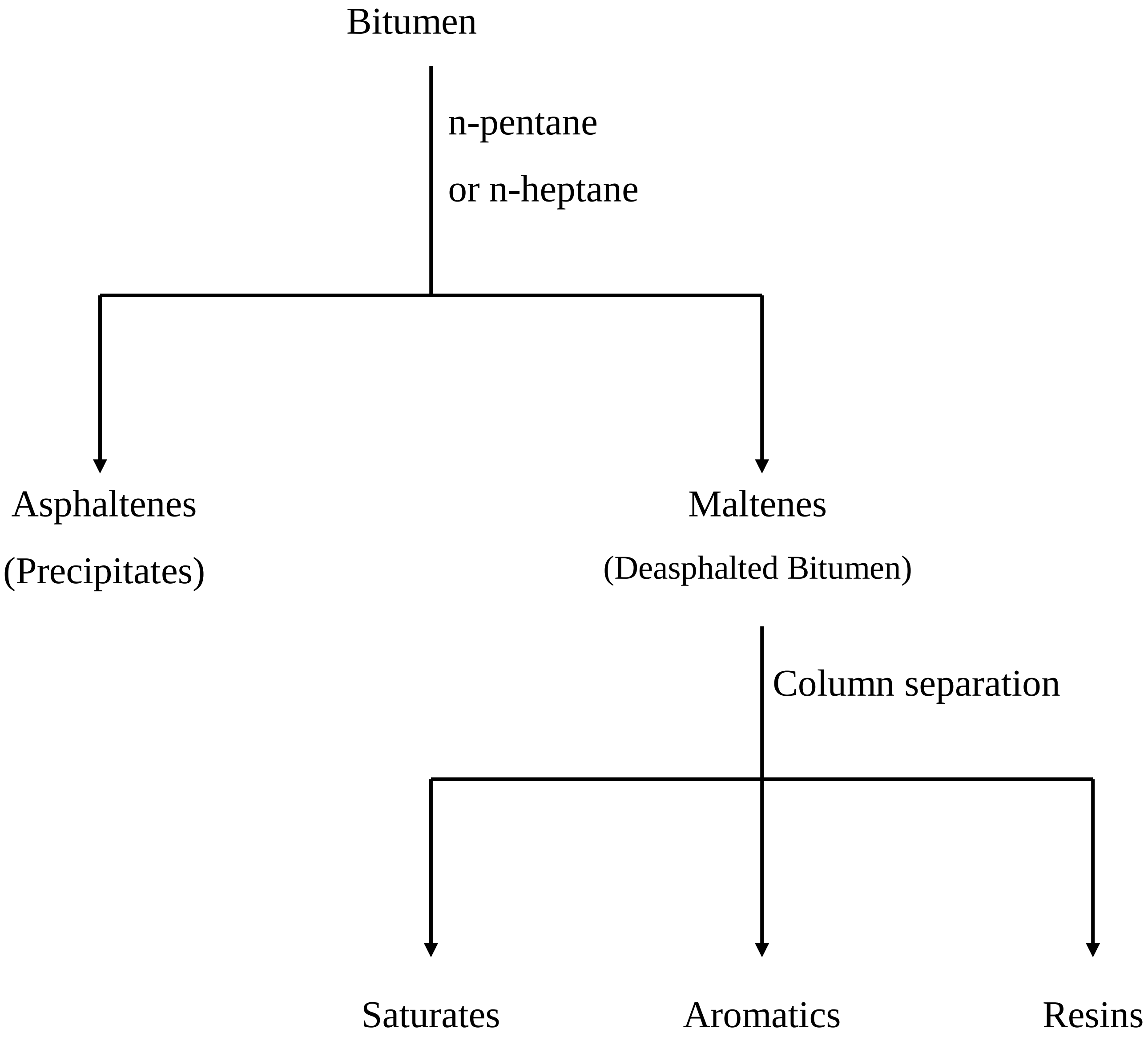

Figure 1.2. Flowchart of bitumen components as a solubility class

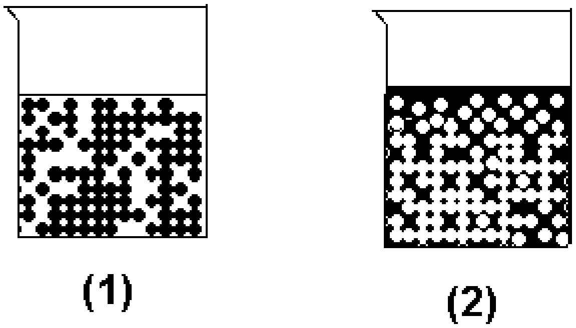

(1) (2)

Figure 1.3. Two types of Emulsions:(1) oil-in-water (O/W) and (2) water-in-oil (W/O)

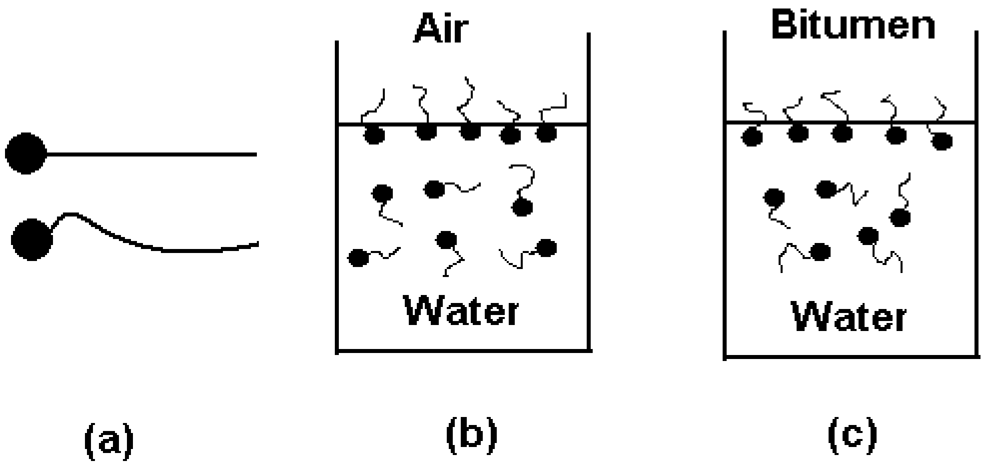

Figure 1.4. (a) Conventional representation of surfactant molecule. (b) and (c) Surfactant at air/water and bitumen/water interfaces, respectively (Masliyah, 2000)

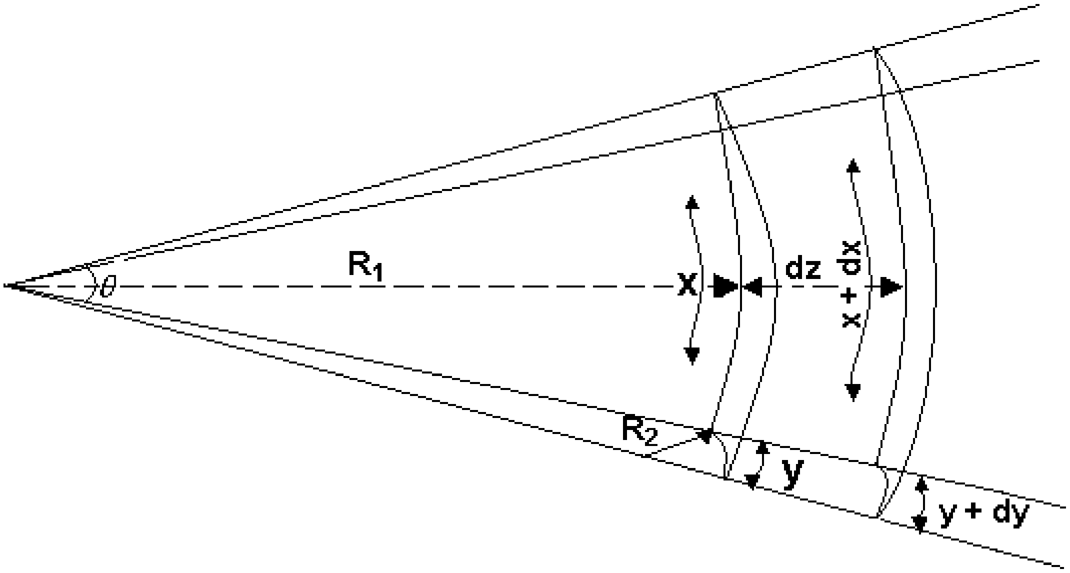

Figure 1.5. Mechanical equilibrium for an arbitrarily curved surface (Adamson, 1976)

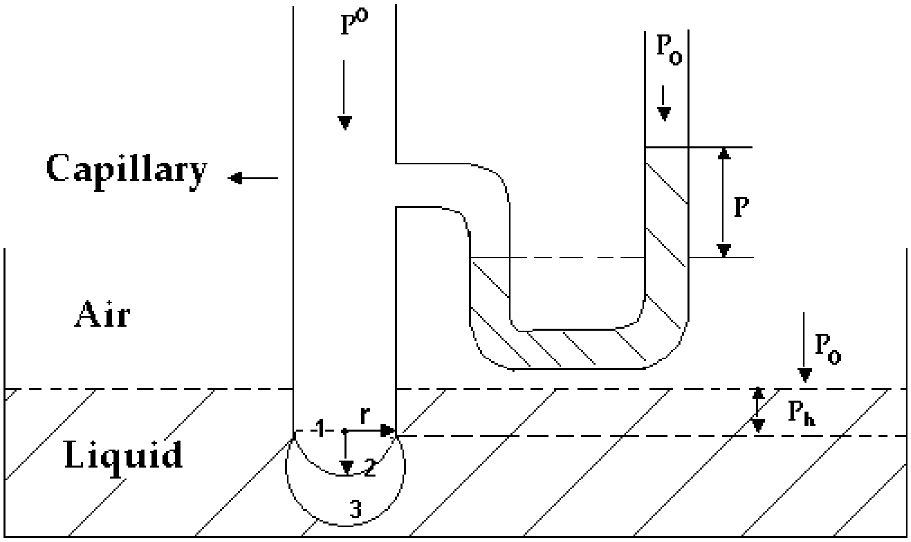

Figure 1.6. Illustration of maximum bubble method

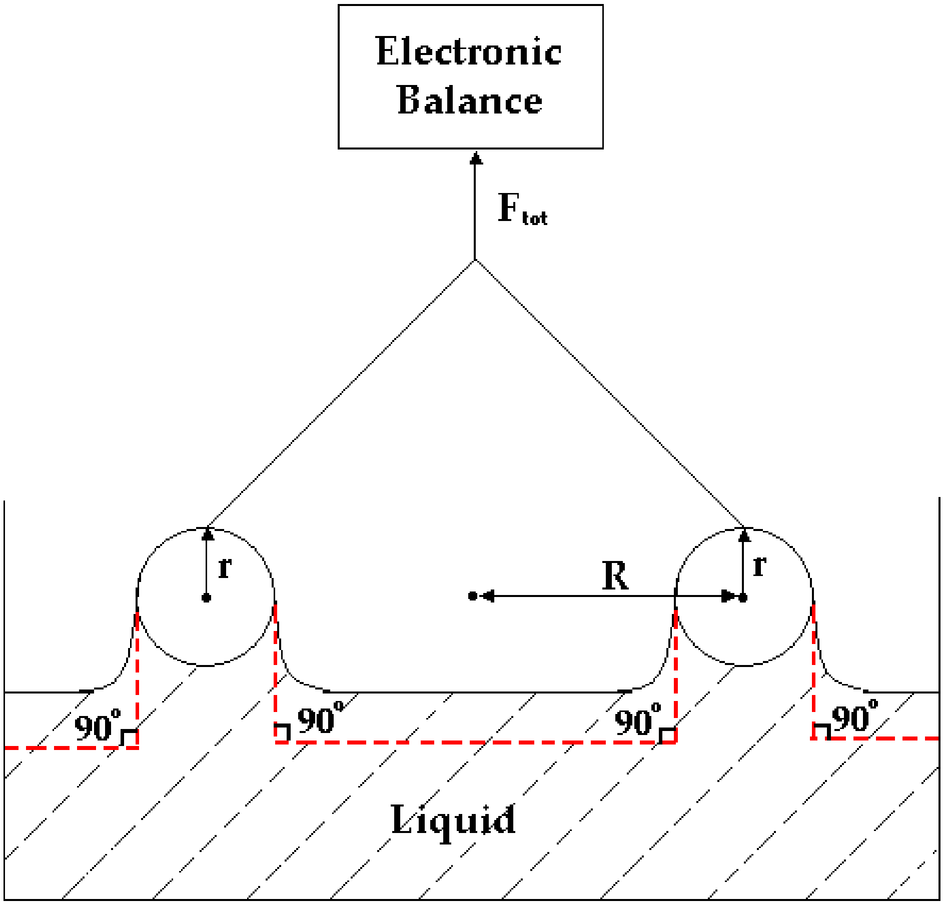

Figure 1.7. Illustration of Du Noüy ring method

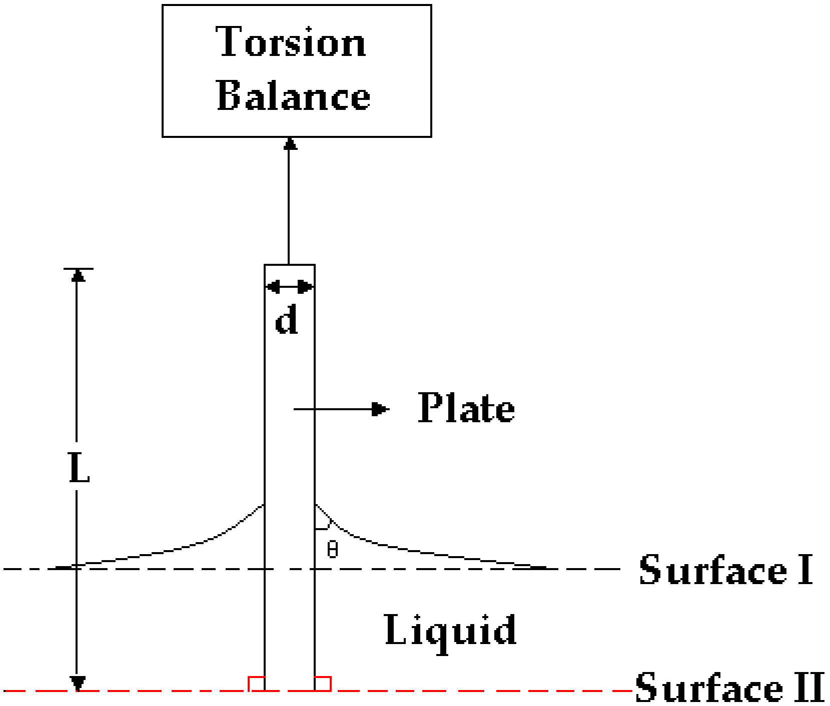

Figure 1.8. Illustration of Wilhelmy plate method

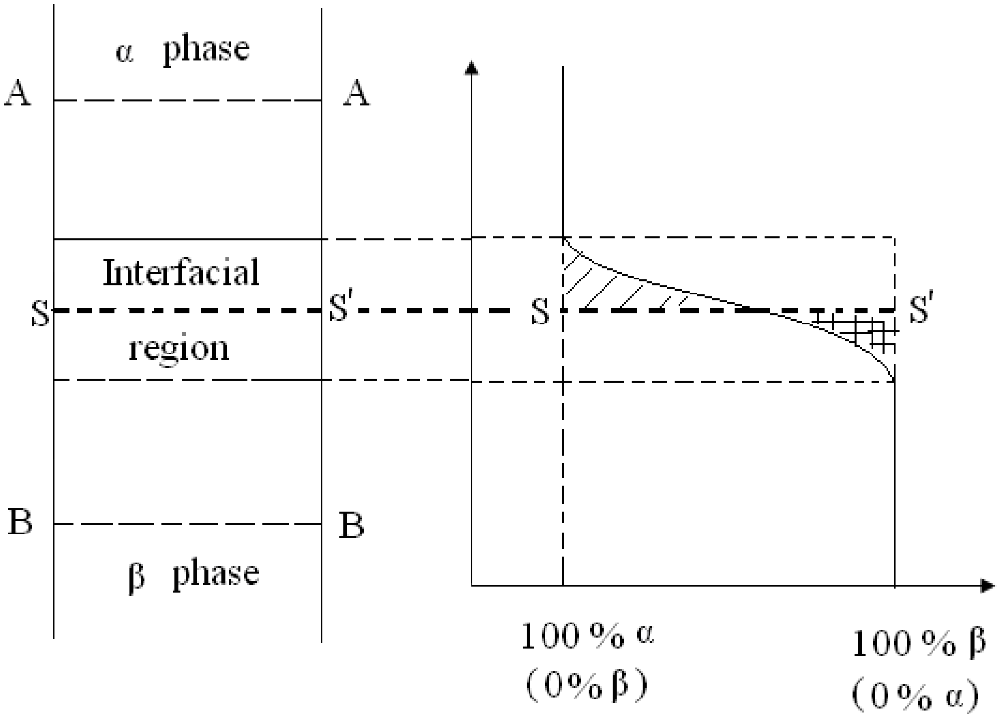

Figure 1.9. Schematic illustration of Gibbs dividing plane, S-S', an arbitrary choice of Gibbs surface reduce the surface concentration to zero (note equality of the two hatched areas)

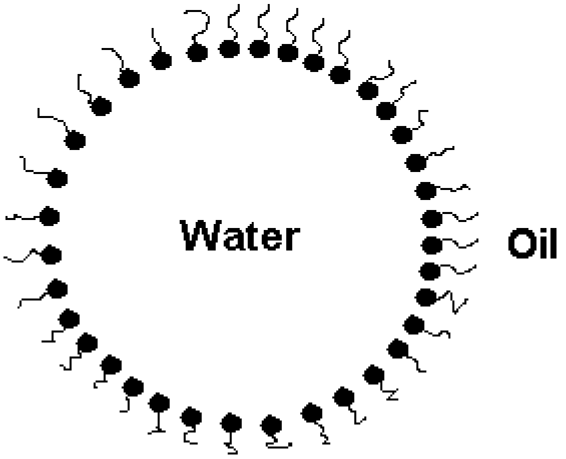

Figure 1.10. A water droplet stabilized by surfactant in the continuous oil phase.

Chapter 2

Experimental techniques

2.1 Micropipette technique

Micropipette techniques used in the biological sciences (Evans and Skalak, 1980; Evans and Rawicz, 1990) were introduced by Yeung et al. (1998) to oil sands research in the study of emulsion systems. The importance of this technique was proven by its recent adaptation in macro-emulsion studies (Yeung et al., 1998; Yeung et al., 1999; Yeung et al., 2000; Kloet et al., 2001; Moran and Czarnecki, 2007; Moran, 2007). The near colloidal scale of this technique maintains surface area-to-volume ratios of the system that are representative of the commercially encountered emulsions. Crumpling ratios based on micromechanical volume contraction experiments are determined to provide a quantitative analysis of the skin formation on the surface of emulsified water droplets. Furthermore, the probability of coalescence is determined to statistically document the droplet interactions.

2.1.1 Experimental setup

The micropipette technique makes it possible to study the behavior of individual emulsion droplets *in situ* with the use of small suction pipettes. As shown in Figure 2.1, micron-sized droplets in the emulsions were observed through an inverted optical microscope with transmission bright-field illumination (Carl Zeiss Canada; model Axiovert 200). Two suction micropipettes were mounted on micromanipulators (Narishige, Tokyo; model MHW-3) to ensure the continuous movements at micrometer scale. A sample cell assembled from microscope cover slips was used to contain the emulsions. It should be noted that both micropipette and sample cell are treated with a methylating agent to make them hydrophobic. This treatment prevented the spreading of water droplets onto glass surfaces, maintaining the integrity of emulsion systems. The methylating chemicals used in the present work were a mixture of dichlorodimethylsilane (Aldrich Chemicals) and cyclohexane at a volume ratio of 1:4. Filtered and deionized water was placed on the sample cell after the introduction of ~50μL emulsion in the cell to prevent the evaporation of components in the emulsion system. A CCD camera (Hitachi Denshi, Japan; model KP M3) and a TV monitor made it possible to visualize the micro-scale experiments in real time. A videocassette recorder (JVC, Japan; model PV-S9670) was used to record the experiments for further analysis. Pressure was applied through syringes and measured using a commercial pressure transducer (Omega Engineering, Stamford CT).

Borosilicate glass tubes with 1mm OD and 0.75mm ID (Friedrich & Dimmock, USA; SYN-BCT-75136) were utilized to produce micropipettes. The tubes were stretched axially in an extruder (David Kopf Instruments, Tujunga, CA; model 730) to produce tapered hollow tubes with fused tips (Moran, 2007). The tapered tubes were truncated to form hollow pipette tips with the inside diameter ranging from 5 to 10μm (as shown in Figure 2.2) on a home-made forging device. All experiments were carried out at room temperatures.

2.1.2 Experimental methods

2.1.2.1 Interfacial tension measurement

A previous study (Yeung, 1998) has shown that the interfacial tension of micron-sized droplets in emulsion system is appreciably different from that measured by conventional tensiometers. In addition, the micropipette method allows interfacial tension measurements to be conducted under emulsion conditions of similar surface area-to-volume ratios as encountered in industrial operating systems and therefore it is an applicable tool in the study of industrial emulsions. In this study, the interfacial tension of emulsified water droplets in different emulsions was measured by a maximum bubble pressure method using a micropipette approach (Moran, 2007). The open and untapered end of a micropipette was connected to a 60 mL syringe through flexible rubber tubes. Positive pressure was applied to a water-filled micropipette immersed in the oil to control the movement of the water-oil interface near the tip of the micropipette. The curvature of the interface increased as the pressure was increased until a critical pressure (maximum pressure) at which, a hemispherical interfacial geometry was formed at the tip, defined by R_p. Beyond this pressure, any increase in applied pressure at the tip caused the interface to spontaneously expand into the oil phase. The critical pressure P_c was recorded via a calibrated pressure transducer. The interfacial tension was then calculated from the Young-Laplace equation (Figure 2.3).

The combination of micropipette technique and maximum bubble pressure method makes it possible to record the change of interfacial tension in real time over a long aging process. Results obtained by this method are reproducible and correspond well with the literature value for reference fluids (Table 2.1).

Table 2.1 Surface and interfacial tensions of pure liquids measured using maximum bubble pressure technique. Selected literature values are also shown. The values shown are the average with standard deviation based on a minimum of 10 measurements at the room temperature. DIW refers to de-ionized water.

Fluid Interface	Micropipette (mN/m)	Previous study (Moran, 2007) (mN/m)	Literature value (Davis, 1963; Adamson, 1997) (mN/m)
DIW/Air	71.8 ± 0.3	72.6 ± 0.1	72.80 (20°C)
Toluene/Air	27.4 ± 0.1	26.9 ± 0.3	28.52 (20°C)
Toluene/DIW	36.5 ± 0.4	36.3 ± 0.3	35.7 (25°C)
n-Heptane/Air	19.9 ± 0.3	20.3 ± 0.1	20.14 (20°C)
n-Heptane/DIW	49.8 ± 0.3		50.2 (20°C)
Heptol/Air	21.2 ± 0.1 [a]	23.4 ± 0.2 [b]	
Heptol/DIW	45.2 ± 0.2 [a]	40.0 ± 0.4 [b]	

[a] The volume ratio of *n*-heptane to toluene is 4:1.

[b] The volume ratio of *n*-heptane to toluene is 1:1.

2.1.2.2 Volume contraction experiment

The volume contraction experiment is the basis for quantitative analysis of skin formation at the surface of emulsified water droplets. In this experiment, a water-filled micropipette is immersed into a continuous oil phase. With the applied positive pressure, a water droplet with a diameter of 20-30 μm is produced at the tip of the micropipette. The shape and volume of the droplet is manipulated to be constant and aged in the continuous oil phase for one minute. This time scale aims to allow the adsorption of surface active components on the surface of water droplet. The droplet is then slowly aspirated into the micropipette by applying a negative pressure at a rate such that the whole droplet will be completely drawn back into the micropipette in one minute. This aspiration rate was selected to eliminate the possible influences of higher order surface mechanics. The decrease of droplet volume is smooth and the shape remains spherical during the contraction process if the droplet surface remains fluid. However, a sudden crumpling of the water-oil interface may occur during the contraction process if a rigid skin is formed at the droplet surface. The crumpling ratio, which is the ratio of the projected area of the water droplet immediately prior to crumpling to its initial projected area, is proposed as a measure of rigid skin formation. The larger, the crumpling ratio, the more rigid, the skin on water droplet surface. It should be noted that crumpling ratio and rigidity are both measures of in-plane surface deformation. In this study, the effect of aspiration rate on the crumpling ratio was not reported.

2.1.2.3 Droplet interaction experiment

Droplet-droplet contact is prerequisite for droplet coalescence. The interaction experiment involves the use of suction pressure to capture emulsified water droplets of diameter ranging from 15-30 µm (the bigger the droplets, the easier the coalescence (Esmaeili et al., 2006)), at tips of two micropipettes in axial alignment. One droplet was directed using a micromanipulator, towards the other droplet held stationary to enable a direct “head-on” contact. A sufficient force was applied by one of the micropipettes to deform both droplets. The contact of the droplets was held under this force for a sufficient period of time (three minutes in this study) to allow for the drainage of the intervening liquid sandwiched in the planar region between the droplets. Previous research (Moran, 2007) showed that the applied pressure at the contact region of two droplets remained constant. No difference was observed if the droplets were held in static contact for more than three minutes. If the droplets did not coalesce or flocculate, they were easily separated when the applied force was removed after the contact. In some cases, coalescence occurred spontaneously upon direct contact of the two droplets. The probability of coalescence, which is defined as the ratio of the number of contact trials in which coalescence was observed to the total number of trials, was employed to describe the statistical nature of emulsified water droplets coalescence (Moran, 2007).

2.2 Langmuir trough

A Langmuir trough technique was developed in the late 1910s and early 1920s to study monolayers at air/water interface (Langmuir, 1917). Several years later, Katherine Blodgett (1935) gave the first detailed description of sequential monolayer transfer onto solid supports. It is one of the most important tools to study insoluble monolayers at the hydrocarbon-water interface in the oil sands industry (Ese, 1998; Zhang et al., 2003, 2005). Using this technique, the properties of the interfacial film at the hydrocarbon-water interface can be evaluated to understand the interfacial properties.

2.2.1 Experimental setup

The standard Langmuir trough is composed of three parts: 1) a lower compartment built with hydrophobic and inert material (typically PTEE) to avoid subphase contamination, 2) a coupled movable barrier to control the surface area and 3) a microbalance sensor used to measure the surface pressure. Schematic views of the Langmuir trough can be found in Figures 2.4 and 2.5. A Wilhelmy plate method is the most commonly used technique to measure the variations of surface pressure.

The Langmuir trough (KSV instruments, Finland) used in this study has an area of 17010 mm^2 and two symmetric barriers (Delrin). Two holes in the barriers allow the upper phase (lighter phase, such as oil) to flow freely while changing the surface area. Contaminants on any part of the trough may cause unreliable results. Consequently, the following cleaning procedures must be adopted before each test (courtesy of Mussone, P):

1) Handle the trough always and only with surfactant free gloves.
2) Wipe the trough and barriers carefully with surfactant free paper (Texwipe wipers).

3) Rinse the trough thoroughly with toluene (HPLC grade) and acetone
4) Wipe and dry the trough with Texwipe wipers.

The temperature of the trough was controlled by a circulation water bath operating at room temperature. A filter paper (Whatman 1 CHR) was used as the Wilhelmy plate due to its advantage of maintaining zero contact angle as it was completely wetted by the water subphase.

2.2.2 Experimental methods

2.2.2.1 Spreading Method

With the barrier in the open configuration, 120 mL of Milli-Q water was carefully poured into the trough. The barrier was compressed at low speed (2 mm / min) to a small area until the surface pressure reading was smaller than 0.10 mN/m. If this target was not achieved, the surface layer would be cleaned with a pipette connected to an aspirator and the compression was repeated. A monolayer was carefully spread on the water phase to avoid phenomena such as self-aggregation, dissolution in the subphase and multilayer formation. The sample solution (20~50 μL) was placed drop-wise and evenly onto the water surface using a 100 μL gas-tight Hamilton syringe (Sigma-Aldrich). A period of typically 20 minutes lapsed to ensure complete evaporation of solvent at the interface. The upper phase (oil phase, 100 mL) was carefully poured from a glass beaker along a glass stirring rod. The glass rod was inclined at an angle so that the oil phase flowed down along it and then spread smoothly on the water phase without disturbing the water subphase (Zhang, 2005). The compression of the interfacial film was conducted after a 2 hour equilibration. All the reading was zeroed before the compression. All compressions were performed at 5mm/min.

2.2.2.2 Langmuir-Blodgett films

A common application of Langmuir trough is to transfer a monolayer onto a solid substrate. It is accomplished by dipping the substrate into the subphase, allowing the formation of monolayer. The surface pressure was kept constant during the deposition process. Hydrophilic silicon wafers were used for the Langmuir-Blodgett (LB) film deposition. Prior to use, the silicon wafers were cleaned by soaking in a 70/30 by volume of 96 % sulfuric acid and 30 % hydrogen peroxide at 90 ^{o}C for 30 minutes, followed by flushing thoroughly with Milli-Q water. The cleaned hydrophilic silicon wafer was stored in Milli-Q water before use. The interfacial film was compressed at 5mm/min until the surface pressure was 2 mN/m (target pressure). Under this constant target pressure, the monolayer was deposited on the silicon substrate; while the substrate was pulled upward though the interface at a rate of 5mm/min. The silicon substrate with deposited LB film was stored in a desiccator for future use.

2.3 Atomic Force Microscopy

Atomic force microscope (AFM) can image both conductor and insulator surfaces with a scan range as small as few fractions of nanometers or as large as 80 μm in air or in liquids on any flat substrate (Hansma et al., 1991). AFM is compatible with a variety of environments, including liquids at varied temperatures (Drake et al., 1989), and is capable of imaging with a force as low as 10^{-7} N in air and 10^{-9} N or less under liquids (Weisenhorn et al., 1989). Recent studies (Weisenhorn et al., 1990; Meyer et al., 1991; Zhang et al., 2005; Torrent-Burgues et al., 2006) reported the microscopic structures of different LB films imaged by AFM.

2.3.1 Experimental setup

A standard AFM consists of a microscale cantilever with a sharp tip at the end, which bends in response to the force between the tip and the sample (Figure 2.6). At first, the tip was directed towards the sample until it was interacting with the sample surface. According to Hooke’s law, the force between the tip and the sample can be expressed as,

$$F = -K\,x \qquad (2.1)$$

where K is the spring constant and x is the cantilever deflection. The deflection is measured by a laser spot reflected from the top of the cantilever into an array of photodiodes. In order to avoid breaking the tip and damaging the surface, a feedback mechanism is adopted to adjust the distance between the tip and sample surface to keep the interaction force constant.

The most common image modes of AFM are contact mode and tapping mode. For the contact mode, the tip is in direct contact with the surface under a special force, where the deflection of the static tip is sensed and compared to the desired value of deflection. Generally, cantilevers with low stiffness would be used to lower the noise and drift of the deflection signal. In a tapping mode (Figure 2.7), the tip was lifted off after contact with the surface to avoid damaging the surface while dragging the tip across the surface. As the oscillating cantilever begins to intermittently touch the surface, the cantilever oscillation is reduced due to energy loss caused by the tip contacting the surface. This reduction in oscillation amplitude is used to identify and measure the surface features (Sophie, 2007).

2.3.2 Experimental method

A multimode AFM with a nanoscope IIIa controller (Veeco, Santa Barbara, CA) was operated under the tapping mode in air to obtain images of LB films at room temperature. A topographical image of the sample can be obtained using a silicon tip (RTESP, Veeco) with a resonance frequency of 260-320 kHz at a scan rate of 1 Hz. Scans were performed at several locations of each sample with scan size ranging from 100 nm to 1μm.

2.4 Brewster angle microscopy

Instead of transferring the monolayer to a solid substrate, Brewster angle microscope (BAM) provides a non-invasive tool to allow the characterization of a monolayer at a liquid-water interface. Polarization means defining the direction of an electric field. A beam of light is p-polarized when the light is in the plane of the incidence while it is defined as s-polarized when it is perpendicular to the same plane. For a beam of p-polarized light on a flat insulating surface, there is a unique angle at which no reflection occurs. This angle is commonly referred to as "Brewster's angle" (discovered by David Brewster, 1781-1868) and can be calculated using the following equation for a beam of light traveling through air,

$$\tan\theta = \frac{n_{subphase}}{n_{air}} \qquad (2.2)$$

where n is the refractive index of the corresponding phase. A small amount of the incident intensity can be reflected by introducing a thin film at the interface of two phases (Figure 2.8). This reflectivity can be measured when a condensed phase of monolayer with different refractive index is spread or deposited at the interface. Moreover, the reflected light can be used to form a high contrast image of the lateral morphology of the monolayer. Based on these early results, the Brewster angle microscope was invented independently and almost simultaneously by two groups: Jacques Meunier in Paris, France and Dietmar Möbius in Göttingen, Germany (Hénon, 1991; Hönig, 1991).

2.4.1 Experimental setup

A standard Brewster angle microscope (BAM) is augmented with an opto-mechanical, electronic control unit, two arms and a personal computer (Figure 2.9). The BAM used in this work (Figure 2.10) is the latest commercial model supplied by Nanofilm Technologies GmbH (BAM2+) (Hannover, Germany). The Z-lift (Figure 2.9) of this BAM is a liner stage with approximately 30mm traverse distance. The vertical distance between the sample and the objective should be controlled to allow some spaces to remain at the lowest point of the Z-lift. The right arm of the BAM aims to produce laser (NdYAG, 532nm, 70mW) with the polarizer and a safety shutter. Both the angle of incidence and the state of the incident beam must be set to the optimal values to get optimal results. The left arm of the BAM contains the objective, analyzer and a CCD camera. The objective has a nominal magnification value of 10X, which images the sample surface onto a CCD chip. The maximum resolution of the apparatus is 2 μm. A quarter wave plate on the path of the incident beam and an analyzer on the path of the reflected beam were added in order to visualize the optical anisotropy of the monolayer. This modification made it possible to show both the s-polarized and the p-polarized components of the reflected light. Consequently, it is possible to adjust the polarization of the incident light when the angle of the analyzer is fixed, and vice versa. In this way, the contrast of the images can be better resolved and the presence of two different phases can be observed due to the different reflected intensity (Paolo, 2007).

2.4.2 Experimental method

The BAM and Langmuir trough (Nima Technology, Coventry England) were mounted on an anti-vibration table and inside a steel cabinet to avoid contamination, air drafts and diffusion of the laser beam. The Langmuir trough was cleaned according to the procedure described in section 2.2.1. A volume of 120 mL of Milli-Q water was carefully poured into the lower component of the trough with the barrier fully open. The sample solution (20~50 μL) was placed drop-wise and evenly onto the water surface using a 100 μL gas-tight Hamilton syringe (Sigma-Aldrich). A typical period of 20 minutes lapsed in order to allow the evaporation of solvent at the interface. After 2 hours of equilibrium, the barrier was compressed at a rate of 5 mm/min. The surface pressure readings were zeroed before the compression. All the images were taken when the surface pressure is less than 5 mN/m to ensure the formation of monolayer. The BAM was oriented to the critical angle (53.15^o) of the air-water interface. For the 10x objective, a laser power of 50 % and maximum gain were used. All the experiments were performed at room temperature.

2.5 Fourier transform infrared spectroscopy

Fourier transform infrared spectroscopy (FTIR) is an excellent tool for primarily and qualitatively characterization of a wide variety of materials. When infrared radiation is passed through a sample, some of the infrared radiation is absorbed by the sample while some is transmitted. The absorbed infrared radiation can excites molecules of the sample into a higher vibration state. The energy difference between the excited vibration and resting molecules is a function of the absorbed radiation wavelength. The resulting spectrum represents a molecular “fingerprint” of the sample, which is unique to the molecular structure.

2.5.1 Experimental setup

A standard FTIR spectrometer contains an interferometer, which modulates each wavelength of infrared radiation at a different frequency. Most interferometers employ a beam splitter which divides the incoming infrared beam into two optical beams. One beam is reflected off a fixed mirror while the other is reflected off a moving mirror (Figure 2.11). These two beams are recombined and exit the interferometer when they meet again at the beam splitter. Since the path that one beam travels is of a fixed length and the other is constantly changing as the mirror moves, the exiting signal, also called interferogram, is the result of two “interfering” beams. This signal is then converted by Fourier transformation into an infrared spectrum. The spectral features of the sample can be obtained by subtracting the sample spectrum with the background spectrum.

2.5.2 Experimental method

In order to eliminate the background characteristics of the spectrometer, a spectrum without a sample in place must be obtained. The spectrum of the sample is then obtained against the spectrum of the background so that the resulting spectrum is solely due to the sample. Standard spectra of samples must be evaluated and installed in the computer system before measurement. In this work, the spectra of the sample were obtained using an FTIR spectroscope (Thermo-Nicolet 8700) together with a variable path length KBr liquid cell (Thermo Instrument Inc.). Prior to use, the KBr liquid cell must be rinsed with methylene chloride several times, dried with a glass syringe and then rinsed with the sample. The sample is then introduced into the cell by using a syringe. The sample port is then plugged and the cell is placed in a sample holder. The resulting interferogram is then processed to generate the spectrum. All the experiments are performed at room temperatures.

In this study, the intensity of characteristic absorbance at corresponding bond vibration was obtained. A quantative relationship between the concentration of the sample and the intensity of characteristic absorbance can be evaluated by comparing with that of standard sample.

2.6 Karl Fisher Titration

This test method covers the determination of water in the range from 0 to 10 % in crude oils. Unisol, a mixture of toluene (optimal grade) and isopropyl alcohol (IPA) at a volume ratio of 70/30, was used to disperse the water evenly in the emulsion. The corresponding principles and procedure largely followed standard ASTM D4377.

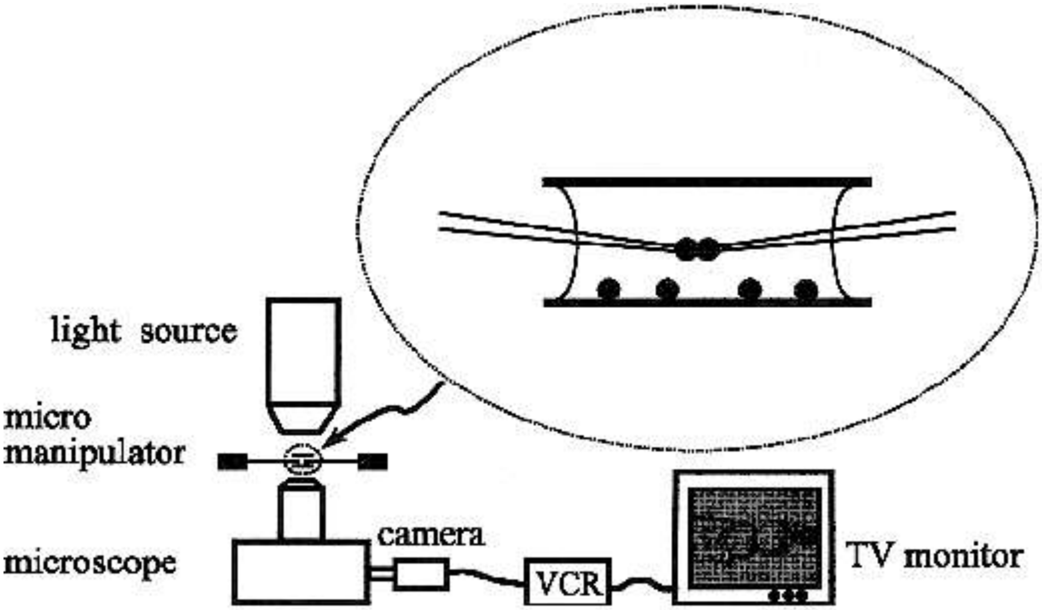

Figure 2.1. A schematic view of micropipette setup (Yeung, 2000).

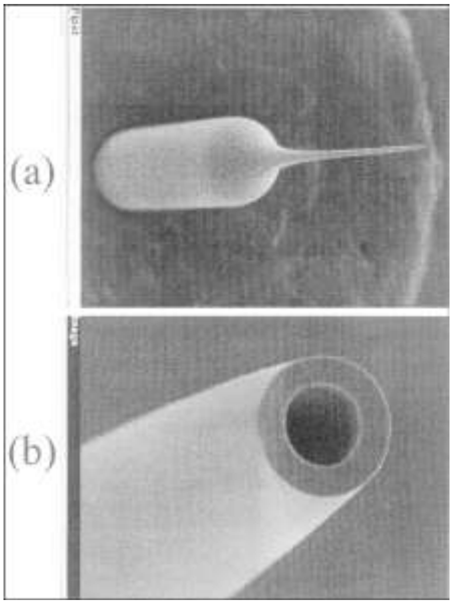

Figure 2.2. Scanning of electron micrographs of a micropipette (Yeung, 2000)

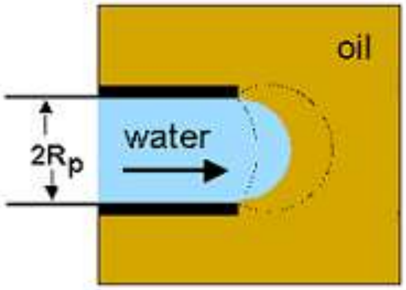

$$\Delta P = \frac{2\gamma}{R_P}$$

Figure 2.3. Maximum bubble pressure method

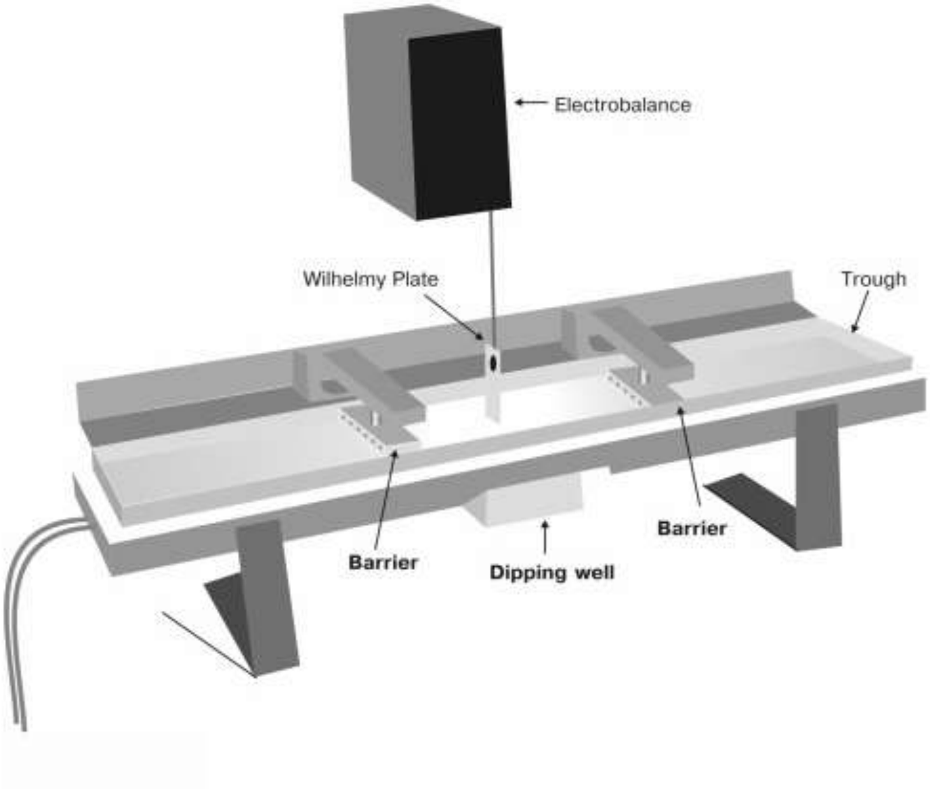

Figure 2.4. Schematic view of the Langmuir trough setup (Zhang, 2007)

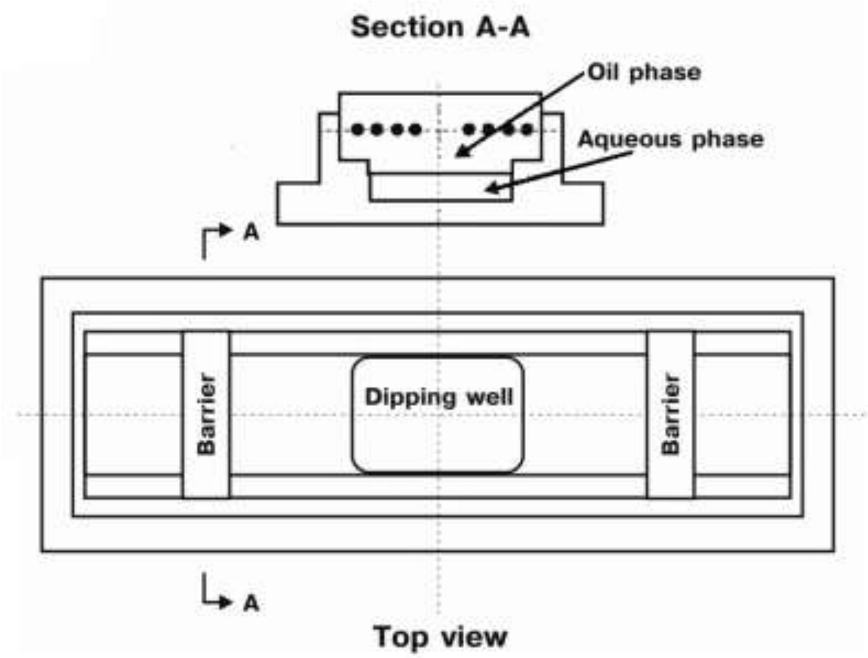

Figure 2.5. Top view of Langmuir trough setup (Zhang, 2007)

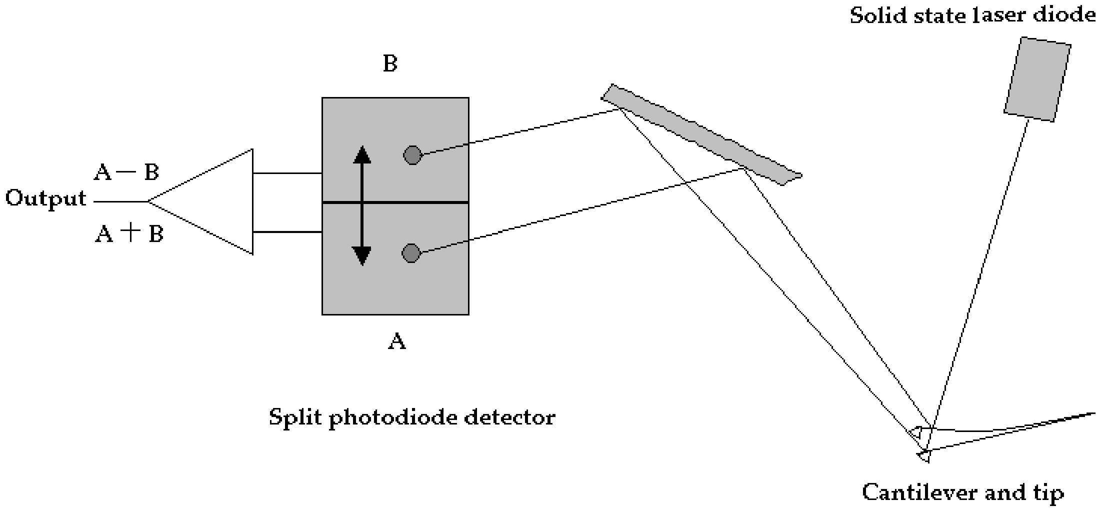

Figure 2.6. Optical system of cantilever deflection

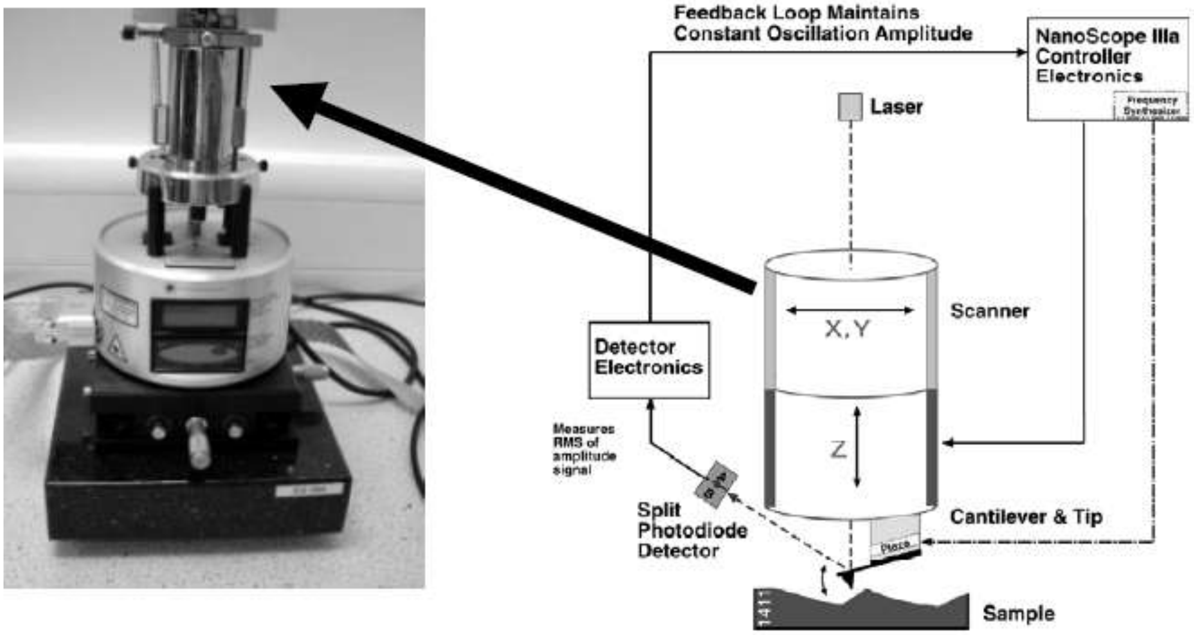

Figure 2.7. (a). Atomic force microscope
(b). tapping mode setup (Sophie, 2007)

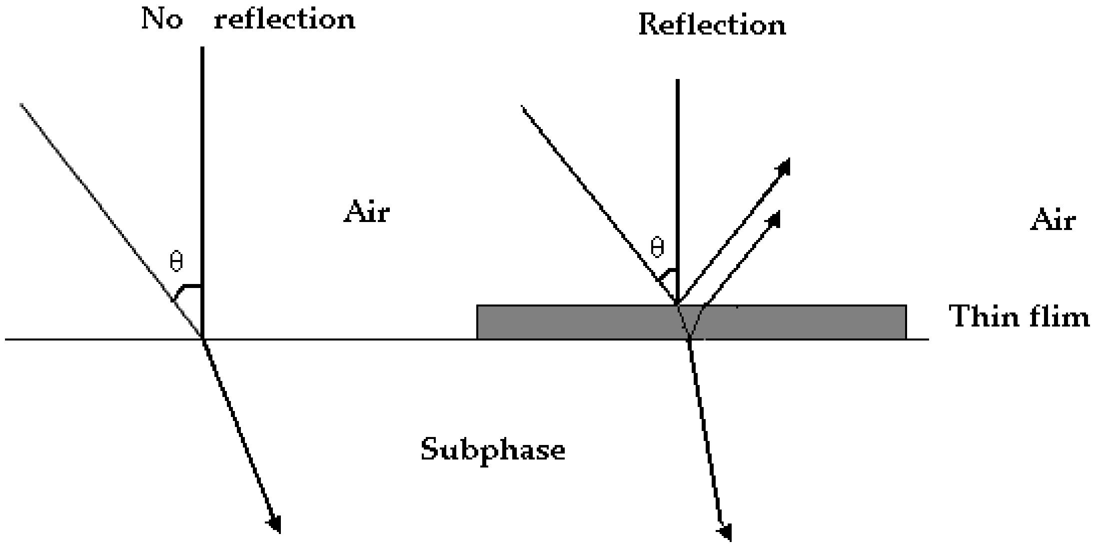

Figure 2.8. Schematic representation of Brewster angle at the air-water interface (left) and with a thin film in between the air-water phase (right).

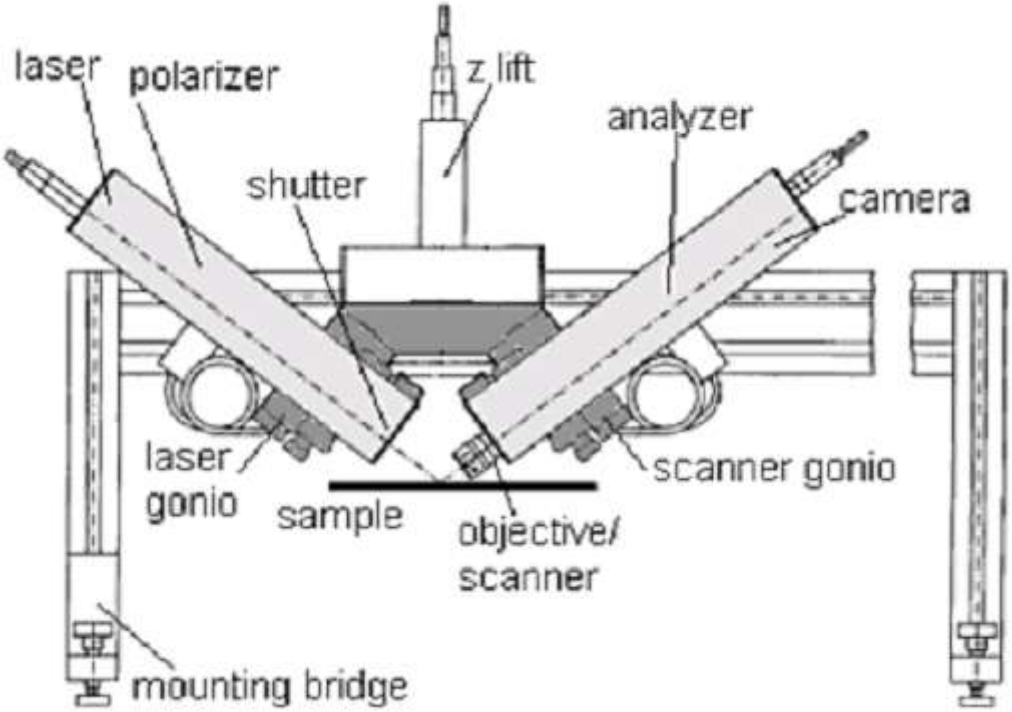

Figure 2.9. Schematic view of a standard Brewster angle microscope
(Taken from the Nanofilm website)

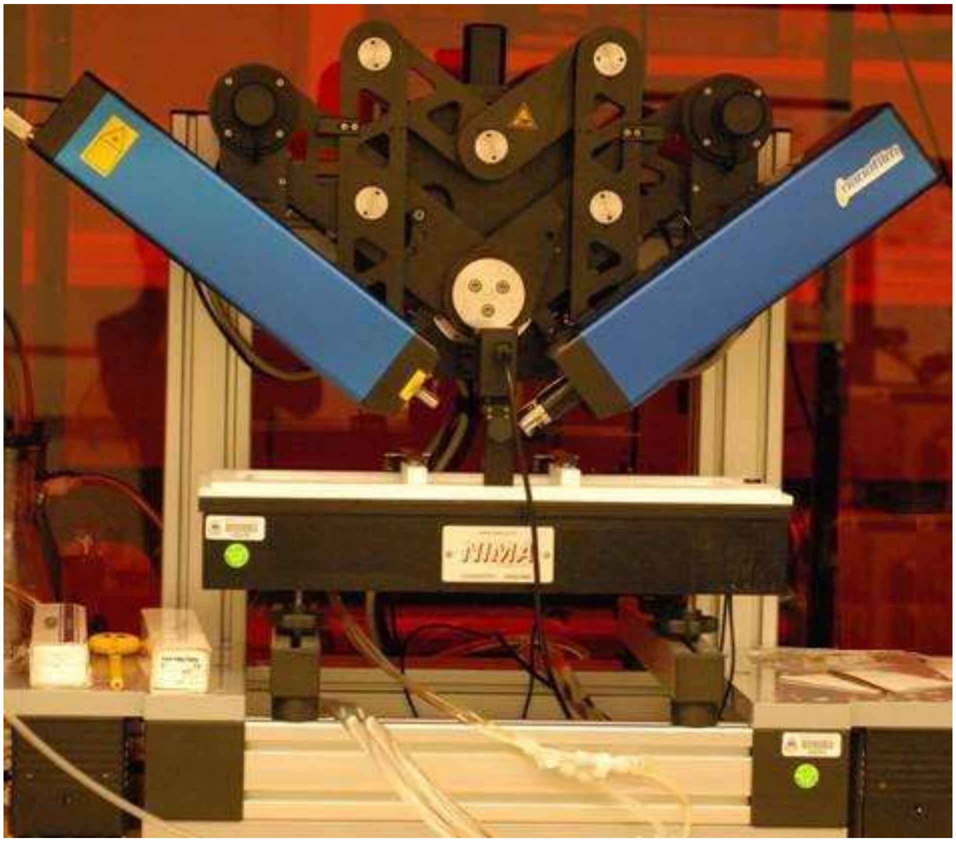

Figure 2.10. Brewster angle microscope with Langmuir trough

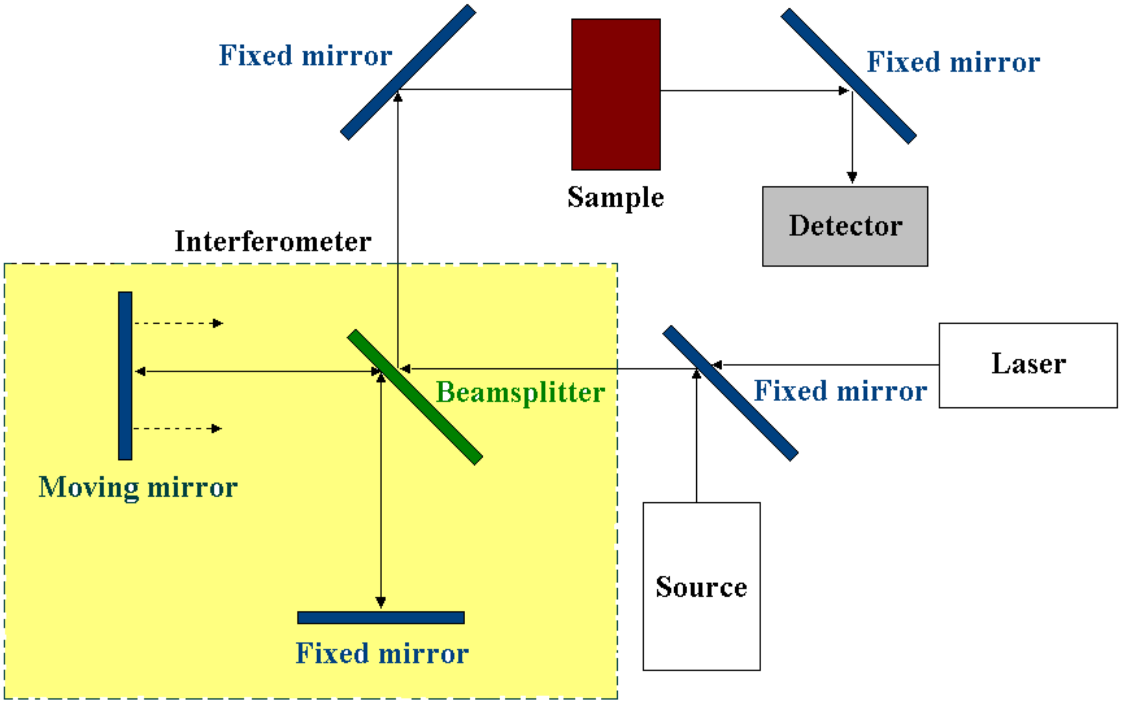

Figure 2.11. Schematic representation of Fourier transform infrared spectrophotometer

Chapter 3

Roles of Bitumen Components in Stabilizing Water-in-Diluted Model Oil Emulsion [*]

3.1 Introductions

In water based bitumen extraction processes, the bitumen froth collected from primary gravity settling vessels, flotation cells and hydrocyclones will be treated to remove the water and solids. However, there is still water remaining after this froth treatment, in the form of emulsified water droplets of diameters around 5 μm or less, in the diluted bitumen (Figure 3.1). These emulsified water droplets carry chlorides that can lead to corrosion problem and catalyst deactivation for downstream upgrading operations (Shaw et al., 1996). Moreover, the presence of fine solids in the bitumen can cause equipment fouling and reactor plugging. Therefore, dewatering via emulsion destabilization is of great concern to the oil sands industry.

Two major mechanisms can describe the stability of water-in-crude oil emulsions (Wasan and Nikolov, 1993; Kumar et al., 2001): Steric stabilization due to an adsorbed layer of asphaltenic molecules, and structural stabilization due to long-range colloidal structure formation inside the film in the presence of a sufficient volume fraction of colloidal particles.

---

[*] Published paper, Gao, S., Moran, K., Xu, Z., Masliyah, J. H., 2009, Energy & Fuels 23, 2606-2612.

Bitumen is composed of various surface active compounds including asphaltenes, resins, saturates, aromatics and suspended fine solids. It is well accepted that the remarkable stability of water-in-oil emulsions is steric in origin. The adsorption of indigenous natural materials forms a steric interfacial layer of non-uniform thickness (Wu et al., 1999) to prevent the coalescence of water droplets. It has been suggested that fine solids and asphaltenes are the main stabilizer of these emulsions (Menon and Wasan, 1986; Yan et al., 1999; Gu et al., 2003; Jiang et al., 2007). A pair of solid surface separated by a thin film of model oil was used to simulate the droplet interactions of water-in-oil emulsions (Claesson et al., 2001). Recent studies have shown that the presence of naturally occurring surfactants can facilitate flocculation of emulsified water droplets but prevent their coalescence (Czarnecki and Moran, 2005, 2007). Asphaltenes are soluble in light aromatic hydrocarbons (i.e., toluene or benzene) but insoluble in paraffinic solvents (i.e., heptane, pentane, or hexane). Asphaltenes may contribute to the emulsion stability through the formation of viscoelastic interfacial films as they are readily adsorbed on water droplet surfaces and can develop into cross-linked three dimensional networks (Kilpatrick and Spiecker, 2001, 2004). The stabilization of emulsions by asphaltenes is strongly mediated by their interfacial activity, aggregation state and partitioning at the water-oil interface. Solids stabilize the emulsion through steric interactions or possibly via depletion mechanisms (Hunter, 1986; Sztukowski and Yarranton, 2004, 2005; Moran, 2007). Resins, which are soluble in most light alkanes (i.e., heptane, petane or hexane) but insoluble in liquid propane, are reported as the dispersants of asphaltenes in crude oil (Gafonova and Yarranton, 2001; León et al., 2002).

To destabilize/dewater the emulsions in diluted bitumen, coalescence (Heimentz and Rajagopalan, 1997) between two emulsified water droplets is of great importance. As two droplets approach each other, direct contact of the droplet surfaces can be realized when the applied external force is greater than the net repulsive colloidal forces (Hunter, 1986). The surfaces within the contact region deform to a planar interface as a precursor to bridging and coalescence. However, a highly viscoelastic film, composed of adsorbed surface active materials responsible for emulsion stability, inhibits droplets deformation by, in part, restricting transport of adsorbates. For this reason, a number of studies have focused on the surface rheology of the emulsion droplets to better understand the stability mechanism.

An early study showed the formation of rigid/elastic interfacial skins of the complex interfacial rheology on emulsified water droplets (Bartell and Neiderhauser, 1949). The stability of water-in-diluted bitumen emulsions is believed to originate from, at least in part, the existence of a steric barrier due to the adsorption of asphaltene-like materials on the emulsified water droplets. Asphaltenes are adsorbed slowly and irreversibly on the interfaces to form rigid/elastic films which resist the compression and deformation of the interface (Freer and Radke, 2004; Czarnecki and Moran, 2005). It was recognized that the thickness of 2-10nm asphaltene interfacial films (Taylor et al., 2002; Sztukowski et al., 2003) is too small to provide a steric barrier. A viscous, cross-linked network of asphaltenes has been proposed to explain the formation of rigid/elastic films (Kilpatrick and Spiecker, 2001). The effects of the interfacial film thickness and bending rigidity on the stabilization of water droplets were not considered in this study. Efforts have been made to characterize the compressibility and elasticity of this interfacial film using Langmuir film balance techniques (Ese et al., 1998; Zhang et al., 2003, 2005), shear viscometric measurements (2004; Eley et al., 1987; Mohammed et al., 1993; Acevedo et al., 1993; Li et al., 2002; Spiecker and Kilpatrick), oscillating drop tensiometer (Bauget et al., 2001; Aske et al., 2002; Freer et al., 2003; Freer and Radke, 2004; Bouriat et al., 2004; Dicharry et al., 2006; Yarranton et al., 2007), and small angle neutron scattering (SANS) technique (Jestin et al., 2007).

The surface properties and behaviors of the emulsified water droplets in diluted bitumen were studied under different conditions at near colloidal scale (Kloet et al., 2001; Moran et al., 2006; Czarnecki and Moran, 2005, 2007; Yarranton et al., 2007). Due to experimental limitations, these techniques have not been applied to study emulsion systems of high bitumen concentrations, which more closely simulate conditions encountered in the industrial practices. The purpose of this work is to understand the rheological behavior of water droplets emulsified in oils/solvents containing different bitumen components (asphaltenes and maltenes) and in diluted bitumen of a concentration range from 10^{-6}wt% to 50wt%. The interfacial tension isotherms are determined to understand adsorption processes of surface active materials at oil-water interfaces. Volume contraction experiments, in which the bulk fluid of a water droplet is aspirated into a micropipette, are used to quantify surface rigidity. In addition, the probability of droplet coalescence is determined to statistically quantify droplet coalescence.

With the use of the existing experimental set-up, the measurements in highly concentrated bitumen solutions were extremely challenging if not impossible due to the opaque nature of the fluids. To address this challenge, an air bubble was carefully produced at the tip of the micropipette and placed within the sample cell to reduce the amount of light absorbed by emulsions. The filter and condenser of the microscope were adjusted to allow the maximum intensity of the transmitted mercury light. By this approach, the image of water droplets in the highly concentrated bitumen solution can be clearly captured as shown in Figure 3.2.

3.2 Materials and Methods

3.2.1 Materials

“Atmospheric-topped” bitumen supplied by Syncrude Canada Ltd. was used in this study. Filtered and deionized water was produced from a Millipore Milli-Q water system equipped with a 0.22μm filter. All the solvents were HPLC grade products purchased from Fisher Scientific.

Asphaltenes and maltenes were separated by adding toluene and n-pentane, at a volume ratio of 1:40, to the bitumen sample. Initially, 1 g of bitumen was completely dissolved in 1 mL of toluene, and then 40 mL of n-pentane was added to the mixture to precipitate the asphaltenes. The precipitated asphaltenes were filtered, repeatedly washed with n-pentane until the effluent was colorless, and finally dried as a powder product for further use. The pentane soluble fraction of bitumen, known as maltenes, consists of saturates, aromatics and resins. The residue toluene in maltenes was removed with a Laborota 4002 rotary evaporator. Quantitative analysis of the same bitumen was completed using Syncrude Analytical Method 5.1 (Bulmer and Starr, 1979). Results indicate that the bitumen used in the present work contains ~20% asphaltenes.

3.2.2 Emulsion preparation

Heptol, a mixture of n-heptane and toluene at a volume ratio of 4:1, was used as a model solvent to form the continuous oil phase. In this study either bitumen, asphaltenes or maltenes was dissolved in the oil phase at concentrations ranging from 10^{-6}wt% to 50wt%. For the convenience of comparison and discussion, the amount of asphaltenes and maltenes were added to reflect their equivalent concentrations as found in whole bitumen and expressed as bitumen equivalent concentration. For example, 10 wt% of bitumen is equivalent for 2 wt% of asphaltenes and 8 wt% of maltenes. All the solvents used in this study were pre-saturated with water in a closed container for 24hr to avoid any dissolution of water in the oil phase during the tests. In preparation of the emulsions, 100μL of aqueous (filtered and deionized water) phase was introduced into 10mL of the continuous oil phase. The emulsion was formed by agitating the mixture in a water-bath sonicator (Fisher Scientific, model No. F56) at ~60^{o}C for 7~10 seconds. The diameter of water droplets created by this method ranges from 5 to 30μm. All the emulsions were aged for 10~20 minutes to allow the water droplets to settle to the bottom of the holding dish before measurements.

3.2.3 Experimental setup and methods

The combination of Brewster angle microscope and Langmuir trough provides a non-invasive method to characterize the monolayer of bitumen, asphaltenens and maltenes at the air-water interface. In order to make the results comparable, the volumes and concentrations of bitumen, asphaltenes and maltenes solution spread at the air-water interface were adjusted to ensure the same surface coverage (Table 3.1). The micropipette technique was performed to measure the *in-situ* interfacial properties of different emulsions. Detailed description of the experimental setup and methods can be found in chapter 2 (Section 2.1 and 2.4).

Table 3.1 Volume and concentration of spreading samples for the BAM images

Solution	Volume	Concentration
Bitumen-in-toluene	20 μL	2 mg/mL
Asphaltenes-in- toluene	50 μL	1 mg/mL
Maltenes-in- toluene	35 μL	2 mg/mL

3.3 Results and Discussion

Emulsions were created in three different oils to measure interfacial tensions, crumpling ratios and the probability of droplets coalescence. An equivalent concentration of original bitumen in the oil phase was used to make the results comparable.

3.3.1 Brewster angle microscopy

The monolayer of bitumen, asphaltenes and maltenes are formed at the air-water interface with a compression rate of 5 mm/min. The BAM images (Figures 3.3, 3.4, 3.5) were obtained at surface pressure less than 5 mN/m. The monolayer of asphaltenes in Figure 3.4 was rigid and tended to repel and deform under further compression, while that of the maltenes in Figure 3.5 is very spongy and fluid. However, the monolayer of bitumen in Figure 3.3 appears as a uniform net, which is softer than aphaltenes but more rigid than maltenes.

3.3.2 Interfacial tension isotherms

The interfacial tensions of water droplet in three different oils were evaluated over a wide range of concentrations by the maximum bubble pressure method. The pressure was recorded via a pressure transducer. Calibration was performed for the pressure transducer to convert the signal to a pressure in dyne/cm^2. A liner relationship was observed between the applied voltage and the measured pressure

(Figure 3.6). The interfacial tension was then calculated from the Young-Laplace equation.

$$\Delta P = \frac{2\gamma}{R_P} \qquad (3.1)$$

where ΔP is the gauge pressure measured by the pressure transducer and R_P is the radius of the water droplet when a hemispherical interfacial geometry was formed at the micropipette tip. In these measurements, a water droplet was aged in oil solutions at the micropipette tip for 3 minutes to enable the system to come to an equilibrium state. The effects of bitumen component concentration in the continuous oil phase on the interfacial tension were evaluated over a concentration range from 10^{-6}wt% up to 50wt%. Data points in Figure 3.7 represent the average measurement using 20 or more water droplets with the standard deviation shown as the error bars.

It is clear that the interfacial tension of the water droplets in the studied oil phase decreases with increasing concentrations of bitumen in continuous oil phase. The decrease of interfacial tension is attributed to the adsorption of surface active material at water-oil interface. The results in Figure 3.7 show a gradual, continuous decrease in the interfacial tension with increasing concentration of bitumen up to 0.001 wt%, suggesting a continuous increase in the adsorption of surface active materials on water droplet surfaces. At the concentrations higher than 0.001 wt%, the interfacial tension decreases almost linearly (at a semilog scale) with increasing concentration of bitumen in continuous oil phase. At concentrations higher than 10wt%, the interfacial tension appears to level off, indicating that the droplet surfaces may be saturated with the surface active materials in bitumen.

The influence of bitumen components on the interfacial tension was examined by plotting the results at equivalent bitumen content, i.e., asphaltenes and maltenes in the continuous oil phase. For a bitumen concentration in the heptol-bitumen mixture of X wt%, the concentrations of pure asphaltenes and pure maltenes will be $0.2 \times X$ wt% and $0.8 \times X$ wt%, respectively. It is evident that maltenes also contain surface active molecules. At the same equivalent bitumen concentration, the interfacial tension of water droplet in diluted model oil decreases in the order of asphaltenes > bitumen > maltenes. This order is extremely interesting as the bitumen contains both asphaltenes and maltenes at a given equivalent bitumen concentration and should have exhibited the highest reduction of interfacial tension with increasing bitumen concentration.

Previous studies (Freer and Radke, 2004; Czarnecki and Moran, 2005) showed that most of the surface active asphaltenic molecules were irreversibly adsorbed at the oil/water interface. In the present study, it appears that more surfactants are adsorbed at the droplet surface in maltenes system than in asphaltenes system at an equivalent bitumen concentration, as shown by the lower interfacial tension. In the bitumen system, with the presence of both apshaltenes and maltenes, the interfacial tension isotherm was higher than maltenes system but lower than asphaltenes system. This may be due to the complex nature of the competitive adsorption among the asphaltenes and maltenes. Alternatively, the presence of asphaltenes in heptol may have tied up some surface active molecules in the maltenes in the model oil to make them less available at the oil-water interface.

To understand the surface active nature of the oil systems, one can approximate the continuous oil phase as an ideal single-component surfactant solution. The Gibbs adsorption principles can be used to evaluate the coverage (Γ, number of adsorbed molecules per unit area) of surface active components at the interface,

$$-d\gamma = kT\,\Gamma d\ln C \qquad (3.1)$$

where γ is the interfacial tension at the oil/water interface, k is the Boltzmann constant ($k = R / N_A$, where R is the universal gas constant and N_A is Avogadro's number), T is the temperature, and C is the concentration of the adsorbates. The "effective" surface coverage (Γ) of an "average" surface active species can be evaluated from equation (3.1), which lumps a complex molecular mixture into an equivalent single type of molecules of the same average molar mass. As per equation 3.1, the slope of the linear regime (Figure 3.7) reflects the effective surface coverage of the adsorbates: the smaller it is, the bigger the effective surface coverage of surfactants is and the more active the adsorbates are. The effective molecular cross section (the area per "site") is given by the reciprocal of Γ. Therefore, it can be concluded from Figure 3.7 that the effective molecular cross section of asphaltenes is only slightly larger than that of maltenes. Table 3.2 shows the estimation of effective average area occupied by each adsorbed surface active molecule in asphaltenes and maltenes systems. Based on the size characterization, the effective cross section of asphaltene molecules is believed to be larger than that of maltenes (Hall and Herron, 1979). The calculated results suggest a complex surface organization that may be due to a wide size distribution of maltenes. The difference between the present result (with an average value of 2.92nm^2) and previous estimations of 1.35nm^2 (Moran and Czarnecki, 2007) and 0.74nm^2 (Yeung et al., 1999) is possibly due to the compositions of crude oil used, water chemistry and properties of solvent. Moreover, the molecular cross section obtained here for asphaltenes agrees well with other research. The literature value of the molecular cross section of single asphaltene molecule is 2.53~5nm^2 (Bhardwaj and Hartland, 1994; Yarranton et al., 2000).

Table. 3.2 Molecular cross section estimated using Gibbs adsorption equation

Surfactants	Asphaltenes	Maltenes
Molecular cross section (nm^2)	3.12 ± 0.6	2.72 ± 0.4

3.3.3 Quantitative characterization of "skin formation"

The stability of water-in-crude oil emulsions has been largely attributed to the skin formation at the interface (also called steric layer). The existence of this steric layer is visualized using micropipette volume contraction experiments (Figure 3.8) (Shaw et al., 1996; Yeung et al., 1999, 2000; Tsamantakis et al., 2005; Moran and Czarnecki, 2007).

In micropipette volume contraction experiments, the surface area of the water droplet which was saturated with surfactants after sufficient aging time was gradually compressed by applying suction pressure. The surface active asphaltenic molecules irreversibly adsorbed at the interface were slowly drawn together as the surface area of droplet was reduced. The incompressible nature of these irreversibly adsorbed molecules results in out-of-plane deflections characterized by visible crumpling behaviors. This irreversible behavior can be observed by dynamically tracking the tension at an interface (Czarnecki and Moran, 2005). Langmuir trough studies and axisymmetric drop shape analysis (ADSA) of asphaltenes at the toluene/water interface provided further evidence for the irreversible adsorption of asphaltenes (Zhang et al., 2005).

To quantify the skin formation, a crumpling ratio (*CR)*, was introduced

$$CR = \frac{A_f}{A_i} = \frac{\pi R_f^2}{\pi R_i^2} = \frac{R_f^2}{R_i^2} \qquad (3.2)$$

where A_i is the initial projected area of the water droplet, A_f is the projected area of water droplet right before the point when crumpling was first observed. In Figure 3.8, I represents the initial state of an equilibrated water droplet, II is the status prior to crumpling, and III shows the first visible sign of crumpling. The crumpling ratio of bitumen, asphaltenes and maltenes were measured as a function of bulk concentration of individual components, and the results are shown in Figure 3.9. Each data point in Figure 3.9 is an average of measurements with 35 or more water droplets; the error bars represent the standard deviation of all measurements. For both bitumen and asphaltenes, crumpling was not observed at very low bitumen or asphaltene concentrations (less than 10^{-4} wt%) due to very little or no adsorption of surface active molecules. The absence of crumpling was also noted in the model solvent (heptol). At bitumen or asphaltene concentrations between 10^{-4}wt% and 10^{-3}wt%, a sharp increase in crumpling ratio was observed, indicating irreversible accumulation of surface active materials at water-oil interface. At higher bitumen and asphaltene concentrations, the interface responds differently to further increase in bitumen and asphaltene concentrations.

In the case of bitumen, the crumpling ratio decreases with further increasing bitumen concentration, indicating the film becomes progressively less rigid. This can be explained by the competitive adsorption of asphaltenes and maltenes in bitumen at interfaces. At higher bitumen concentration, more maltenes will adsorb at the water droplet surface, perhaps due to favorable partitioning, reducing available space for asphaltenes. It is also possible that increasing maltene in oil phase makes asphaltene less surface active. Alternatively, maltenes may be more surface active than asphaltenes due to the favorable solubility of naturally occurring surfactants, such as naphthenic acids (Yang and Czarnecki, 2005). In the case of asphaltenes, the crumpling ratio continues to increase with increasing asphaltene concentration, although at a reduced rate. It is anticipated that increasing asphaltenes concentration in heptol would force more asphaltenes move to the water-oil interface, leading to a more rigid interface and hence higher crumpling ratio, although the impact is less significant as the interface approaches its saturation. This result agrees well with previous studies (Czarnecki and Moran, 2005; Yarranton et al., 2007a, 2007b) on the inference of asphaltenes as the main stabilizer of water-in-crude oil emulsion.

The results of Figure 3.9 agree well with those of Wu (2005), where it was found that at low bitumen concentrations the hydrogen to carbon ratio (H/C) of the surface active material at the water-diluted bitumen interface is consistent with that of asphaltenes. However, at higher bitumen concentrations, the H/C ratio of the surface active material at the water-diluted bitumen interface resembles more like bitumen. No crumpling was observed for the maltenes (Figure 3.10) at any concentration. This behavior may be attributed to the absence of asphaltenic molecules or complex molecular structure on the water droplet surface. It is interesting to note that maltenes are more active in reducing interfacial tensions as shown in Figure 3.7. However, the adsorbed molecules do not associate with each other to form a rigid interfacial film, leading to reversible contraction. Clearly, asphaltenes are mostly responsible for interfacial skin formation, and the presence of maltenes mitigates the formation of asphaltene interfacial skins. This study clearly shows that interfacial tension itself is not a good indicator for emulsion stability or interfacial film properties.

3.3.4 Droplet interaction

While the interfacial tension isotherm and crumpling ratio experiments provide information on the adsorption behavior of surface active materials, they are inadequate to describe the stability of an emulsion. In order to link these measurable parameters with emulsion stability, the visual observation of droplet coalescence becomes extremely valuable. Considered together with characteristics of interfacial tension and interfacial film rigidity, water drop coalescence experiments provide insight into the stabilization mechanism. Two droplets, grabbed at the tip of two micropipettes, coalesce immediately upon contacting each other in the absence of the steric layer as shown in Figure 3.11.

With a steric barrier at their surfaces, the droplets remain intact after removing the applied force pressing them in contact for a sufficient period of time (three minutes in present study) (Figures 3.12 and 3.13). In these experiments, the applied force was sufficient to deform the droplets (Moran, 2007) as visually confirmed. The statistic nature of the droplet coalescence is represented by the probability of coalescence, Φ. In the present study, an average of three sets of interaction experiments for a minimum of 50 water droplet pairs is tried for every data point with the standard deviation shown by the error bars. The results in Figure 3.14 show the same trend in coalescence probability as a function of component bulk concentration for bitumen and asphaltenes. In highly diluted model oils ($<10^{-3}$ wt%), coalescence is often observed due to the absence of irreversibly adsorbed asphaltenic molecules (Figure 3.9), which are believed to be responsible for the formation of steric layer (interfacial skin). A sharp decrease in coalescence probability was observed over a very narrow bitumen or asphaltene concentration around 10^{-3} wt%. At a bitumen concentration above 10^{-2} wt% or asphaltene concentration above 0.1wt%, the probability of coalescence reduced to zero, i.e. no droplet coalescence was observed. This concentration range corresponded well with skin formation at water-oil interface shown in Figure 3.9.

Clearly the presence of a steric layer by the irreversible adsorption of asphaltenic molecules at water-oil interface resists the coalescence of droplets for both the bitumen and asphaltenes system.

For maltenes, the coalescence probability was around unity over a wide range of maltene concentration up to 1 wt%. At higher maltene concentrations, a reduction in coalescence probability was observed, even though skin formation is not observed in volume contraction experiments at the same concentrations. This observation indicates the adsorption of maltenes on water droplet surface might contribute, to some extent, to the emulsion stability, without skin formation, provided that its concentration is sufficiently high. The similarity of water droplet coalescence in Heptol-diluted bitumen or asphaltenes solutionos suggests that asphaltenes are mainly responsible for stabilization of water-in-diluted heptol emulsions, although maltenes may facilitate emulsion formation due to a more significant reduction in interfacial tension. Maltenes itself will not contribute to interfacial rigidity due to the fast equilibrium adsorption.

3.4 Conclusions

Asphaltenes and maltenes are separated from bitumen to investigate the role of bitumen components in stabilization of water-in-crude oil emulsions using micropipette technique. The interfacial properties of the emulsified water droplets in heptol containing bitumen or its components are studied by examining interfacial adsorption behaviors, droplet surface rigidity and coalescence probability. The adsorption of naturally occurring surfactants, contained within both asphaltenes and maltenes, reduces the interfacial tension. The crumpling test of water droplets reveals that surface active components in asphaltenes are the major contributor to the formation of steric layer at the surface of water droplets. This is further supported by the droplet coalescence tests. Water droplets in pure maltenes, without asphaltenes, tend to coalesce quickly. However, water droplets do not coalesce in Heptol containing 0.1wt% or more bitumen or bitumen-equivalent asphaltenes. Certain naturally occurring small surface active species in maltenes contribute to the stabilization of water-in-diluted model oil emulsions without causing observable skin formation. This study clearly shows that interfacial tension alone is not sufficient to describe probability of emulsified water droplets coalescence and hence the stability of water-in-diluted model oil emulsions. Further research is required to identify the species responsible for stabilization of water-in-diluted bitumen emulsions and establish conclusive stabilization mechanisms. The knowledge from micrometer-scale study provides foundation for design of demulsification systems in industrial oil sands extraction processes.

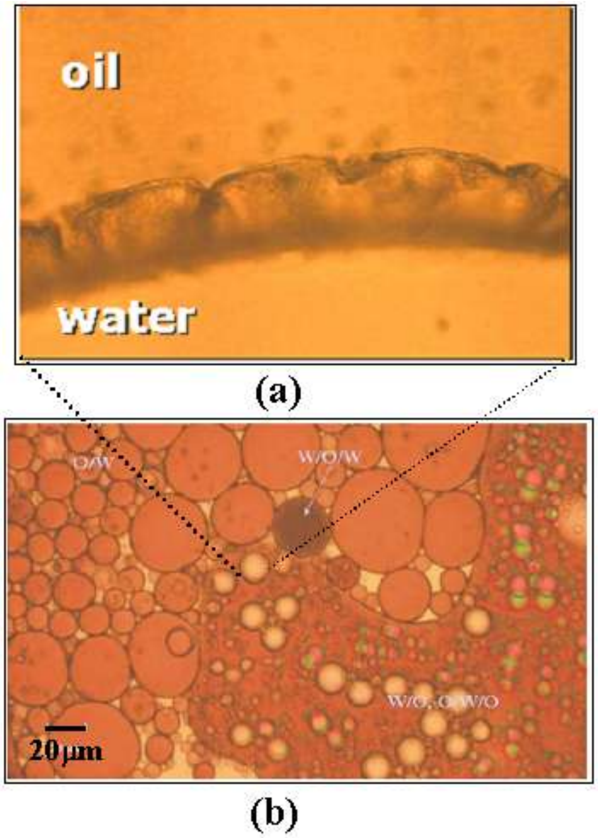

Figure 3.1. Emulsified water droplets in diluted bitumen froth (b) and the interface between water droplet and diluted bitumen (a) (Moran and Czarnecki, 2006).

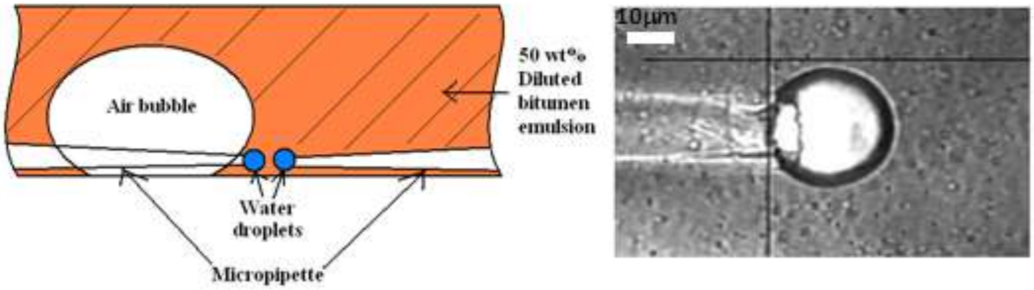

(a) (b)

Figure 3.2. Micropipette view of a water droplet in a 50wt% heptol-diluted bitumen emulsion, (a) schematic side view, (b) in situ view.

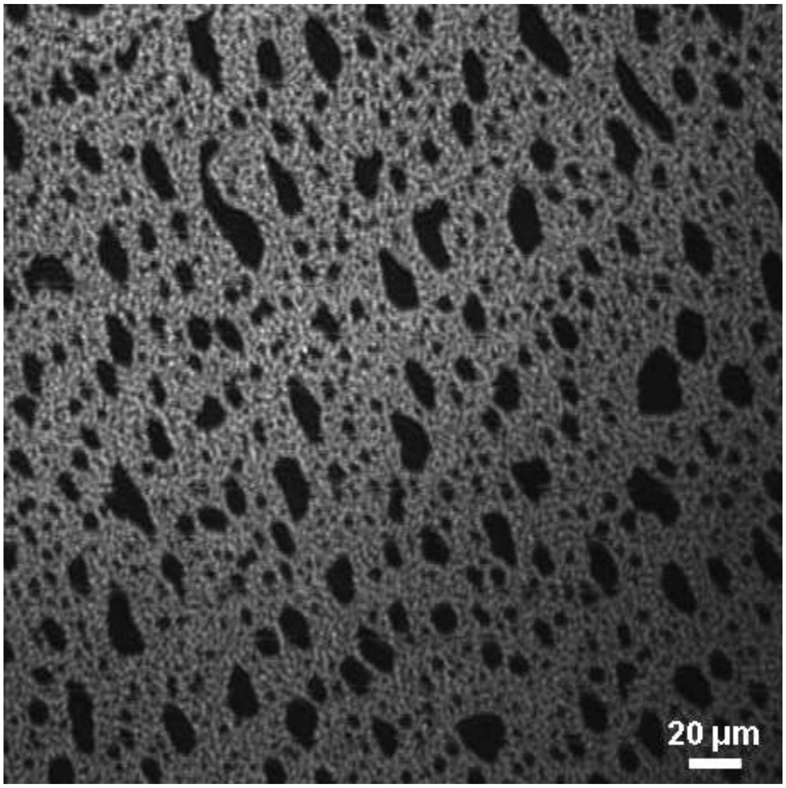

Figure 3.3. Brewster angle microscopy of a bitumen monolayer with a Langmuir trough compression rate of 5 mm/min and surface pressure less than 5 mN/m; dimensions of the image is 250 μm × 250 μm. (Courtesy of Mussone, P)

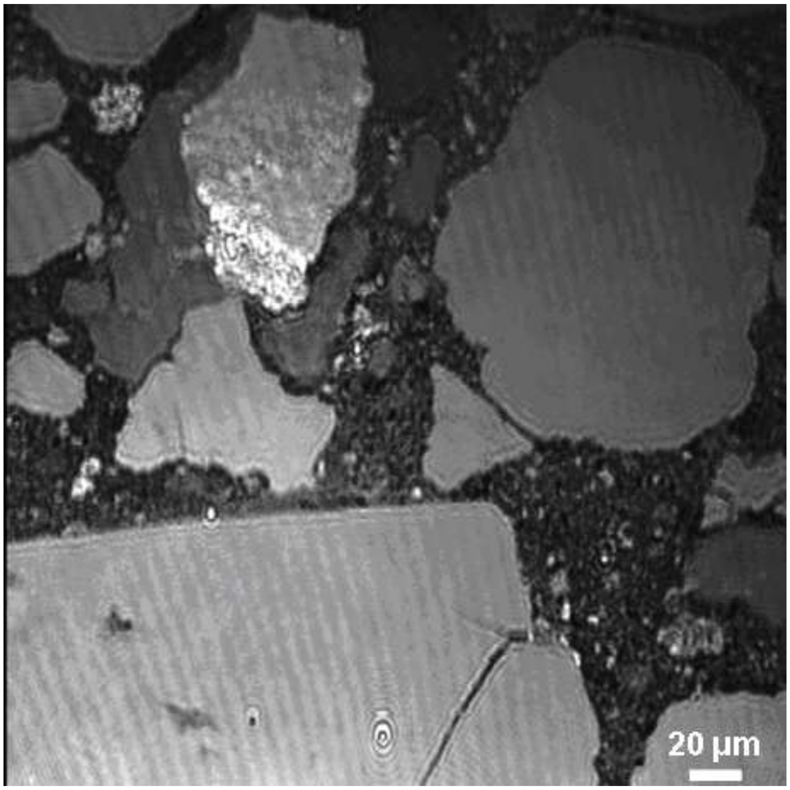

Figure 3.4. Brewster angle microscopy of an asphaltene monolayer with a Langmuir trough compression rate of 5 mm/min and surface pressure less than 5 mN/m; dimensions of the image is 250 µm × 250 µm. (Courtesy of Mussone, P)

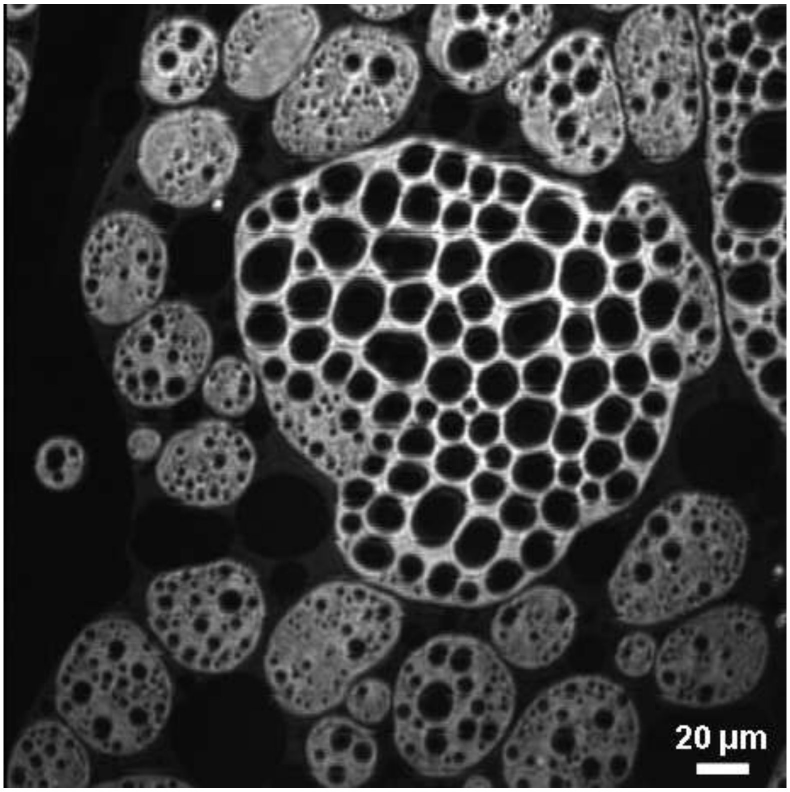

Figure 3.5. Brewster angle microscopy of a maltene monolayer with a Langmuir trough compression rate of 5 mm/min and surface pressure less than 5 mN/m; dimensions of the image is 250 μm × 250 μm.

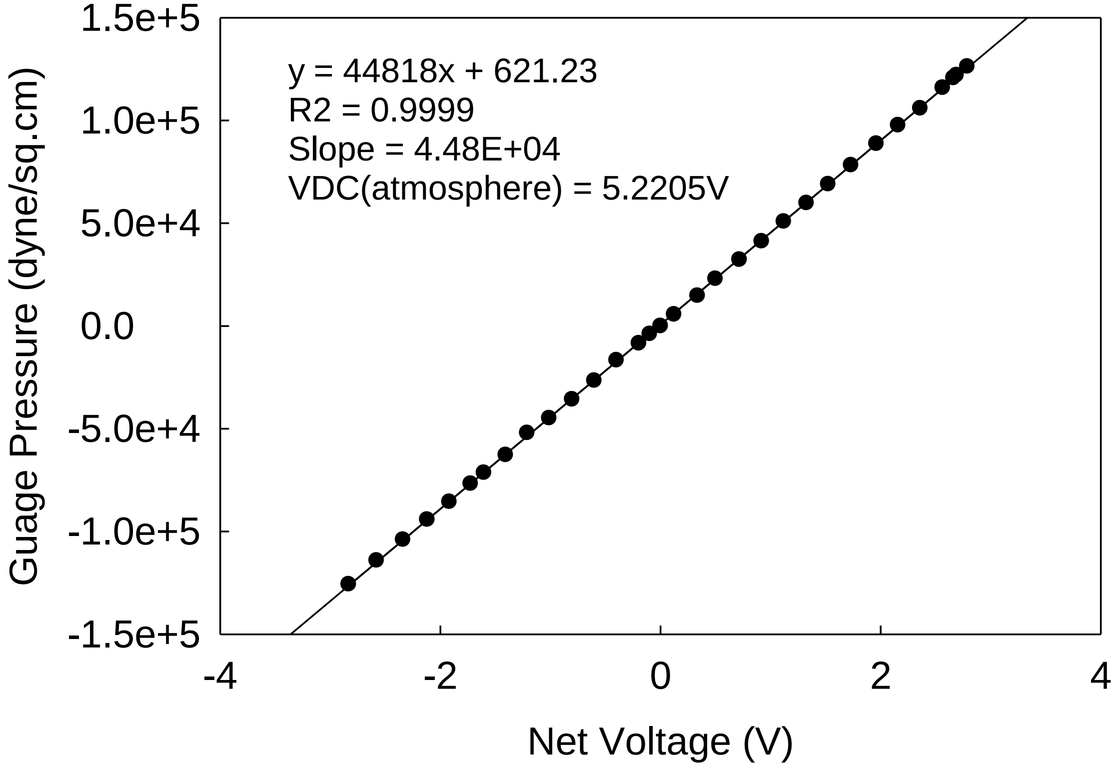

Figure 3.6. Calibration for the pressure transducer, VDC is the reading of pressure transducer at atmosphere pressure.

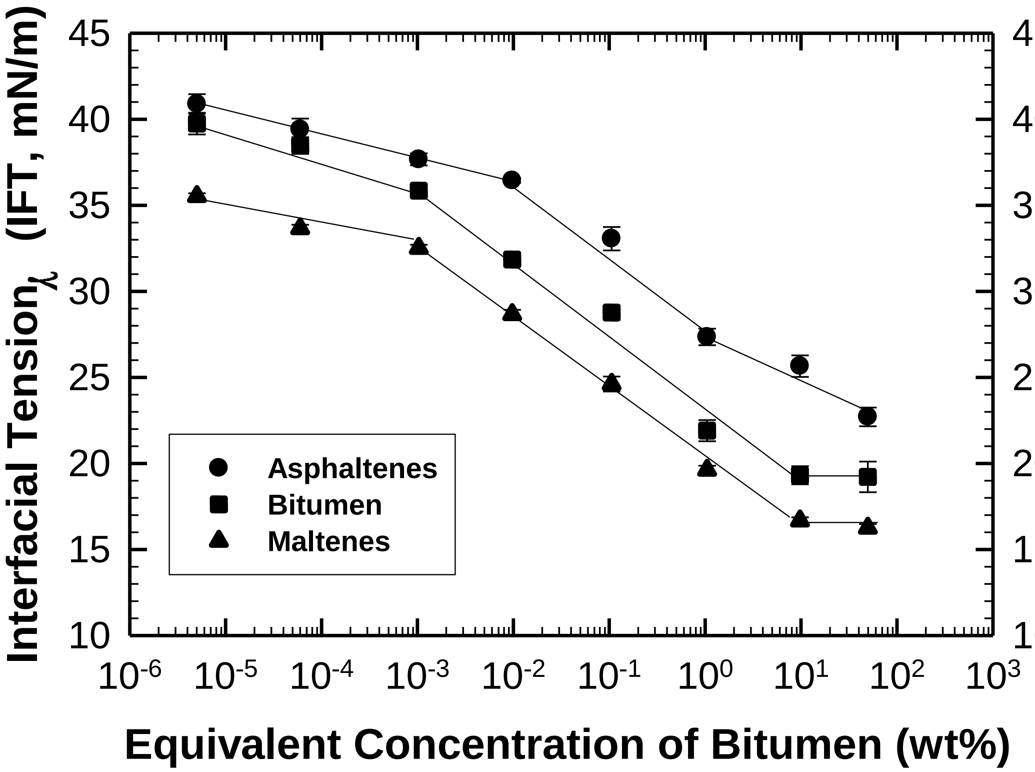

Figure 3.7. Comparison of IFT of three systems at equivalent concentration in bitumen; asphaltenes system (solid circles), bitumen system (solid squares) and maltenes system (solid triangles)

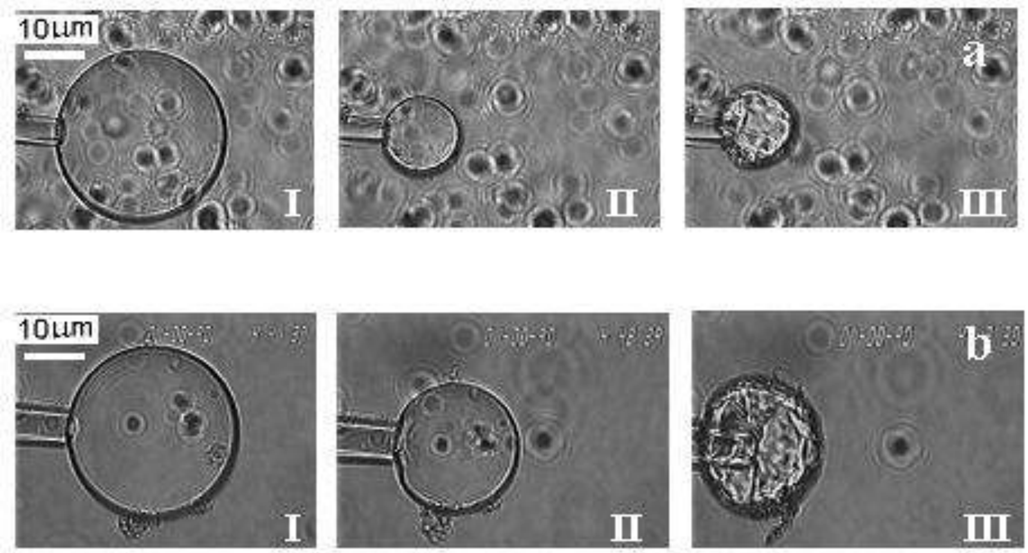

Figure 3.8. Skin formation (steric layer) at water droplet surfaces in(**a**) 0.1 wt% bitumen and (**b**) 0.001 wt% bitumen

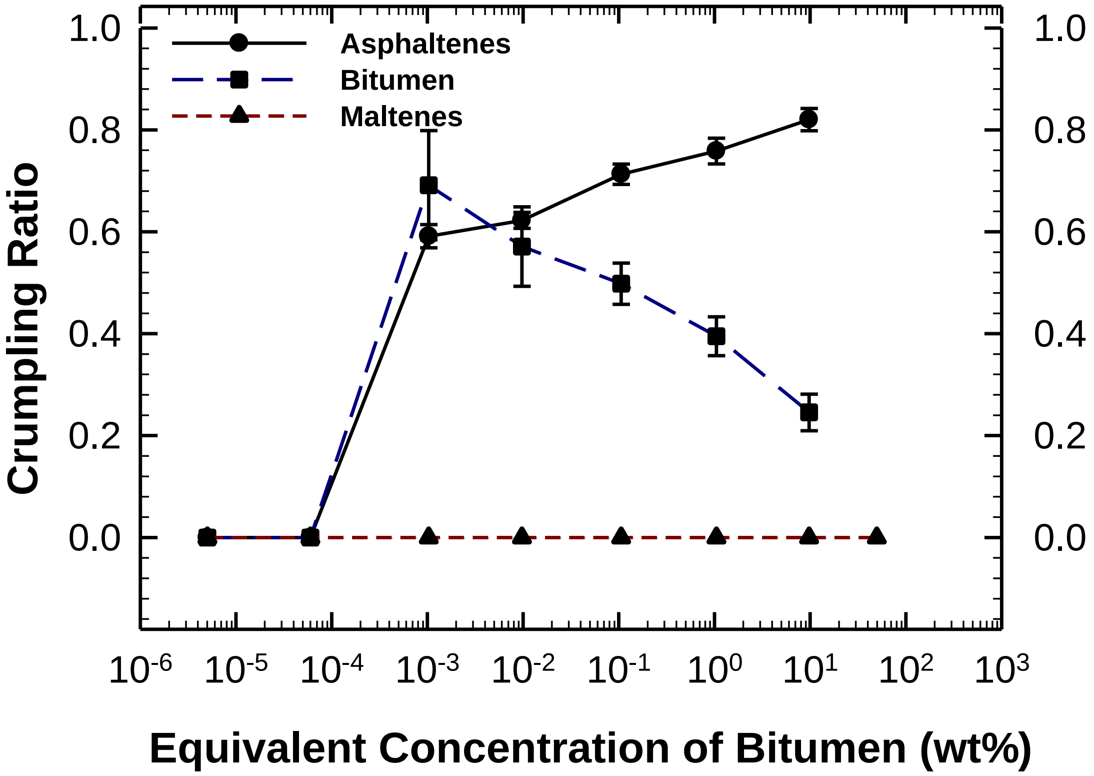

Figure 3.9. Comparison of crumpling ratio at equivalent concentration in bitumen; asphaltenes system (solid circles), bitumen system (solid squares) and maltenes system (solid triangles)

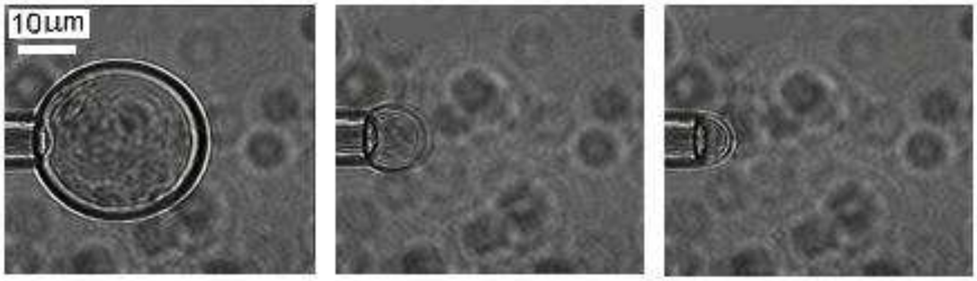

Figure 3.10. No sign of skin formation in 1 wt% maltenes

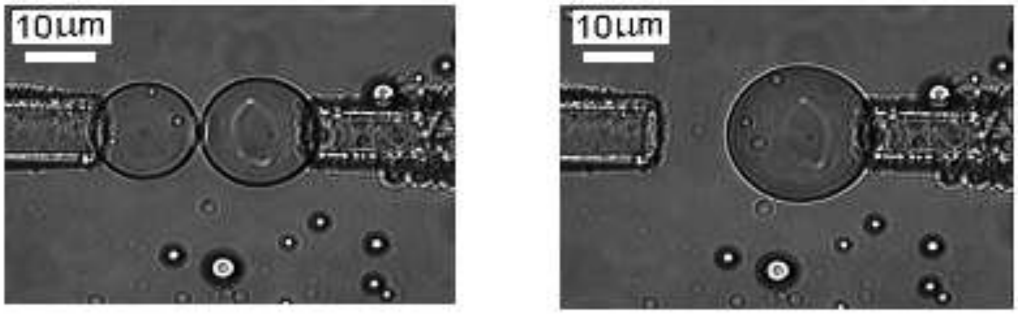

(a) (b)

Figure 3.11. Sequential micrographs of the coalescence of two water droplets in 1 wt% maltenes: (a) brought in contact; and (b) spontaneous coalescence.

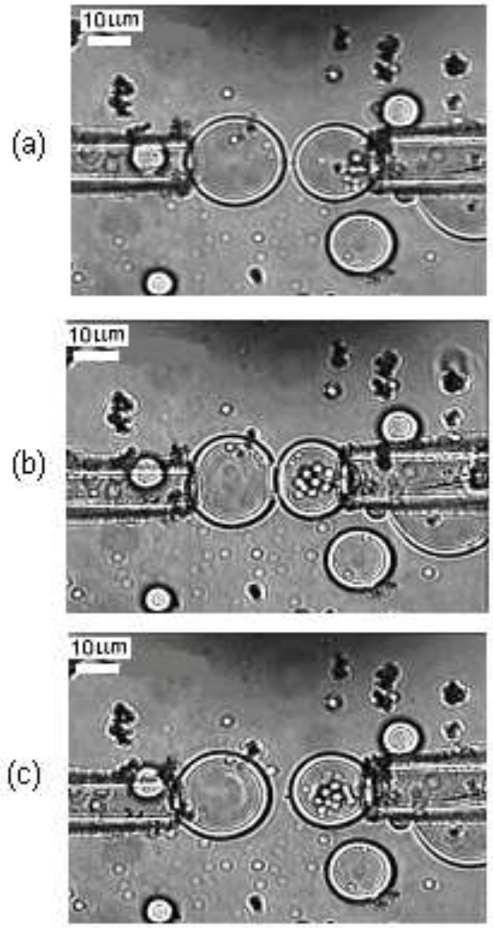

Figure 3.12. Sequential series of micrographs (a-b-c) describing droplet interactions in 0.1wt% bitumen

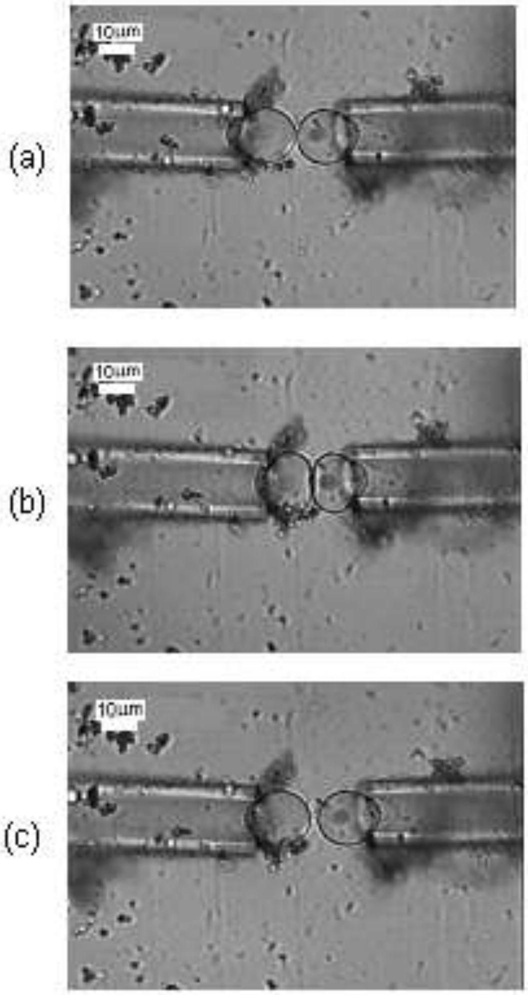

Figure 3.13. Sequential series of micrographs (a-b-c) describing droplet interactions in 1wt% asphaltenes

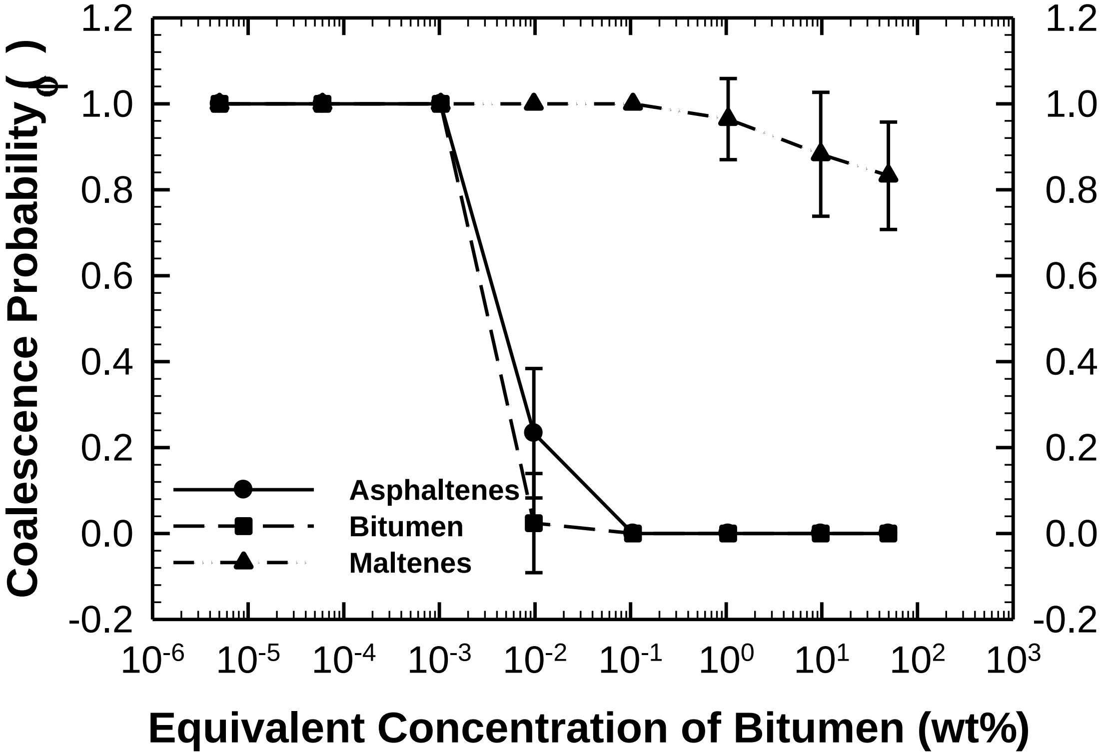

Figure 3.14. Probability of coalescence at equivalent concentration in bitumen; asphaltenes system (solid circles), bitumen system (solid squares) and maltenes system (solid triangles)

Chapter 4

Roles of Naphthenic Acids in Stabilizing Water-in-Diluted Oil Emulsions [*]

4.1 Introduction

Surfactants are prevalent in many stages of the petroleum recovery and processing, including oil well drilling, reservoir injection, oil well production, surface plant processing, pipeline and seagoing transportation of petroleum emulsions (Schramm and Marangoni, 2000). The amphiphilic nature of surfactants can be ascribed to the presence of a hydrophilic head group and a hydrophobic chain in the molecule. The nature of the polar head group provides a basis to categorize different surfactants. At high concentration, a large number of surfactant molecules tend to aggregate in an organized manner, called micelles. In aqueous solutions, micelles are formed by associating the hydrophobic tails in the interior and leaving the hydrophilic heads exposed to the aqueous phase. Figure 4.1 shows the tendencies for the polar part to contact with the aqueous medium, and for the alkyl chains to avoid energetically unfavorable contacts with aqueous phase. At a specific concentration, known as the critical micelle concentration (CMC), the physico-chemical properties of surfactants solutions vary dramatically. It has been demonstrated that the adsorption of surfactants at the

---

[*] Submitted to The Journal of Physical chemistry

liquid interfaces can affect emulsion stability by lowering interfacial tension, increasing surface elasticity and possibly increasing surface viscosity.

Stable water-in-oil emulsions have been a major concern in the oil sands industry because the chlorides carried by the emulsified water droplets can adversely affect downstream bitumen upgrading to sweet crude oil. Extensive research has been carried out to study the role of bitumen components, e.g., asphaltenes, resins and other naturally occurring surfactants on emulsion stability. Asphaltenes, the highest molecular weight components of bitumen, are soluble in light aromatic hydrocarbons (i.e., toluene and benzene) but insoluble in paraffinic solvents (i.e., heptane, pentane and hexane). Asphaltenes are adsorbed slowly and irreversibly at interfaces to form rigid/elastic films which resist the compression and deformation of the interface. The stability of water-in-oil emulsions is believed to originate from a steric asphaltene-rich interface on the emulsified water droplet surface. A fluid interface can be observed in more concentrated bitumen solutions due to the competitive adsorption of asphaltenes and maltenes (i.e., deasphalted bitumen) in bitumen (Gao et al., 2009).

In conventional bitumen extraction, sodium hydroxide is used as a process aid to release (saponify) natural surfactants from the bitumen to the aqueous phase. Previous studies have shown that the surfactants released from the bitumen were mainly carboxylic salts of naphthenic acids along with some sulfonic acids (Bowman, 1967; Baptista and Bowman, 1969; Leja and Bowman, 1968).

Naphthenic acids (NAs) are a complex mixture of cyclic carboxylic acids that may contain aliphatic side chains (Strausz, 1988). The molecular weight of these surfactants ranges from about 166 to 450 g/mol (Schramm et al., 2000). Most of the indigenous naphthenic acids (~90%) in Athabasca bitumen are C_{21}-C_{24} tricyclic terpenoid acids (Cyr and Strausz, 1983, 1984; Strausz, 1989). Under the alkaline conditions (e.g., NaOH) of bitumen extraction, the naphthenic acids can be converted to sodium naphthenates (NaN). It has been reported that these sodium naphthenates mainly remain soluble in the maltenes fraction when precipitating asphaltenes with n-pentane (Yang and Czarnecki, 2005). The presence of sodium naphthenates has been known to "soften" the rigid layer of the emulsified water droplets in water-in-0.1 wt% diluted bitumen emulsions (Moran and Czarnecki, 2007). Concentrated surfactant solutions can form mesomorphic phases, such as liquid crystalline phase (Horvath et al., 2002). The presence of this phase can increase the stability of hydrocarbon emulsions due to its multilayered structure. The liquid crystalline sodium naphthenates have been observed as thick, viscous layers at oil-water interfaces (Pauchard et al., 2009a, 2009b). However, the phase equilibria of sodium naphthenates in sodium naphthenates-toluene-water system suggest that it is difficult to form such liquid crystalline phase at industrial operating conditions (Horvath-Szabo et al., 2001). A detailed investigation on the impact of sodium naphthenates on stability of water-in-diluted bitumen components (i.e., asphaltenes and maltenes) emulsions is not available. Also, the role of the indigenous naphthenic acids in determining emulsion stability remains unclear. These issues will be a primary focus of this chapter.

Bitumen, extracted from Athabasca oil sands, was used to obtain maltenes via the precipitation of asphaltenes. A protocol is established to extract the indigenous naphthenic acids from maltenes. The characters of rigid oil/water interfacial film were measured in a Langmuir trough. Mechanical aspects of diluted model oil emulsions were studied using micropipette technique. The micropipette technique makes it possible to visualize *in situ* the interactions of water droplets in the diluted model oil emulsions, at surface area to volume ratio of industrial relevance.

4.2 Experimental Materials and Methods

4.2.1 Materials

“Atmospheric-topped” bitumen supplied by Syncrude Canada Ltd. was used in this study. Deionized water was produced from a Millipore Milli-Q water system equipped with a 0.22μm filter. Spectral grade methylene chloride was purchased from Fisher Scientific. Heptol, a mixture of n-heptane (optima grade) and toluene (optima grade) at a volume ratio of 4:1, was used as model oil. All the other solvents were HPLC grade products purchased from Fisher Scientific. The commercial sodium naphthenates (NaN) was purchased from Acros

Organics/Fisher Scientific and used as received. Sodium hydroxide (Fisher Scientific) was supplied as solid. The standard naphthenic acid was from Fluka.

4.2.2 Separation of asphaltenes and maltenes

Asphaltenes and maltenes were separated by solvent extraction from the bitumen sample. Initially, 1 g of bitumen was completely dissolved in 1 mL of toluene, and then 40mL of n-pentane was added to the mixture to precipitate the asphaltenes. The precipitated asphaltenes were filtered, repeatedly washed with n-pentane until the supernatant become colorless, and then dried in a vacuum oven at 110^{o}C for 4 hours to obtain dry powder form for further use. The pentane soluble fraction of bitumen, known as maltenes, consists of saturates, aromatics and resins. The residue pentane and toluene in maltenes were removed with a Laborota 4002 rotary evaporator. Quantitative analysis of the bitumen was completed using Syncrude Analytical Method 5.1(Bulmer and Starr, 1979). The bitumen used in the present study was found to contain ~20 wt% asphaltenes.

4.2.3 Extraction of indigenous organic naphthenic acids from maltenes

Photoacoustic Fourier Transform Infrared (PAS-FTIR) analysis shows that naphthenic acids mainly remain soluble in the maltenes when precipitating asphaltenes with n-pentane. A protocol (Figure 4.2) was established to extract different amounts of naphthenic acids from maltenes by incremental addition of sodium hydroxide aqueous solutions. The concentration of sodium hydroxide was selected to ensure only naphthenic acids will be extracted. This was confirmed by the following FTIR analysis. Sodium hydroxide solution of 0.0005 mol/L (0.0005N) concentration was added to the maltenes at a mass ratio of 5:1 at each step. The mixture was stirred for 30 minutes at 70-80^{o}C and then left for 1 hour to allow the separation of layers. Precisely weighed 10 g of leached maltenes (maltenes with extractable naphthenic acids left) from each step were dissolved in toluene and centrifuged to remove the excess aqueous phase. The residue toluene in these leached maltenes was removed with a Laborota 4002 rotary evaporator. The leachate from each step was sent for FTIR analysis to measure the content of the extracted NAs.

4.2.4 Emulsion Preparation

Heptol, a mixture of n-heptane and toluene at a volume ratio of 4:1, was used as a model solvent to form the continuous oil phase. In this study either bitumen, asphaltenes or maltenes was dissolved in the oil phase at concentrations ranging from 10^{-6} wt% to 50 wt%. For the convenience of comparison and discussion, the amount of asphaltenes and maltenes were added to reflect their equivalent concentrations as found in whole bitumen and expressed as bitumen equivalent concentration. All the solvents used in this study were pre-saturated with water in a closed container for 24hr to avoid any dissolution of water in the oil phase during the tests. In preparation of the emulsions, 100μL of aqueous (filtered and deionized water) phase was introduced into 10mL of the continuous oil phase. The emulsion was formed by agitating the mixture in a water-bath sonicator (Fisher Scientific, model No. F56) at ~60^{o}C for 7~10 seconds. The diameter of water droplets created by this method ranges from 5 to 30μm. All the emulsions were aged for 10~20 minutes to reach equilibrium state before measurements.

4.2.5 Experimental Setup and methods

4.2.5.1 Micropipette technique

The micropipette technique makes it possible to study the *in situ* behaviors of emulsions at surface area-to-volume ratios that are representative of the commercially encountered emulsions. Two micropipettes, with an inside diameter ranging from 5 to 10μm at the tip, were mounted on micromanipulator (Narishige, Tokyo; model MHW-3) to ensure the continuous movements on micrometer scale in the studied emulsions. The important parameters in evaluating emulsion stability, including interfacial tensions (based on maximum bubble pressure method), crumpling ratios and the probability of droplet coalescence, were measured using this technique. Detailed description of the experimental setup and procedures can be found in Chapter 2 (Section 2.1).

4.2.5.2 Fourier Transform Infrared spectroscopy

Naphthenic acids (NAs) have characteristic absorbance bands at 1740cm^{-1} (monomer) and 1703cm^{-1} (dimer), and can therefore be quantified by FTIR (Scott et al., 2008). In the liquid or solid state, most carboxylic acid exist as a dimer due to hydrogen bonding between neighboring –COOH groups. The dimer gives a single sharp intense C=O stretch band at 1703 cm^{-1}. In diluted solutions, equilibrium exists between monomers and dimers. The monomer C=O stretch band is at 1740 cm^{-1}. In this study, FTIR spectroscopy was used to determine naphthenic acid content in the leachate from each step (Figure 4.2). Samples were thoroughly mixed with spectral grade methylene chloride, loaded into the sample cell, and then analyzed against a methylene chloride background. FTIR spectra were acquired using a Thermo-Nicolet FTIR spectrometer (8700) equipped with a variable pathlength KBr liquid cell (Thermo Instrument Inc.). The spectra over wavenumber range of 400-7400 cm^{-1} were acquired at a resolution of 4 cm^{-1}. The instrument was operated at interferometer mirror velocity of 0.6329cm/s, 128 scans per run, and data spacing of 1.928 cm^{-1}.

4.2.5.3 Langmuir trough

The monolayer behavior of three samples at heptol-water interfaces was characterized using a commercial Langmuir interfacial trough (KSV instruments, Finland). A standard Langmuir trough is composed of three parts: 1) a lower compartment built with hydrophobic and inert PTEE to avoid subphase contamination, 2) a pair of coupled movable barriers to control the surface area, and 3) a microbalance sensor to measure the surface pressure. A detailed description of this technique can be found in Chapter 2 (Section 2.2). The interfacial pressure was measured using the Wilhelmy plate made of a strip filter paper. A standard procedure was used to obtain interfacial pressure-area (π-A) isotherms. The trough was initially filled with 120 mL of Milli-Q water as the subphase. A given volume of solutions (25 μL of 1 mg/mL asphaltene-in-toluene, 25 μL of 0.1wt% commercial naphthenic acids, and 50 μL of the mixture of the two at a volume ratio of 1:1) was spread dropwise and evenly on the subphase using a Hamilton Microlitter Syringe (Sigma-Aldrich). The top phase was formed by carefully introducing 100 mL of heptol (optima grade) on the interface using a glass rod. All the solvents used in this study were pre-saturated with water in a closed container for 24hr to avoid any dissolution of water in the oil top phase during the tests. The whole system was aged for 3hrs before the pressure-area (π-A) isotherm measurements. The isotherms were obtained by compressing the barriers at a constant rate of 5 mm/min. After the compression, the top phase was carefully collected, spread on a clean subphase and compressed again to make sure that no surface materials migrated during the first compression. All the measurements were conducted at room temperature. In order to ensure reliability of the results, measurements were repeated at least three times.

4.3. Results and Discussion

4.3.1 Surface/interfacial tensions of commercial NaN

In early studies, lamellar liquid crystals and micelles were observed to form in the aqueous NaN solutions (Pauchard et al., 2009a, 2009b). The surface tension isotherms of these systems in Figure 4.3 show that the surface tension decreases with increasing NaN concentration and levels off around 31mN/m at a critical micelle concentration (CMC) of 1.0wt%. The difference in the CMC value obtained here from the reported value (Moran and Czarnecki, 2007) is attributed to the source and extraction method of naphthenates, which vary from one source to another and depends on solvent ratio used in extraction. The CMC obtained from the interfacial tension isotherm of NaN aqueous solution in contact with heptol agrees well with the value from surface tension isotherm. The interfacial tension at the CMC of sodium naphthenates is around 3mN/m.

Previous research showed that the addition of sodium naphthenates at low concentrations (10^{-5} wt% to 0.01 wt%) had little or no effect on interfacial properties of diluted bitumen in which ample amount of surface active components are present (Moran and Czarnecki, 2007, Figure 4.4). However, the added sodium naphthenates dominated the water-diluted bitumen interface at sodium naphthenates concentration higher than 1.0wt% (CMC) (Figure 4.4). in this study, 0.1wt% sodium naphthenates concentration was used to investigate its influence on a diluted asphaltene system.

4.3.2 NAs Concentration in Serial Leaching of Maltenes

The indigenous acids (naphthenic acids) were extracted from maltenes by the incremental addition of 0.0005 mol/L sodium hydroxide aqueous solution, as described above. The concentrations of the naphthenic acids remaining in organic phase were quantified by FTIR with the absorbance bands at 1740cm^{-1} and 1703cm^{-1} (Figure 4.5). A relationship was established between the contents of extracted naphthenic acids and sodium hydroxide addition (Figures 4.6 and 4.7).

Figure 4.7 shows the quantitative relationship between caustic addition and extractable naphthenic acids from maltenes. The pH of the extract after each step (open diamonds) varied from 9.1 to 9.5, which is close to the value of industrial conditioning process. It can be concluded that the total extractable naphthenic acids from this maltene was 1123ppm (i.e., 0.1 %). The extractable naphthenic acids were removed from the maltenes with the addition of sodium hydroxide until their concentration reached 75ppm (i.e., with the addition of 400ppm sodium hydroxide). The surface properties of maltenes with partial naphthenic acids removal were measured to understand the influence of naphthenic acids in maltene system.

4.3.3 Pressure-area (π-A) Isotherms

Interfacial pressure (π) is defined as:

$$\pi = \gamma_0 - \gamma \qquad (4.1)$$

where γ_0 is the interfacial tension after the aging process at the original trough area (i.e., no barrier compression), γ is the interfacial tension at a given compression of the trough area. The observed interfacial pressures are due to the interactions of the surface active materials (asphaltenes or sodium naphthenates) residing at the heptol-aqueous interface. The interfacial film behaviour of asphaltenes, sodium naphthenates solution (0.1 wt%), and the mixture of asphaltenes and sodium naphthenates solution (0.1 wt%) at a volume ratio of 1:1 are illustrated in Figure 4.8.

Clearly, the adsorption of asphaltenes at the interface tends to form the most rigid interfacial film, indicating a strong barrier to coalescence. However, the adsorption of sodium naphthenates at the interface shows little resistance to compression. The behavior of the mixture does not show additive nature. It appears that the presence of NaN hindered asphaltene adsorption. Such a behavior is similar to the effect of the chemical demulsifiers in a water-in-oil emulsion (Jones et al., 1978). This finding indicates that sodium naphthenates can effectively and partially displace asphaltenes adsorbed at the water-oil interface to reduce the rigidity of the interface. Such performance tends to destabilize the emulsion and eventually leads to demulsification.

4.3.4 Influence of NaN on the stability of water-in-asphaltenes emulsions

While the interfacial pressure isotherm provides valuable information to understand the stability of water-in-oil emulsions, it is inadequate to assess emulsion stability. To further understand the role of NA in emulsion stabilization as encountered in oil sands industry, emulsions were produced in heptol containing bitumen, asphaltenes, the mixture of asphaltenes and 0.1 wt% commercial sodium naphthenates solution, referred to as model oil to measure interfacial tensions, crumpling ratios and the probability of droplet coalescence. An equivalent concentration of asphaltenes as found in the original bitumen was used in the model oil in an attempt to make the results comparable.

4.3.4.1 Interfacial tension isotherms

The interfacial tensions of water droplets in three different model oils were evaluated by the maximum bubble pressure method. A water droplet was aged in an oil solution at a micropipette tip for 3 minutes to enable the system to reach an equilibrium state. Data points in Figure 4.9 represent the average of measurements using 20 or more water droplets with the standard deviation shown as the error bars.

The decrease of interfacial tension with increasing crude oil concentration is attributed to the adsorption of surface active materials at the water-oil interface. If a bitumen concentration in the heptol diluted bitumen is X wt%, the concentration of the pure asphaltenes in heptol will be 0.2 X wt%, and 0.1 wt% of NaN aqueous solution was introduced in the heptol diluted asphaltene to form the mixture solution. At the same equivalent concentration, the interfacial tension of bitumen system is lower than that of asphaltenes system due to competitive adsorption among the bitumen components (i.e., asphaltenes and non-asphaltenic surfactants in maltenes, such as naphthenic acids). It is apparent that the presence of additional sodium naphthenates is gaining the competition by displacing or limiting the irreversible adsorption of asphaltenic molecules at the interfaces, which can be concluded from the low interfacial tension for asphaltenes with addition of sodium naphthenates.

The Gibbs adsorption principle can be employed to evaluate the coverage (Γ, number of adsorbed molecules per unit area) of surface active components at the interface,

$$-d\gamma = kT\,\Gamma d\ln C \qquad (4.2)$$

where γ is the oil/water interfacial tension, k is the Boltzmann constant (k = R / N_A, where R is the universal gas constant and N_A is the Avogadro's constant), T is a temperature, and C is the concentration of the adsorbates. The surface coverage (Γ) of an "average" surface active species can be evaluated from equation (4.2), which lumps a complex molecular mixture into an equivalent single molecular species of the same average molar mass. The slope of the linear regime (Figures 4.3 and 4.9) reflects the surface activity of the adsorbates; the steeper the slope, the greater the surface coverage of surfactants, which indicates more surface active adsorbates. The molecular cross section (the area per "site") (Tsamantakis et al., 2005) is given by the reciprocal of Γ (Table 4.1). The similar values of surface coverage of diluted bitumen and asphaltenes suggest that large asphaltene molecules dominate the interface.

Table 4.1 Estimation of average surface area occupied by surface active species

Interface	Molecule cross section (nm^2)
Diluted bitumen (10^{-3}~1wt%)-water	2.97
Diluted asphaltenes (10^{-3}~1wt%)-water	3.12
Air-NaN solution	0.97
Heptol-NaN solution (0.1~1wt%)	0.51

4.3.4.2 Quantitative characterization of skin formation

It is well documented that the steric layer (skin) at the interface is the key contributor to the emulsion stability. This skin formation has been largely attributed by the irreversible adsorption of surface active asphaltenic molecules at the oil-water droplets interface. The incompressible nature of these irreversibly adsorbed molecules result in out-of-plane deflections when they are drawn together with a reduction in surface area of the water droplets. Droplet volume extraction experiments aim to quantify the skin formation by introducing crumpling ratio (CR),

$$CR = \frac{A_f}{A_i} = \frac{\pi R_f^2}{\pi R_i^2} = \frac{R_f^2}{R_i^2} \qquad (4.3)$$

where A_i is the initial projected area of the water droplet, A_f is the projected area of water droplet right before the point when crumpling was first observed.

The crumpling ratio of bitumen, asphaltenes and asphaltenes-0.1 wt% NaN was measured as a function of bulk concentration of individual components. A high CR as defined in equation 4.3 represents a more stable interface. Each data point in Fig. 4.10 is an average of measurements with 35 or more water droplets and the error bar represents the standard deviation of all measurements. Crumpling was not observed at very low bitumen or asphaltene concentrations (less than 10^{-4} wt%) due to very little or no irreversible adsorption of surface active materials. Between 10^{-5} and 10^{-4} wt% of bitumen concentration, a sharp increase in crumpling ratio was observed, indicating formation of irreversibly adsorbed interfacial films. At higher bitumen concentration, the crumpling ratio decreases with increasing bitumen concentration because of the competitive adsorption between asphaltenes and surfactants in maltenes. It shows that maltenes at much higher concentrations are easier, compared with asphaltenes, to adsorb at the water droplet surface due to favorable partitioning, depleting the room available for asphaltenes. In the case of asphaltenes, the crumpling ratio increases steadily with increasing asphaltenes concentration, which means increasing irreversible adsorption. It is anticipated that increasing asphaltenes concentration in heptol would force more asphaltenes to move to the water-oil interface, leading to a more rigid interface and hence higher crumpling ratio, although more difficult as the interface approaches its saturation. It is interesting to note that the sharp increase in crumpling ratio occurred at 10^{-5} wt% concentration for both asphaltene and bitumen, indicating that asphaltene dominates the oil-water interfacial behavior of low bitumen concentration. However, with the addition of 0.1 wt% NaN in the asphaltene system, the crumpling ratio drastically drops from 0.6 to ~0 at 10^{-4} wt% concentration. This finding, in conjunction with the interfacial tension isotherm and surface coverage data, demonstrates that NaN can hinder the development of a rigid interface, perhaps by fast adsorption-desorption kinetics (reaching equilibrium state). Meanwhile, at a fixed NaN concentration (0.1 wt%), increasing asphaltene content in the system will slightly increase the crumpling ratio (0~0.3). This is because more asphaltenic molecules compete for irreversible adsorption at the interfaces.

4.3.4.3 Droplet-droplet interaction

Droplet interactions are measured to understand demulsification potential of NaN by flocculation or coalescence. As two droplets are pressed against each other by micropipettes, the direct contact of droplets allows the drainage of the intervening liquid sandwiched in the planar region between the droplets by mechanical forces. In these experiments, the droplets will be easily separated when the applied force is removed if the droplets do not flocculate. It should be noted that the applied force was sufficient to deform the droplets (Moran, 2007) as visually confirmed. The statistic nature of the droplet coalescence is represented by the probability of coalescence, Φ. In the present study, an average of three sets of interaction experiments for a minimum of 50 water droplet pairs are tried for every data point with the precision being given by standard deviation.

As can be seen from Figure 4.11, the probability of coalescence for all three systems at very low concentration of surface active components (10^{-6}~10^{-4} wt%) is 1, indicating the absence of irreversibly adsorbed asphaltenic films to prevent coalescence. At intermediate concentrations (10^{-4}~0.1 wt%), a sharp decrease in the coalescence probability was observed for all the three systems due to build up of irreversibly adsorbed asphaltenic films. At an equivalent concentration of bitumen above 0.01 wt%, the probability of coalescence reduced to zero, i.e. no droplet coalescence was observed regardless of compositions of oil systems. In the intermediate concentration (10^{-4}~0.1 wt%) region, the addition of 0.1 wt% NaN in the asphaltenes greatly increases the possibility of coalescence. The presence of NaN makes the interface more fluid by winning the competitive adsorption with asphaltenes. It should be noted that the probability of coalescence for all three systems was identical (zero) at high concentration (> 0.1 wt%)due to the excessive amount of asphaltenes.

Table 4.2. Qualitative description of the skin formation at the interface and droplet interactions in the presence of NaN.

Sodium naphthenates	Oil phase	Skin formation	Droplet-droplet interaction
0.1-10 wt%	Pure heptol	No	Coalescence
0.1 wt%	10^{-6}~10^{-4} wt% Diluted asphaltenes	No	Coalescence
0.1 wt%	10^{-4}~0.1 wt% Diluted asphaltenes	Limited	Coalescence & flocculation
0.1 wt%	0.1~10 wt% Diluted asphaltenes	Yes	No coalescence but some flocculation

To better understand the influences of NaN in asphaltenes, Table 4.2 shows the qualitative description of the skin formation at the interface and droplets interactions in different systems. It should be noted that there is no skin formation on the water droplet surfaces in the NaN-pure heptol system. Moreover, coalescence is observed inevitable for all the droplet interactions in the NaN-pure heptol system. Regarding the asphaltene-heptol-0.1 wt% NaN system, results depends on the concentration of asphaltene in the oil phase. In the highly diluted region (10^{-6}~10^{-4} wt%), coalescence is often observed due to the absence of irreversibly adsorbed asphaltenic films, which agrees well with the absence of skin formation at the interfaces. With an increasing concentration of asphaltenes in the oil phase (10^{-4}~0.1 wt%), less coalescence is observed while a limited formation of rigid skin is noticed. Flocculation (Figure 4.12) is often observed in this regime. At high concentration (0.1~10 wt%), the presence of large amounts of asphaltenes eventually dominates the interface, resulting in a no coalescence region.

4.3.5 Influence of indigenous NAs on the stability of water-in-maltenes emulsions

Since most of the indigenous NAs remain in the soluble maltene fraction, a protocol (see above) was established to remove different amount of naturally occurring NAs from the maltene fraction to identify their influence on the emulsion stability. Results in Chapter 3 showed that the adsorption of maltenes on water droplets may contribute, to some extent, to the emulsion stability without skin formation, provided that its concentration is sufficiently high. Consequently, three maltene-in-heptol solutions (0.85 wt%, 7 wt% and 45 wt%) were used to create bulk samples for the extraction of naturally occurring NAs. Based on the proposed protocol, the indigenous NAs in the bulk solution are divided into two parts, the extractable and un-extractable fraction under a given pH condition. In this study, the total amount of extractable naphthenic acids is 1123ppm. Apparently, the higher the concentration of maltene-in-heptol solution is, the more the indigenous NAs (including the un-extractable NA for a given pH) will be left in the bulk solution at the same amount of sodium hydroxide addition. By this way, emulsions containing different amounts of indigenous NAs are prepared for the micro-scale measurements. Interfacial tensions, crumpling ratio and probability of coalescence of these emulsions were evaluated to understand the influence of naturally occurring NAs on the emulsion stability.

For the purpose of comparison, a blank emulsion was created by introducing the extracted indigenous NAs into pure heptol. Regardless of the concentration of the indigenous NAs, no skin formation was observed while performing the volume contraction experiment. Also, coalescence was always observed in such systems.

4.3.5.1 Interfacial tension isotherms

The effect of indigenous NAs remaining in the model oil phase on the interfacial tension was evaluated as a function of extractable NAs in maltene system for a given pH. Data points in Figure 4.13 represent the average of measurements using 20 or more droplets with the standard deviation shown as the error bars. It is clear that, at the same maltene-in-heptol concentration, the interfacial tension decreases with the increasing amount of extractable NAs left in the maltenes, although at a reduced value as the droplet surface approaches its saturation. This can be explained by the preferential adsorption of NAs at the droplet surface as compared with other naturally occurring components in the maltenes. Alternatively, the presence of NAs may displace or interact with other naturally occurring components to make them less available at the oil-water interface. For the same amount of extractable NAs left in maltenes, the higher the maltene-in-heptol concentration is, the more the un-extractable NAs will be left in the emulsion, leading to a lower interfacial tension. Based on the Gibbs adsorption equation (4.2), the slope of the linear regime reflects the surface activity of the adsorbates (indigenous NAs and other naturally occurring components in maltenes). The similarity in slopes of interfacial tension curves in Figure 4.13 suggests the competitive adsorption among NAs and other naturally occurring components and a complex surface organization of these species.

4.3.5.2 Quantitative characterization of “skin formation”

It has been demonstrated that maltenes alone do not contribute to the formation of the rigid skin at the water droplet surface. This can be explained by the fast-reversible adsorption kinetics of some indigenous components in maltenes. Figure 4.14 shows the trend of skin formation with changing extractable NAs content in maltenes. Each data is an average of measurements with 35 or more water droplets and the error bar represents the standard deviation of all measurements. At higher maltene-in-heptol concentration (45 wt% and 7.5 wt%), the crumpling ratio remains zero (i.e., no skin formation) regardless of extractable NAs content in maltenes. This suggests reversible adsorption kinetics at the water-oil interface due to the presence of abundant naturally occurring NAs in maltenes. However, at a maltene-in-heptol concentration of 0.85 wt%, the crumpling ratio increases with decreasing extractable NAs left in maltenes when there is a limited naturally occurring NAs present in the system. It has been shown that no skin formation occurs in the indigenous NAs-heptol system. This finding indicates that the adsorption of certain components in maltenes, other than NAs, can cause skin formation. It should be noted that the contribution (0<CR<0.14) in this system is much smaller compared to the case of asphaltenes (0.2<CR<1).

4.3.5.3 Droplet-droplet interactions

Droplet contact is prerequisite for droplet coalescence, which eventually leads to destabilization of the emulsion. In the present study, an average of three sets of interaction experiments for a minimum of 50 water droplet pairs are tried for every data point with the standard deviation shown by the error bars. For given maltene-in-heptol concentration, the probability of coalescence decreases with decreasing extractable NAs left in the maltenes (Figure 4.15), suggesting an increase of emulsion stability. This finding indicates that the adsorption of an increasing amount of NAs at the droplet surfaces can gradually remove the barrier for coalescence. The trends of 45 wt% and 7.5 wt% maltene-heptol solutions are nearly identical. This can be explained by the saturated adsorption of excess naturally occurring surfactants at high concentrations. Only the behavior of the 45 wt% maltene-heptol is considered in the following discussion. It is perhaps surprising that the 45 wt% maltene-in-heptol solution still can contribute to the emulsion stability, even without skin formation. Recall that neither skin formation nor the barrier to coalescence is caused by the presence of indigenous NAs. This phenomenon has two implications. It shows that the adsorption of other naturally occurring components can be partially masked by the presence of high concentration of NAs (as confirmed by the crumpling ratio). Furthermore, the adsorption of the naturally occurring material will provide a barrier for coalescence at high maltene concentrations. However, flocculation (Figure 4.16) can be present for all the interactions in which coalescence was not observed. Moreover, the more the extractable NAs left in maltenes, the stronger is the flocculation. Therefore, the adsorption of NAs tends to “soften” the droplet surface and promote the coalescence of water droplets.

4.4. Conclusions

In conventional bitumen extraction processes, a natural surfactant group, naphthenic acids (NAs) is released through the addition of sodium hydroxide. The level of NAs in the oil varies with caustic addition (sodium hydroxide) and the source and properties of the ore.

Current investigation demonstrated that the level of NAs could affect the surface properties of water droplets in diluted bitumen component (asphaltenes and maltenes) in heptol solutions. NAs are capable of reducing the interfacial tension, soften the rigid asphaltenic film and promote the coalescence of water droplets, all of which would lead to destabilization of water-in-oil emulsions. This indicates that there may be a critical level of NAs to allow for minimum rag layer development in the commercial bitumen production processes. Possibly, a predictor can be found to optimize bitumen recovery and diluted bitumen quality based on the relationship between caustic addition and content of NAs released from the oil sands during processing.

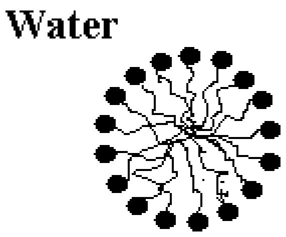

Figure 4.1. Schematic representation of an aqueous micelle

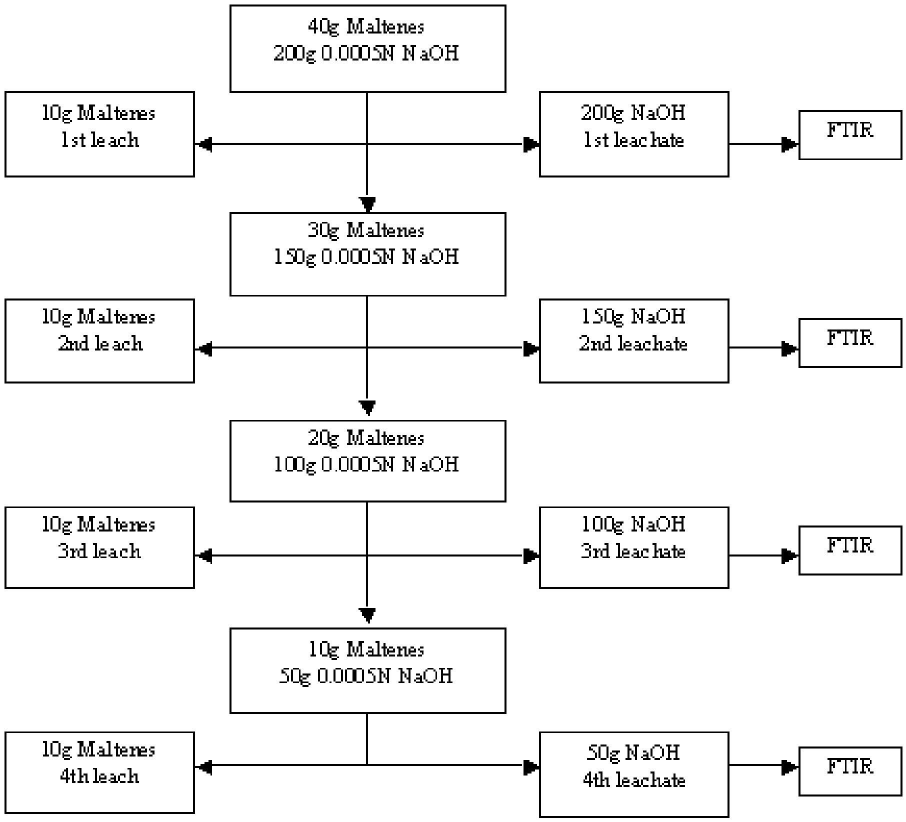

Figure 4.2. Procedure for extraction of naphthenic acids from maltenes using caustic soda

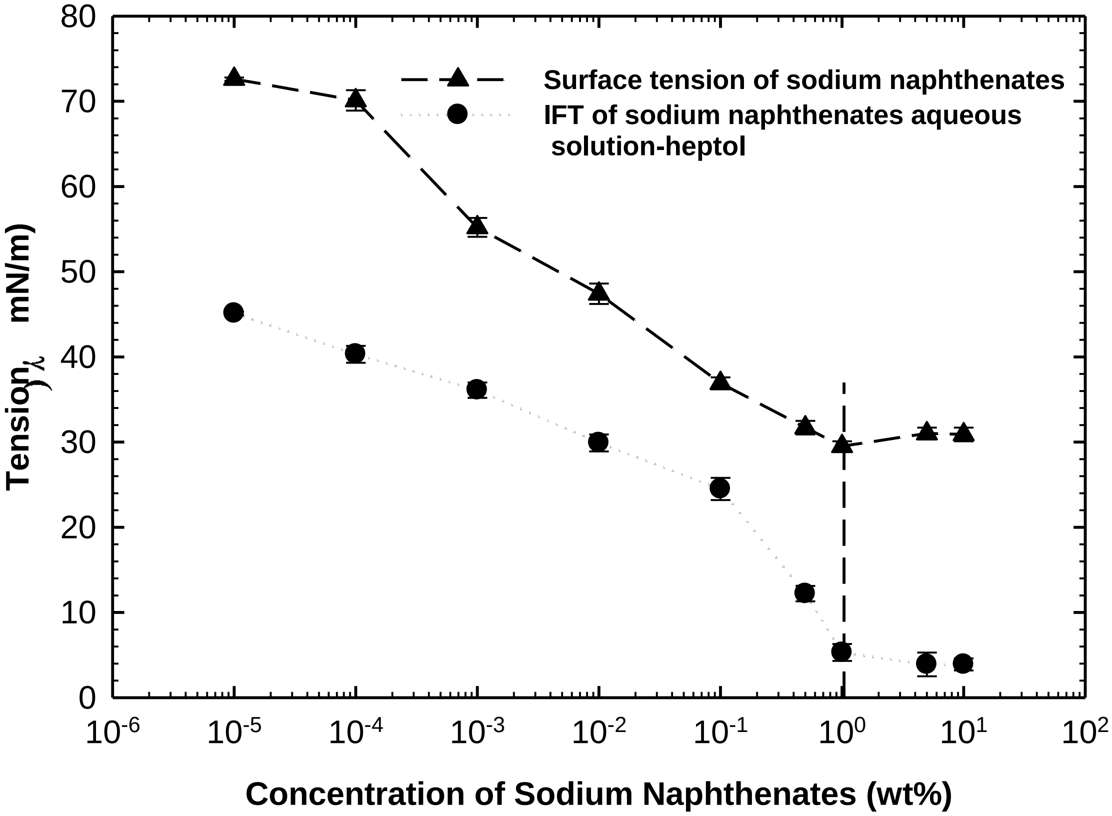

Figure 4.3. Surface tension of aqueous sodium naphthenates solution (solid triangles) and interfacial tension of aqueous sodium naphthenates solution against heptol (solid circles). Both surface tension and interfacial tension tend to level off at a sodium naphthenates concentration of 1.0 wt% (critical micelle concentration).

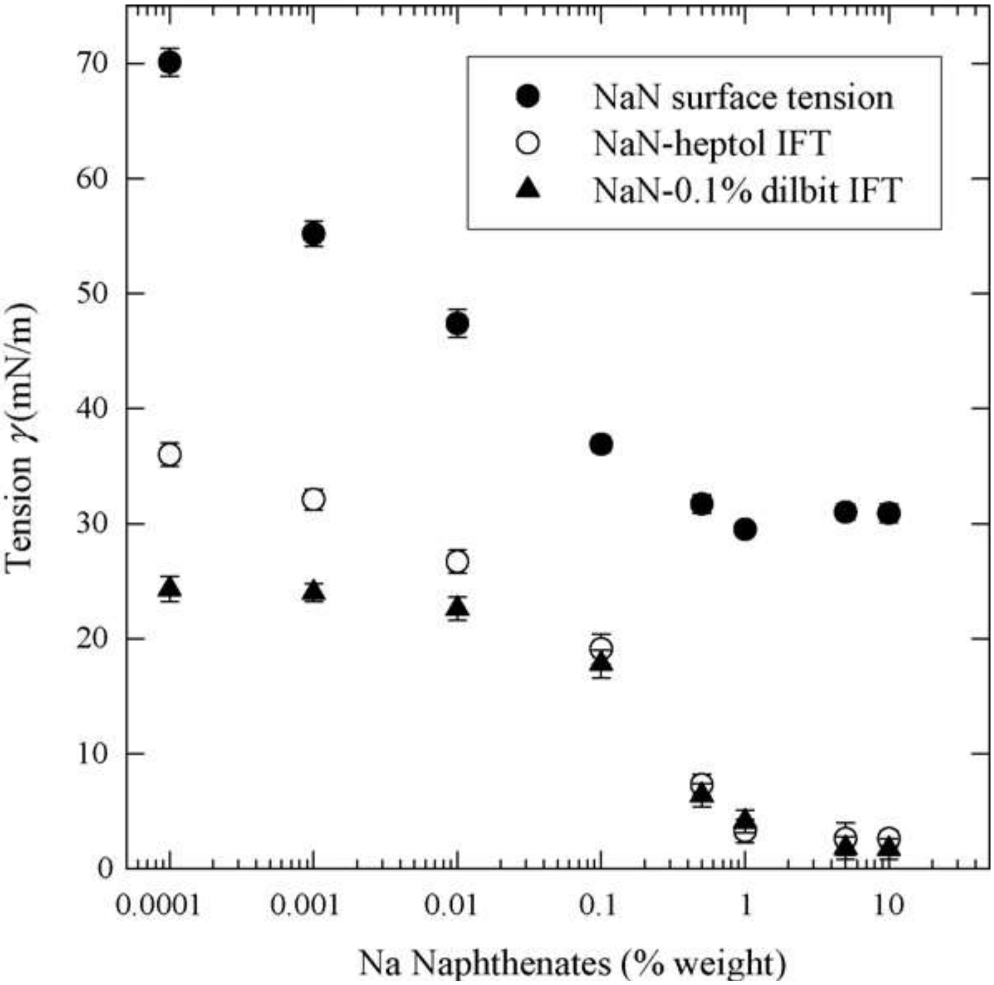

Figure 4.4. Tension isotherms of aqueous solutions of sodium naphthenates (NaN). Surface tension (solid circles) and interfacial tension against heptol (open circles) or heptol-diluted bitumen ('dilbit', 0.1% bitumen by volume; triangles) were measured using the maximum bubble pressure method. Data points represent the average of a minimum of 10 measurements while the error bars give the standard deviation. (Moran and Czarnecki, 2007)

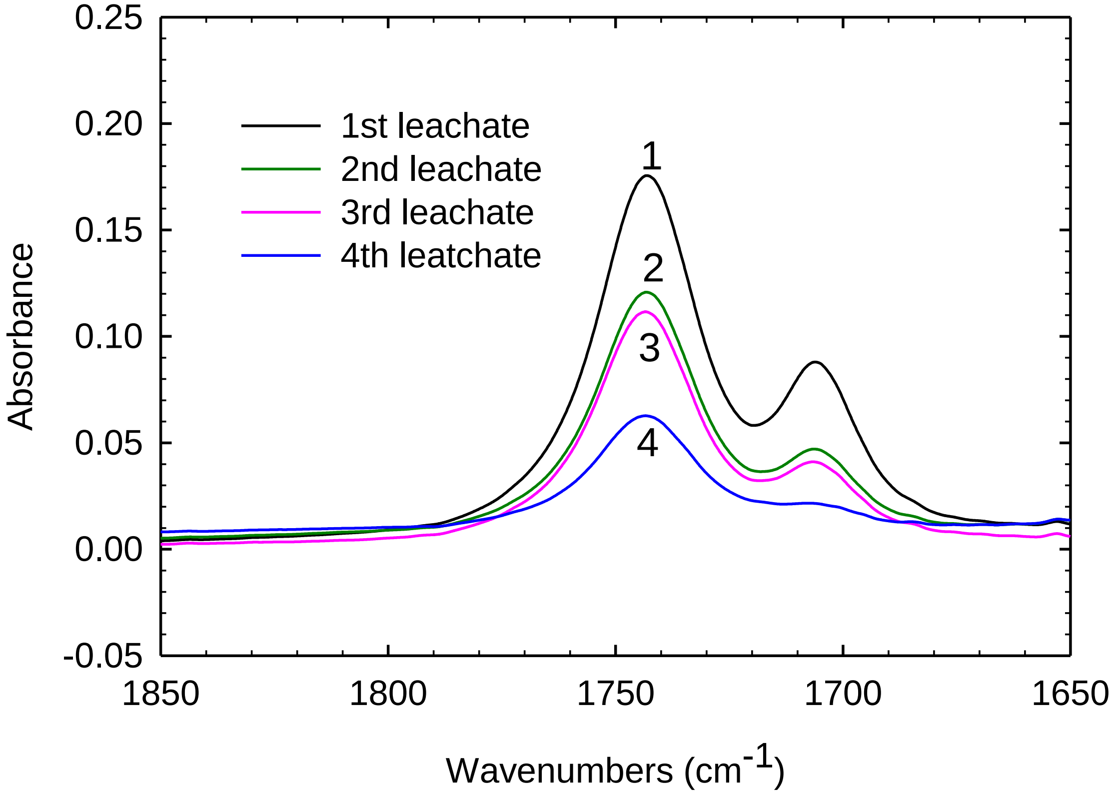

Figure 4.5. FTIR spectra of the indigenous NAs in the leachates extracted from maltenes. NAs have characteristic absorbance bands at 1740cm^{-1} and 1703cm^{-1}, and therefore can be quantified by FTIR.

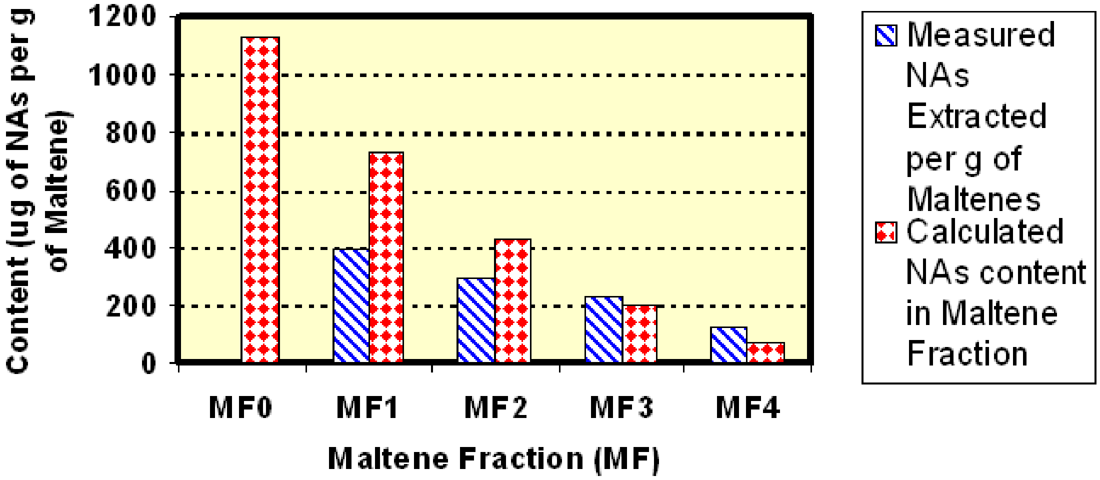

Figure 4.6. Naphthenic acids concentration in Maltenes (μg/g)
MF0 refers to the original maltenes, MF1, MF2, MF3 and MF4 refer to the maltenes after the first, second, third and fourth leaching, respectively.

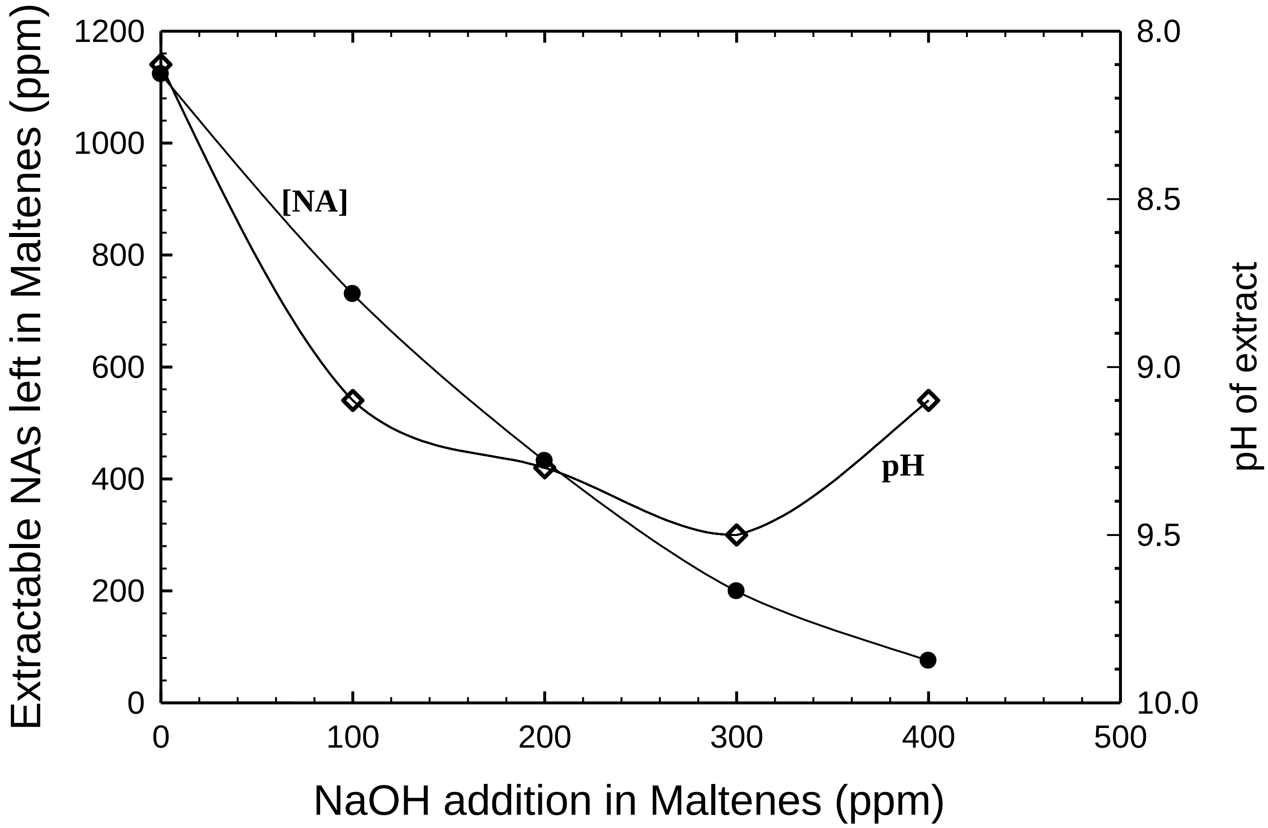

Figure 4.7. Quantative relationship between caustic addition and extractable NAs left in maltenes, solid circles represent the extractable NAs left in maltenes, open diamonds represent the pH of extract after the extraction of NAs under given conditions.

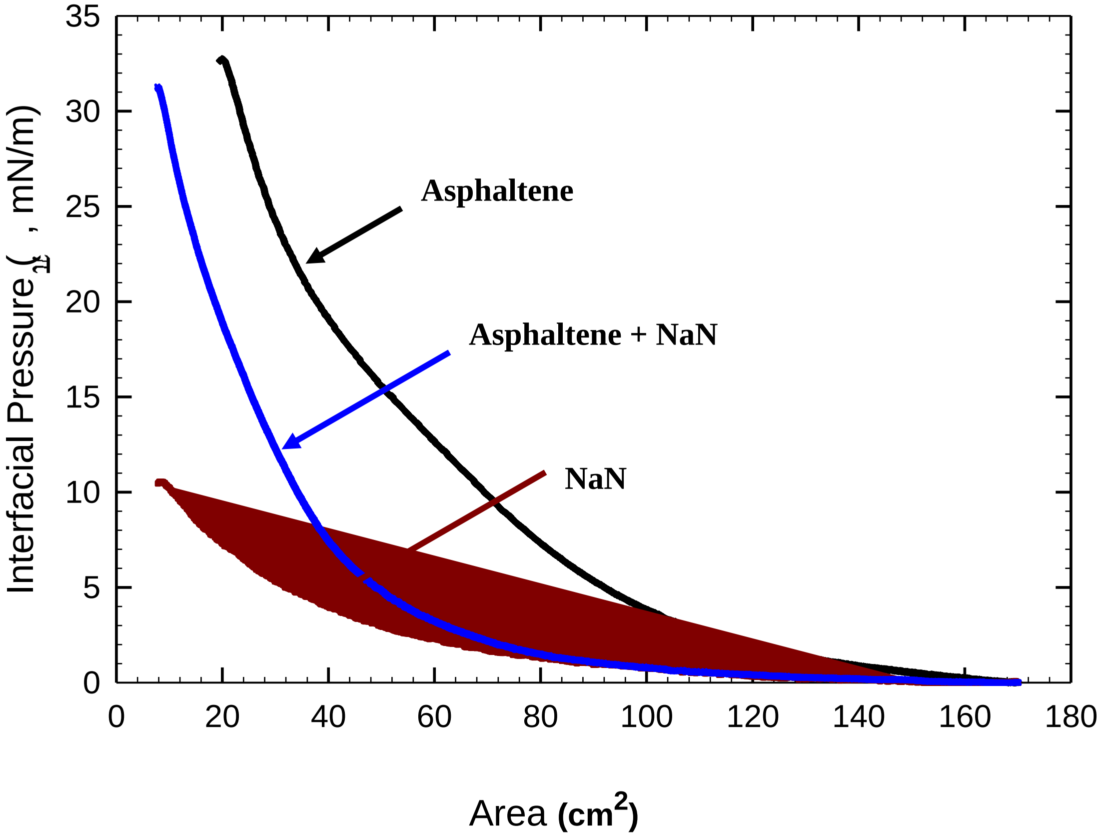

Figure 4.8. Interfacial pressure-area isotherms for asphaltene (25 μL) at heptol-water interface (black line), sodium naphthenates (NaN) (25 μL) at heptol-water interface (brown line), a mixture of asphaltene and NaN (50 μL, volume ratio 1:1) at heptol-water interface (blue line).

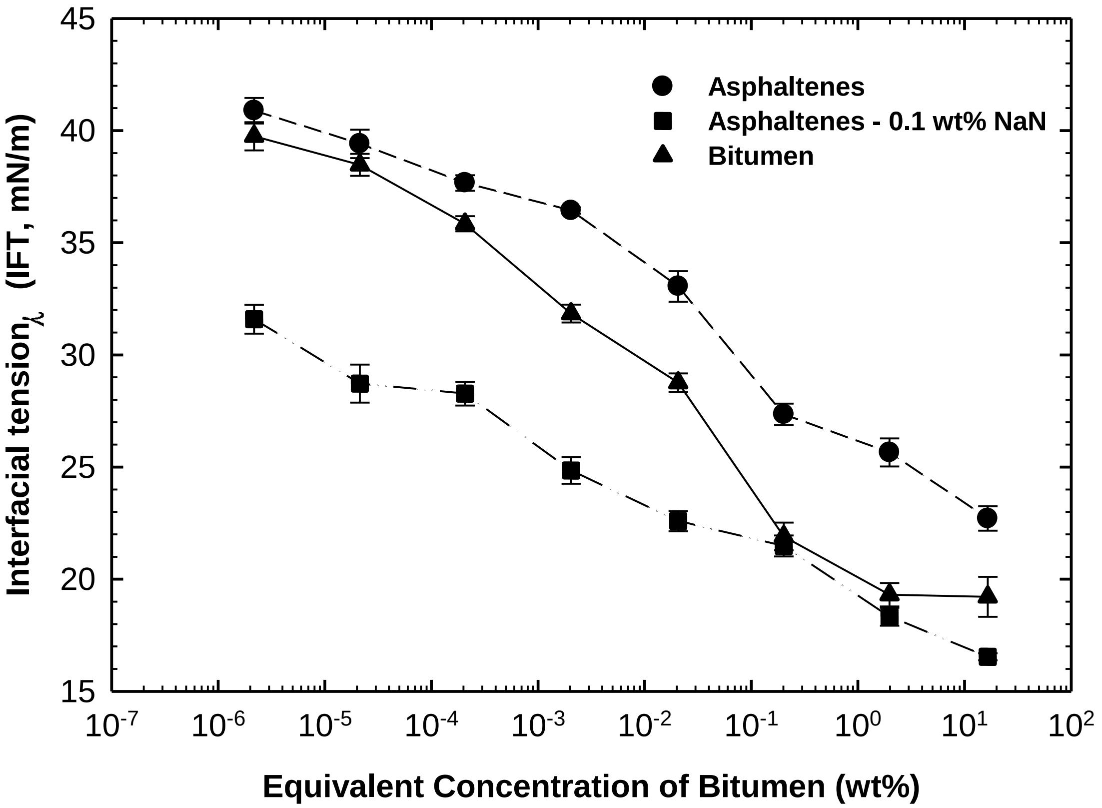

Figure 4.9. Comparison of interfacial isotherms for diluted bitumen-heptol (solid triangles), diluted asphaltene-heptol (solid circles) and asphaltene -heptol-0.1 wt% NaN (solid squares).

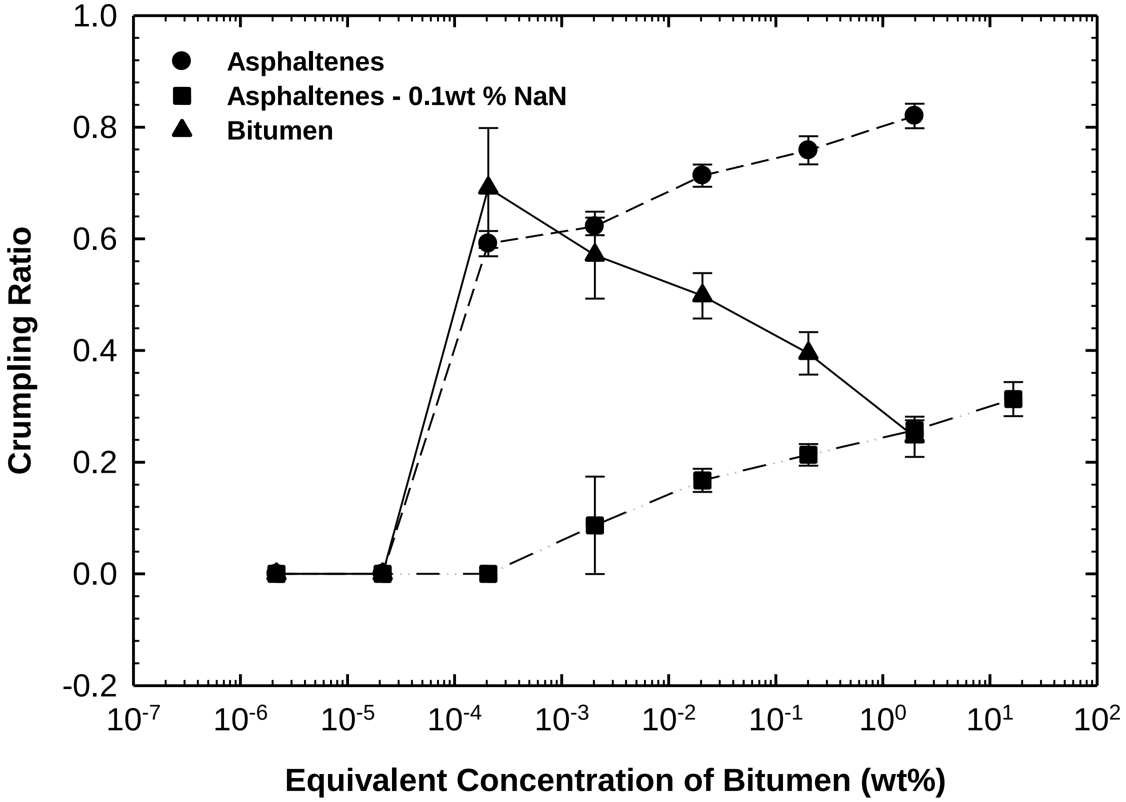

Figure 4.10. Comparison of crumpling ratio for diluted bitumen-heptol (solid triangles), diluted asphaltene-heptol (solid circles) and asphaltene-heptol-0.1 wt% NaN (solid squares) systems.

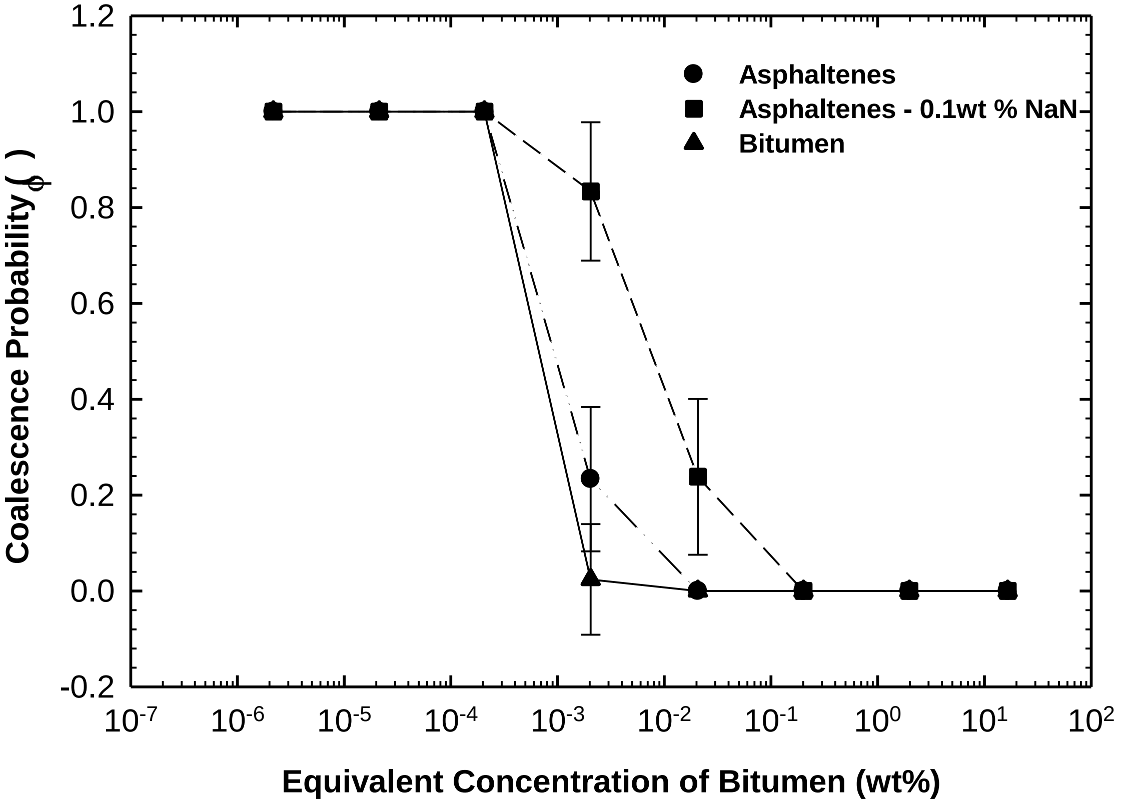

Figure 4.11. Coalescence probability of emulsified water droplets for diluted bitumen-heptol (solid triangles), diluted asphaltene-heptol (solid circles) and asphaltene-heptol-0.1 wt% NaN (solid squares) systems.

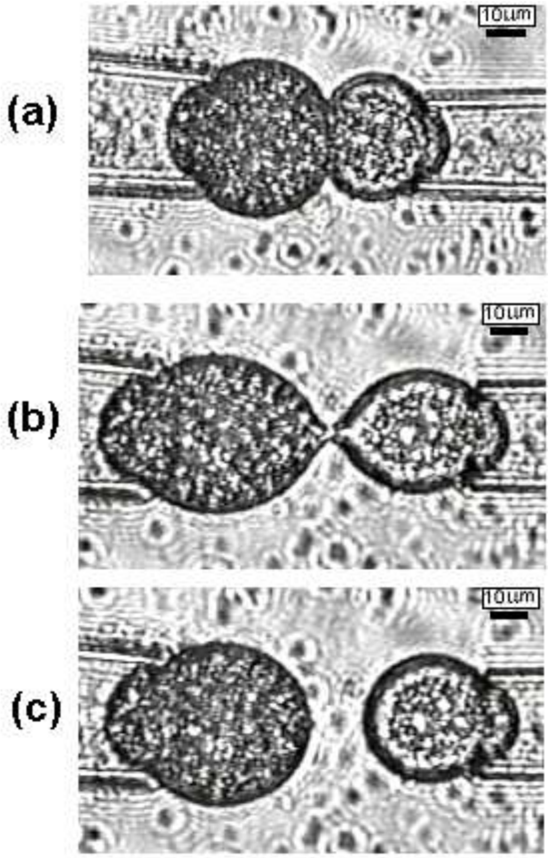

Figure 4.12. Sequential series of visualization (a-b-c) describing droplet flocculation in 0.1 wt% NaN-0.1 wt% asphaltene-heptol system. (a). One droplet is directed toward another static droplet to enable a “head-on” contact and external force is applied to cause noticeable deformation of the contacting region for a sufficient time (allowing for the film drainage between the droplets and attainment of equilibrium droplet shapes). (b). The droplets show a sign of flocculation and deformation when the external force is gradually removed. (c). The droplets return to its original state after the flocculation state is removed.

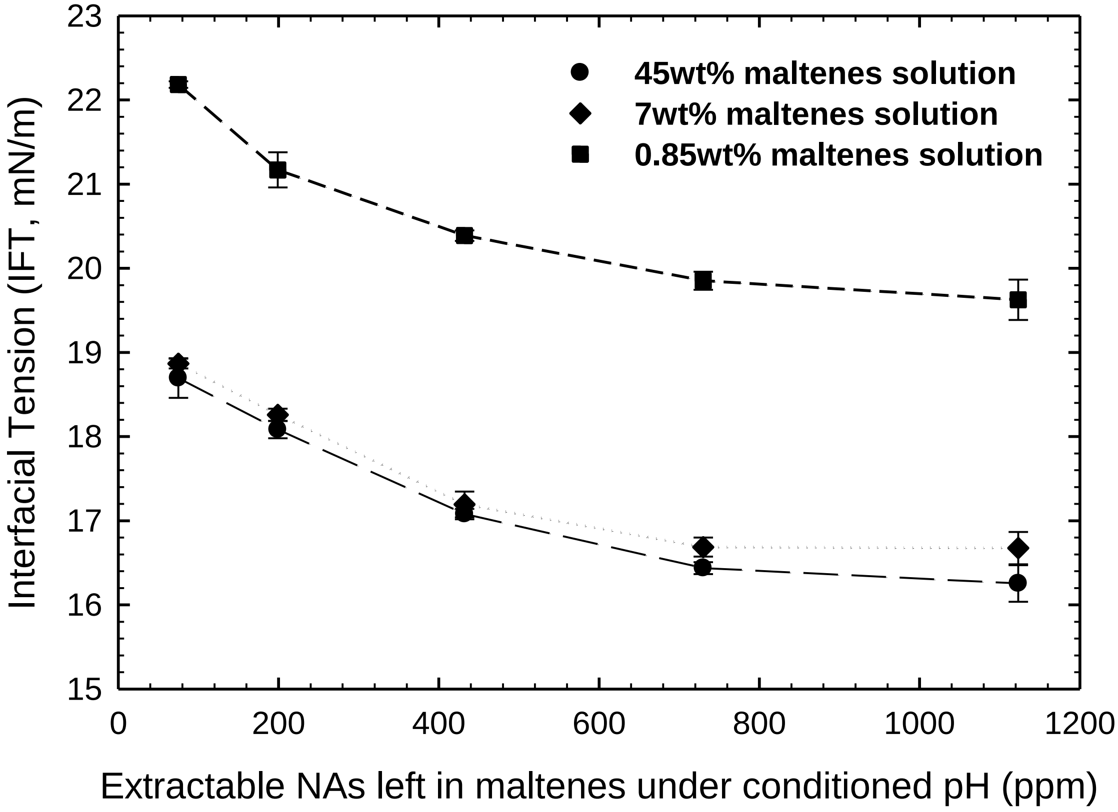

Figure 4.13. Comparison of interfacial tension isotherms in diluted maltene-heptol with different amount of extractable indigenous NAs left in the system. The maltenes are diluted in heptol to create three concentrations: 45 wt% (solid circles), 7.5 wt% (solid diamonds) and 0.85 wt% (solid squares).

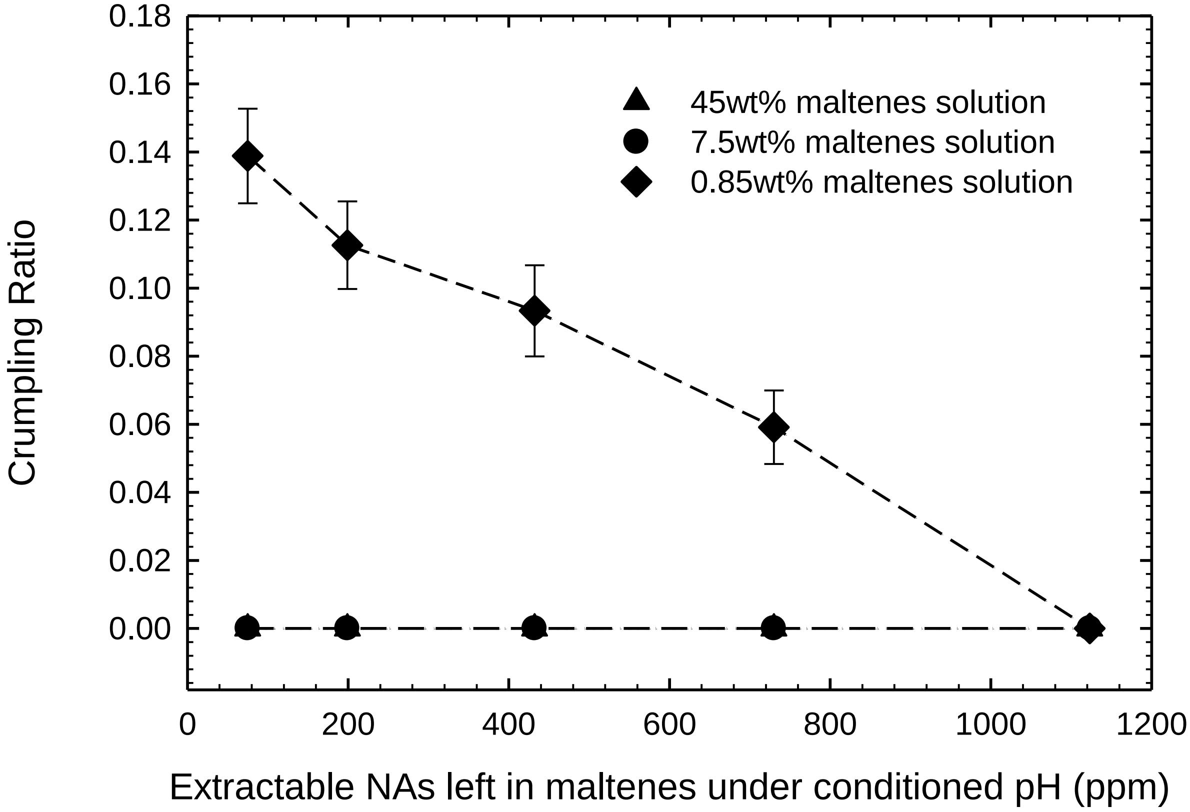

Figure 4.14. Comparison of crumpling ratio in diluted maltene-heptol systemes with different amount of extractable indigenous NAs left in the oil. The maltenes are diluted in heptol to create three concentrations: 45 wt% (solid triangles), 7.5 wt% (solid circles) and 0.85 wt% (solid diamonds).

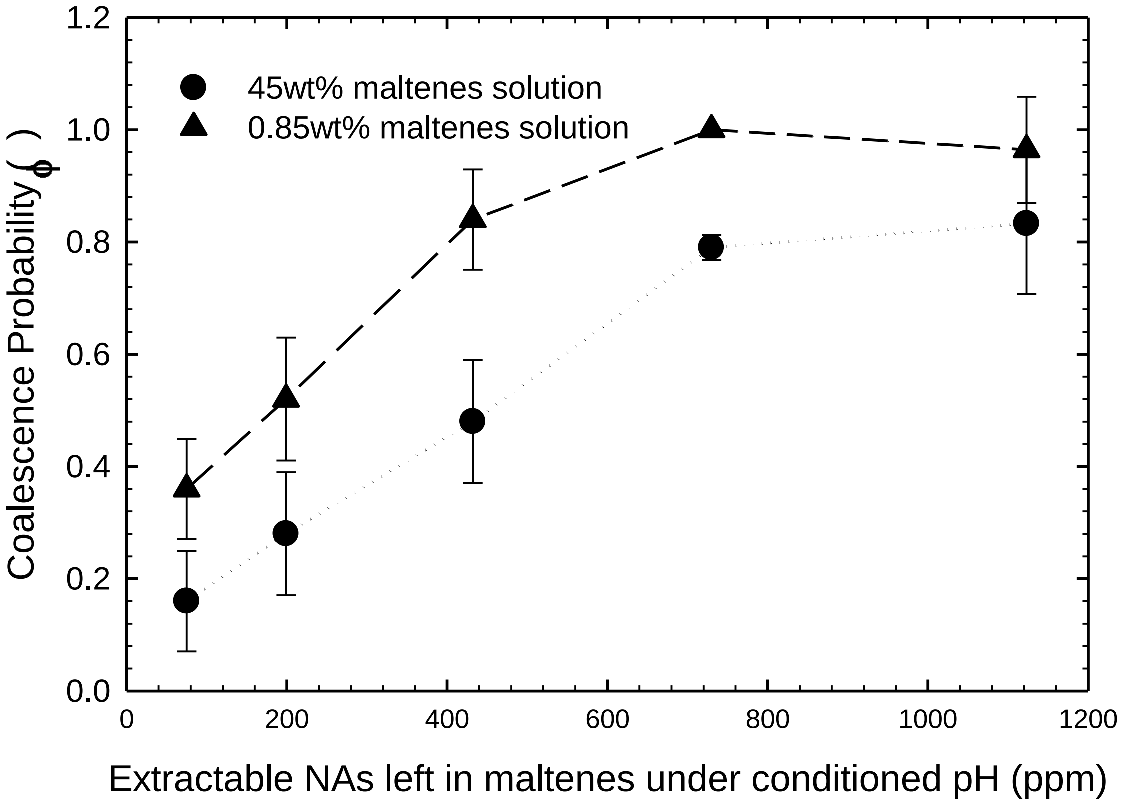

Figure 4.15. Comparison of probability of coalescence for droplet interactions in diluted maltene-heptol with different amount of extractable indigenous NAs left in the system. The maltenes are diluted in heptol to create two concentrations: 45 wt% (solid circles) and 0.85 wt% (solid triangles).

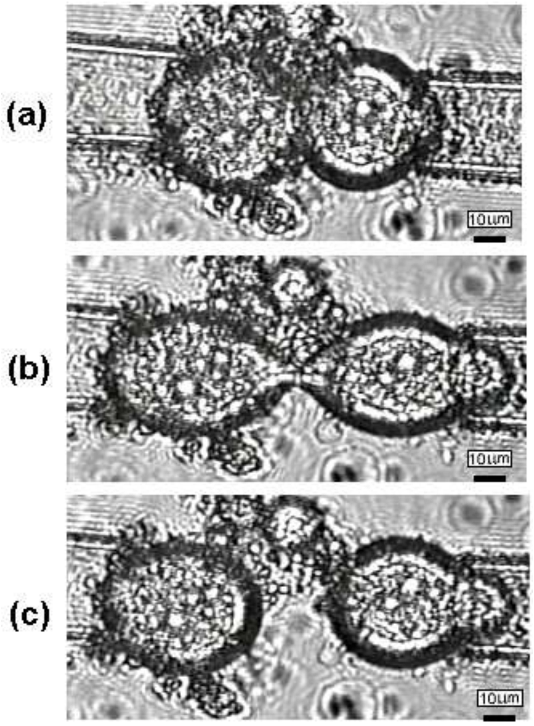

Figure 4.16. Sequential series of visualization (a-b-c) describing droplet flocculation in 0.85 wt% maltene-heptol with 432 ppm extractable NAs left in the system. (a). One droplet is directed toward another static droplet to enable a “head-on” contact and external force is applied to cause noticeable deformation of the contacting region for 2 minutes (a sufficient time allowing for the film drainage between the droplets and attainment of equilibrium droplet shapes). (b). The droplets show a sign of flocculation and deformation when attempt is made to remove the external force. (c). The droplets return to its original state after the flocculation is detached.

Chapter 5

Demulsification of water-in-diluted bitumen emulsions via ethylcellulose *

5.1 Introduction

Chemical demulsification is widely employed to remove water from heavy oils so that the content of bottom solids and water (BSW) in oil is less than 0.5 vol% (Mikula and Munoz, 2000). Demulsifiers are surface active substances (surfactants), which can destabilize emulsions by changing the interfacial film properties, such as interfacial tension, mechanical strength, elasticity and thickness of interfacial film to promote coalescence and/or through flocculation of water droplets (Urdahl et al., 1993; Singh, 1994; Kumar et al., 2001; Zhang et al., 2003; Sjoblom et al., 2001). The mechanism of demulsification and the principal role of demulsifiers have been studied by many researchers (Zapryanov et al., 1983; Eley et al., 1987; Krawczyk, et al., 1991; Mohammed et al., 1994; Kim and Wasan, 1996; Djuve et al., 2001; Wu et al., 2005; Feng et al., 2009).

An efficient demulsifier should migrate rapidly through the continuous phase to reach the droplet surface and have a strong attraction to the interface. At certain

---

* Related publication: Feng, X., Mussone, P., Gao, S., Wang, S., Wu, S., Masliyah, J. H., Xu, Z., 2009, *Langmuir*, DOI: 10.1021/la9029563

concentrations, the demulsifier will counteract the agent stabilizing the emulsion, and facilitate the formation of flocs and/or coalescence of the dispersed phase (Smith and Arnold, 1992; Stalass et al., 1991; Berger et al., 1987; Monson and Stenzel, 1946; Van Os et al., 1993; Bessler, 1983; Mukherjee and Kushnick, 1989). For water-in-oil emulsions, the demulsifiers are typically oil-soluble to allow them to access the oil/water interface through the continuous oil phase.

Commercial demulsifiers used in oil sands industry are mostly nonionic surfactants due to their advantages on compatibility, stability and efficiency. A typical nonionic demulsifier contains hydrophilic groups, such as oxyethylene, hydroxyl, carboxyl and amine, and hydrophobic groups, such as alkyl, alkyphenol and oxypropylene. It is well known that ethylene oxide (EO) and propylene oxide (PO) block copolymers (Figure 5.1) are particularly active at the oil/water interface. There are two stages in the collapse of emulsions: flocculation, in which some clustering of emulsion droplets takes place, and coalescence, in which the number of distinct droplets decreases (Adamson, 1997) (Figure 5.2). Recent research demonstrated that low molecular weight polymeric surfactants have high interfacial activity and adsorb irreversibly at the oil/water interface, leading to film rupture and water droplets coalescence (Sjoblom et al., 2001), while high molecular weight polymeric surfactants tend to flocculate water droplets to realize the separation (Pena et al., 2005). It was proposed that polymers with dendrimer structures destabilize water-in-oil emulsions through both flocculation and coalescence of water droplets (Zhang et al., 2005).

Various parameters, including molecular weight (MW), hydrophilic- lipophilic balance (HLB), partition coefficient, relative solubility numbers and others, have been utilized to predict the performance of demulsifiers (Griffin, 1949; Makhonin et al., 1983; Binyon, 1984; Márquez-Silva, 1997). Demulsifiers were characterized by measuring molecular weight, interfacial tension, interfacial viscosity, and by conducting infrared spectroscopy and elemental analysis (Aveyard et al., 1990; Williams, 1991; Bhardwaj and Hartland, 1998; Sams and Zaouk, 2000). Microscopy also provides an important tool for characterization and evaluation of the performance of demulsifiers. The techniques include light microscopy (LM), cryogenic scanning electron microscopy (SEM), confocal laser scanning microscopy (CLSM) and infrared microspectroscopy (IRM) (Galopin and Henry, 1972; Mason, 1983; Pawley, 1990; Messerschmidt and Harthcock, 1988).

Unlike traditional demulsifiers with EO/PO structure, a biodegradable ethylcellulose (EC) was introduced by Feng et al. (2009) to remove water in naphtha-diluted bitumen and bitumen froth. Ethylcelluose is synthesized from cellulose and ethyl chloride. The properties of ethylcellulose can be finely tuned by controlling the degree of substitution (DS) of hydroxyl groups (Figure 5.3).

An empirical parameter to categorize surfactants is the hydrophilic-lipophilic balance (HLB):

$$HLB = \sum number\ of\ \ hydrophilic\ groups - \sum number\ of\ \ lipophilic\ groups + 7$$

In general, a surfactant of HLB value lower than 9 is considered as lipophilic (oil soluble), while a surfactant of HLB value higher than 11 is considered to be hydrophilic (water soluble). The HLB for EC of DS=1 is slightly lower than 9 to promote its partitioning at the water-oil interface. Moreover, this polymer is non-toxic and biodegradable, making it attractive for commercial applications. Further investigations are currently in progress to understand the properties of this polymer.

In this study, the demulsification mechanism of the EC polymer was investigated. The interfacial properties with the addition of EC polymer to water-in-diluted bitumen were examined by micropipette technique. The interfacial films of bitumen at the naphtha-water interface in the presence and absence of EC were prepared by a Langmuir trough. The morphology of the films was examined by atomic force microscope (AFM) imaging following the transfer of the films onto solid substrates by Langmuir-Blodgett (LB) technique. Moreover, the dewatering performance of EC was compared with a commercial demulsifier, DA, used in oil sands industry.

5.2 Materials and Methods

5.2.1 Materials

“Atmospheric-topped” bitumen supplied by Syncrude Canada Ltd. was used in this study. Filtered and deionized water was produced from a Millipore Milli-Q water system equipped with a 0.22μm filter. The optima grade toluene and isopropyl alcohol were provided by Fisher Scientific. All the other solvents were HPLC grade products purchased from Fisher Scientific. Heavy naphtha was supplied by Champion Technologies Inc. Ethylcellulose (EC) with 48% ethoxyl was purchased from Sigma-Aldrich and used as received. The molecular weight of the polymer was determined by an intrinsic viscosity measurement to be 46 kDa (Feng et al, 2009). EC was dissolved in heavy naphtha and stirred for 24 h prior to its use. The commercial demulsifier, DA, was provided by Champion Technologies Inc. and it is currently used commercially.

5.2.2 Emulsion preparation

The continuous oil phase was prepared by dissolving bitumen into naphtha at a bitumen concentration of 0.1 wt%. All the solvents used in this study were pre-saturated with water in a closed container for 24hr to avoid any dissolution of water in the oil phase during the tests. In preparation of the emulsions, 100μL (0.1mL) of aqueous (filtered and deionized water) phase was introduced into 10mL of the continuous oil phase. The emulsion was formed by agitating the mixture in a water-bath sonicator (Fisher Scientific, model No. F56) at ~60^{o}C for 7~10 seconds. The diameter of water droplets created by this method ranged from 5 to 30μm. All the emulsions were aged for 10~20 minutes to reach equilibrium state before measurements. Various amounts of ethylcellulose solution (0.5 wt% in heavy naphtha) were then added to the emulsion to study the demulsification performance. For studies using Langmuir-Blodgett interfacial film and atomic force microscopy, solutions of 1 g/L diluted bitumen in naphtha and ethylcellulose in naphtha were used.

5.2.3 Experimental setup and methods

5.2.3.1 Micropipette technique

Detailed description of the micropipette experimental setup and procedures can be found in Chapter 2 (Section 2.1). Briefly, two micropipettes, with an inside diameter ranging from 5 to 10μm at the tip, were utilized to measure interfacial tensions (based on maximum bubble pressure method), crumpling ratios and the probability of droplet coalescence, relevant to water-in-oil emulsion.

5.2.3.2 Langmuir-Blodgett film

Langmuir-Blodgett (LB) films were prepared using a Langmuir interfacial trough (KSV instruments, Finland). The trough and barriers were cleaned according to the procedures described in Chapter 2 (Section 2.2.1). A mixture of 20 µL of 1 mg/mL diluted bitumen in naphtha or/and 20 µL of 1 mg/mL ethylcellulose was then evenly placed drop-wise on the water surface using a Hamilton microsyringe. A volume of 100 mL of heavy naphtha, instead of industrial-grade naphtha, was used as top phase in this set of experiments to avoid potential interference of impurities in industrial-grade naphtha with true interfacial LB films. A hydrophilic silicon wafer (0.5 µm thickness, 10 cm diameter, polished on one side, purchased from Ultrasil, Hayward, CA) was used to deposit the interfacial film at a constant surface pressure (2 mN/m) reached by compressing the barriers at 5 mm/min. The transfer was performed by pulling the substrate upward through the interface at a rate of 5 mm/min. The deposited film was stored in a desiccator for atomic force microscope image. The detailed description of this procedure can be found in Chapter 2 (Section 2.2).

5.2.3.3 Atomic force microscopy

Images of LB films were obtained using a Multimode Atomic Force Microscope (AFM) with a nanoscope IIIa controller (Veeco, Santa Barbara, CA) operating under tapping mode in air. AFM imaging was carried out at room temperature using a multimode scanning probe microscope head and a J-scanner. A silicon tip (RTESP, Veeco) with a resonance frequency of 260-320 kHz was used for imaging at the scan rate of 1 Hz. Images were obtained at several locations for each sample. At least two independent samples, prepared under the same deposition condition, were imaged. A detailed description about the procedure can be found in Chapter 2 (Section 2.3).

5.2.3.4 Demulsification performance

Bitumen was dissolved in naphtha at a naphtha/bitumen mass ratio of 0.65 in keeping with that encountered in industrial practices. In preparation of emulsions, aqueous (deionized water) phase was introduced into naphtha-diluted bitumen. The emulsion was formed by agitating the mixture in a water-bath sonicator (Fisher Scientific, model No. F56). The resultant emulsion contained 5 wt% water. In the dewatering test, different amounts of the test demulsifiers were introduced into the emulsion at concentrations ranging from 0 ppm to 150 ppm. 5 mL of the mixture was introduced into a 20 mL vial using disposal pipette and the mixture was allowed for gravity settling for 30 minutes before measurements.

To determine the water content in the emulsion, Unisol solvent, a mixture of toluene (optimal grade) and isopropyl alcohol (IPA) at a volume ratio of 70/30, was used. The Unisol was dehydrated in the molecular sieve (Fisher Scientific, Grade 514) overnight before use. The dried Unisol solvent (5 mL) was then added to the emulsion with the presence of EC (5 mL mixture) at a volume ratio of 1/1. This mixture (10 mL) was homogenized using an Analog vortex mixer (Fisher Scientific) operating at 3200 rpm for 1 minute. A syringe (Hamilton, CR-700) was used to immediately transfer and inject 0.5 mL of the sample emulsion into a Karl Fisher Titrator (Moisture analyzer, Fisher Scientific) after mixing. The water content reported was the average of three measurements.

In another set of tests, diluted bitumen samples (without addition of any demulsifier) from a froth treatment pilot process streams were used to examine the dewatering efficiency of EC and DA by an optical microscope (Carl Zeiss, Axioplan KS 400, Germany) equipped with an Olympus imaging system (DP72, Germany).

Ethylcellulose (EC) with a molecular weight of 46 kDa (Feng et al., 2009) was dissolved in heavy naphtha to a concentration of 0.5 wt%. Different amounts of EC solution were added to prepared emulsions (water-in-naphtha system, water-in-naphtha diluted bitumen system) to understand the influence of EC on the stability of water-in-diluted bitumen emulsions.

5.3 Results and Discussion

5.3.1 Interfacial tension measurements

The surface properties of ethylcellulose were evaluated by measuring their interfacial tension against naphtha (Figure 5.4, solid circles). Further, the influence of ethylcellulose addition on the interfacial tension of emulsified water droplet in diluted bitumen was also characterized (Figure 5.4, solid diamonds).

The surface activity of ethylcellulose is observed from the interfacial tension measurement - the interfacial tension of naphtha-water decreases with increasing EC concentrations (solid circles) in naphtha. This trend continues up to an EC concentration of around 150 ppm, where the interfacial tension levels off at around 8 mN/m. This finding indicates the saturated adsorption of EC at the naphtha-water interface. The interfacial tension isotherm for EC-0.1 wt% diluted bitumen in naphtha system reveals some interesting features (solid diamonds). At lower EC concentrations (0-15 ppm), the isotherm lies below that for pure naphtha system. This observation indicates that the naturally occurring components in bitumen (such as asphaltenes and maltenes) adsorb at oil/water interface at low EC concentration, and contribute to the decrease of interfacial tension. At an EC concentration higher than 50 ppm, the interfacial tension isotherms for EC-naphtha and EC-0.1 wt% diluted bitumen becomes almost identical, leveling off at the similar value of 8 mN/m. This finding clearly demonstrates that the added EC polymer at high concentrations dominates the interfacial properties, possibly completely displacing the adsorption of bitumen components at a sufficient amount.

5.3.2 Quantitative characterization of “skin formation”

Volume contract experiments were performed to assess the effects of adsorbed EC at the oil/water interface. Crumpling Ratio (CR, Equation 3.2) was employed to quantify the rigid skin formation. Figure 5.5 shows the trend of skin formation in EC-0.1 wt% diluted bitumen in naphtha system with increasing EC concentration. Each data point is an average of measurements of 35 or more water droplets and the error bar represents the standard deviation of all measurements.

A blank emulsion was created by introducing EC into pure naphtha. Regardless the concentration of EC, no skin formation was observed while performing the volume contraction experiment.

For EC-0.1 wt% diluted bitumen in naphtha emulsions, crumpling (CR ~ 0.5) was observed in the absence of EC due to the irreversible adsorption of indigenous surface active asphaltenic molecules at the water droplet surfaces (cf. Chapter 3). At an EC concentration lower than 100 ppm, the crumpling ratio decreases with increasing EC concentration, indicating that the presence of EC mitigates the development of interfacial rigidity. This is consistent with the preferable adsorption of EC at the oil/water interface. At an EC concentration higher than 130 ppm, it is surprising that the crumpling ratio increases with increasing EC concentration. In the presence of 200 ppm EC in the system, the crumpling ratio is even higher than that without the addition of EC. This observation suggests the existence of a critical value for EC to minimize the skin formation at the water droplet surfaces. Any value higher than this concentration would cause overdosing. Note that EC itself won’t cause any skin formation in the blank experiment. In other words, excessive adsorption of EC at the interface in the presence of bitumen may result in certain kind of association at the water droplet surfaces, acting as an irreversibly adsorbed layer.

5.3.3 Droplet-droplet interaction

Droplet-droplet interactions were determined to evaluate the influence of adsorbed EC on the ability of emulsified water droplets to flocculate or coalescence. Coalescence probability, which is defined as the ratio of the number of contact experiments in which coalescence was observed to the total number of trials, was employed to describe the statistical nature of emulsified water droplets coalescence. Figure 5.6 shows the relationship between the coalescence probability and concentration of EC in the emulsion. An average of three sets of interaction experiments for a minimum of 50 water droplet pairs were tried for every data point with the standard deviation shown by the error bars.

A blank emulsion was created by introducing EC into pure naphtha. Regardless the concentration of EC, coalescence was always observed in such systems.

With an EC concentration up to 100 ppm, the coalescence probability increases with increasing EC concentration in the diluted bitumen–naphtha system. Clearly, the preferable adsorption of EC facilitates the coalescence of water droplets by bridging the deformed planar interface between two water droplets (Figure 5.7). It must be noted that flocculation (Figure 5.8) is prevalent for all the interactions even where coalescence is not observed. However, further increase of EC dosage (over 100 ppm) decreased the coalescence probability. This observation was surprising, especially considering that the interfacial tension isotherm indicated an interface dominated by adsorbed EC polymer over a concentration greater than 50ppm (Figure 5.4). Note that the similar concentration dependence was observed in the volume contraction experiment and coalescence always happens in the EC-naphtha system. This implies, in the presence of bitumen, that adsorption of excessive amount of EC on the water droplet surfaces could cause certain degree of association among different species in the system. This specific association inhibits the coalescence due to the steric repulsion between the hydrophobic groups (Figure 5.9). On the other hand, the increasing dosage of EC can accelerate the coalescence process. For example, the coalescence with the presence of 35 ppm EC occurs after approximately 30 seconds of direct contact, while for an emulsion with 130 ppm EC, coalescence often happens immediately upon the contact (Figure 5.10). The dynamic behavior of the coalescence process has not yet been studied in any detail.

5.3.4 Atomic force microscopy

To better understand the demulsification mechanisms of EC, interfacial films of bitumen and EC/bitumen mixtures transferred from a naphtha-water interface by LB method were imaged using an AFM.

A typical AFM image of bitumen interfacial LB films was shown in Figure 5.11. It was characterized by random, close-packed discoid nanoaggregates which are similar to those reported for asphaltenes (Gawrys et al., 2006; Chandra et al., 2008). Figure 5.12 shows the morphology of EC/bitumen mixture (1:1) LB film transferred from naphtha-diluted bitumen interface. Clearly, the bitumen interfacial film was pushed to a few microdomains of similar nanostructures while

EC occupied the majority of the interface. This distribution area of EC provides the possibility for the flocculation and/or coalescence of water droplets.

5.3.5 Demulsification performance

At the time of this work, a commercial demulsifier, DA, was tested for comparison. DA was known to be a good demulsifier in the industrial bitumen extraction process. This demulsifier was then diluted to 10 wt% with xylene to increase its solubility in diluted bitumen. Normalized water content was employed as a parameter to evaluate the demulsification efficiency of the demulsifiers. It is defined as the ratio of water content in the emulsion with the presence of certain amount of demulsifier to that without demulsifier addition (also called blank sample). The emulsified water content was evaluated by a Karl Fisher Titrator.

Figure 5.13 displays the normalized water content remaining in the emulsions as a function of demulsifier dosage. It can be seen that there is around 40 wt% of water will naturally settle down after aging process. The addition of either EC polymer or DA led to a sharp decrease in the water content. The water content decreased with increasing demulsifier dosage. Over a low dosage range (0 to ~60 ppm), the dewatering efficiency of DA is better than that of EC polymer. A further increase in dosage clearly shows the dewatering priority of EC polymer compared to DA. At a dosage of ~100 ppm, for example, the normalized water content in the EC-emulsion was only ~4 wt%, while that in DA-emulsion was ~17 wt%. A dosage over 100 ppm would not cause any further significant reduction in the water content.

The dewatering efficiency was also evaluated visually by an optical microscope. EC and DA were added to an industrial pilot diluted bitumen emulsion (with the water content 8-10 wt%) at a dosage of 35 ppm. A lower water content and larger water droplet size represents a higher dewatering efficiency. The water droplet size was around 5 μm without demulsifier addition. The presence of either EC or DA can cause a significant increase of water droplet size. At a dosage of 35 ppm, water droplet size in EC-diluted bitumen was 10-15 μm and that in DA-diluted bitumen was 20-30 μm, suggesting the coalescence of water droplets. Eventually, the water content in the diluted bitumen would decrease, which agrees favorably with the results from Karl titration measurements.

5.4 Conclusions

Ethylcellulose (EC), a biodegradable polymer, was found effective in dewatering of water-in-diluted bitumen emulsions. To some extent, the addition of EC can promote the flocculation and coalescence of water droplets to realize phase separation. However, volume contraction experiments and droplet interactions also indicate the presence of a critical value for EC. At molecular level, AFM imaging revealed that the addition of EC can effectively disrupt the continuous interfacial films formed by surface active components of bitumen. The demulsification performance of EC is compared with a commercial demulsifier, DA, currently used in oil sands industry. Results revealed that the dewatering efficiency of EC could outperform that of DA, even though DA performs better than EC at low concentration.

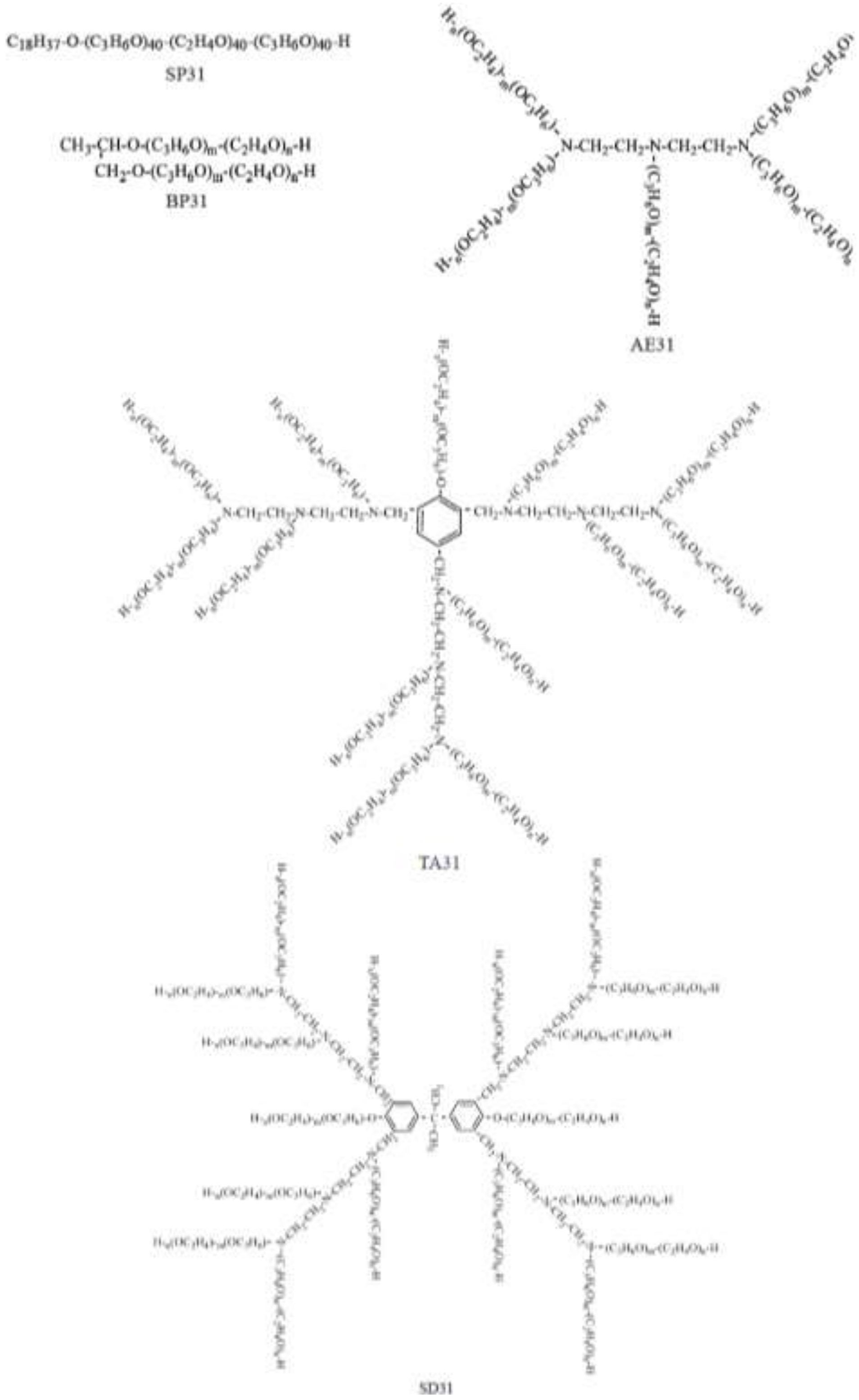

Figure 5.1. Molecular structures of five linear, star and dendrimer block copolymers (Zhang, 2005)

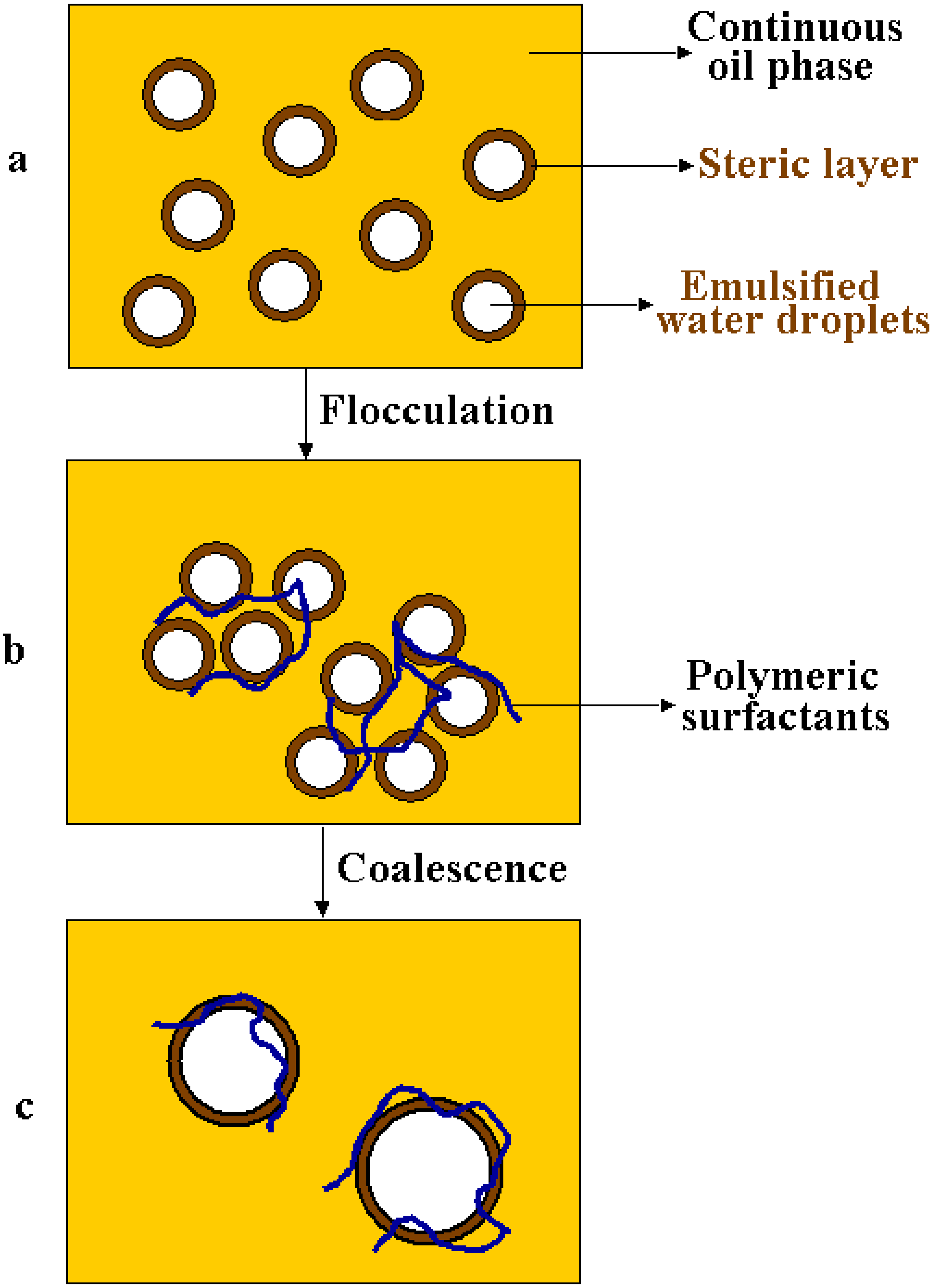

Figure 5.2. Two stages in the collapse of emulsions: flocculation and coalescence

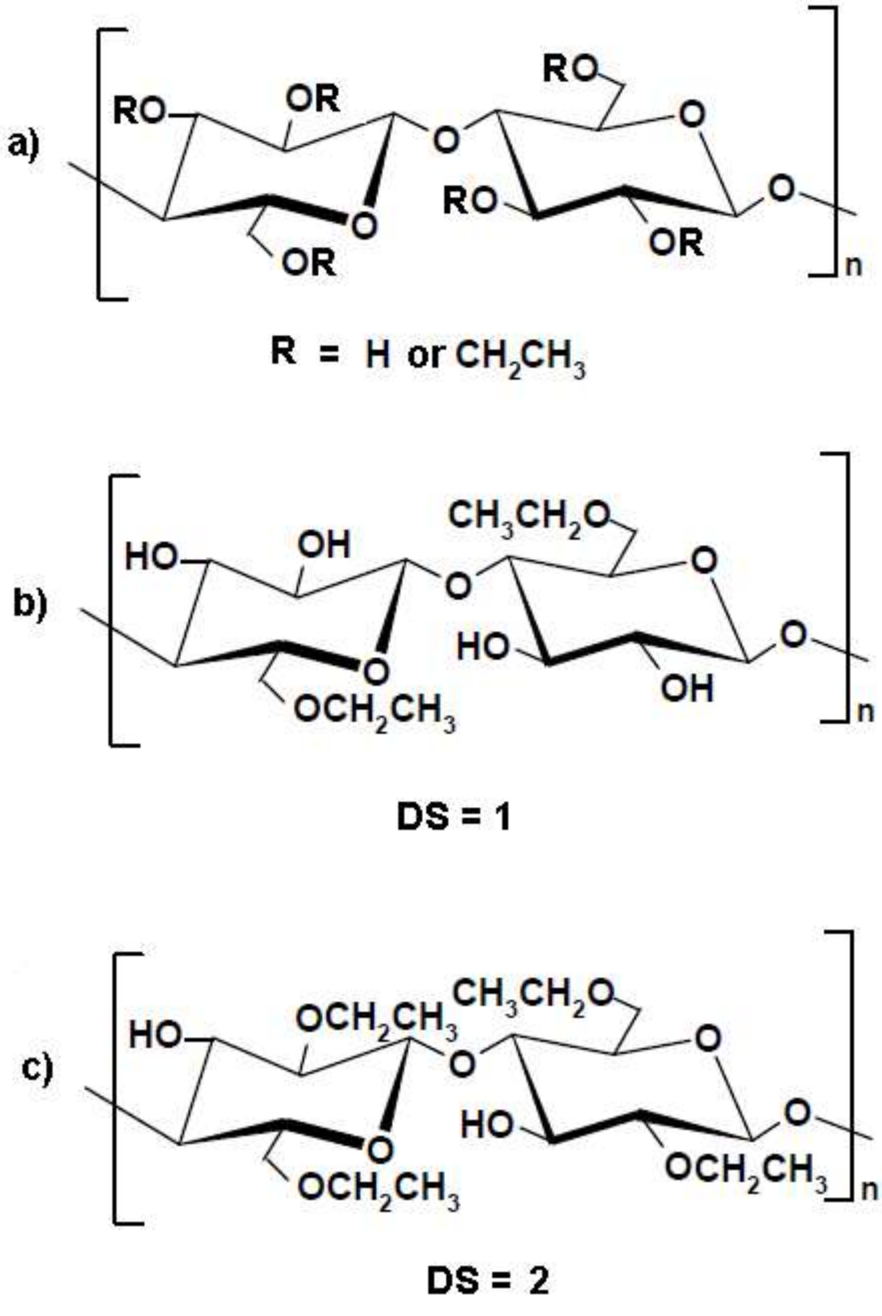

Figure 5.3. Structure of a) ethylcellulose, b) ethylcellulose with a degree of substitution of 1, and c) ethylcellulose with a degree of substitution of 2.(courtesy of Feng, X)

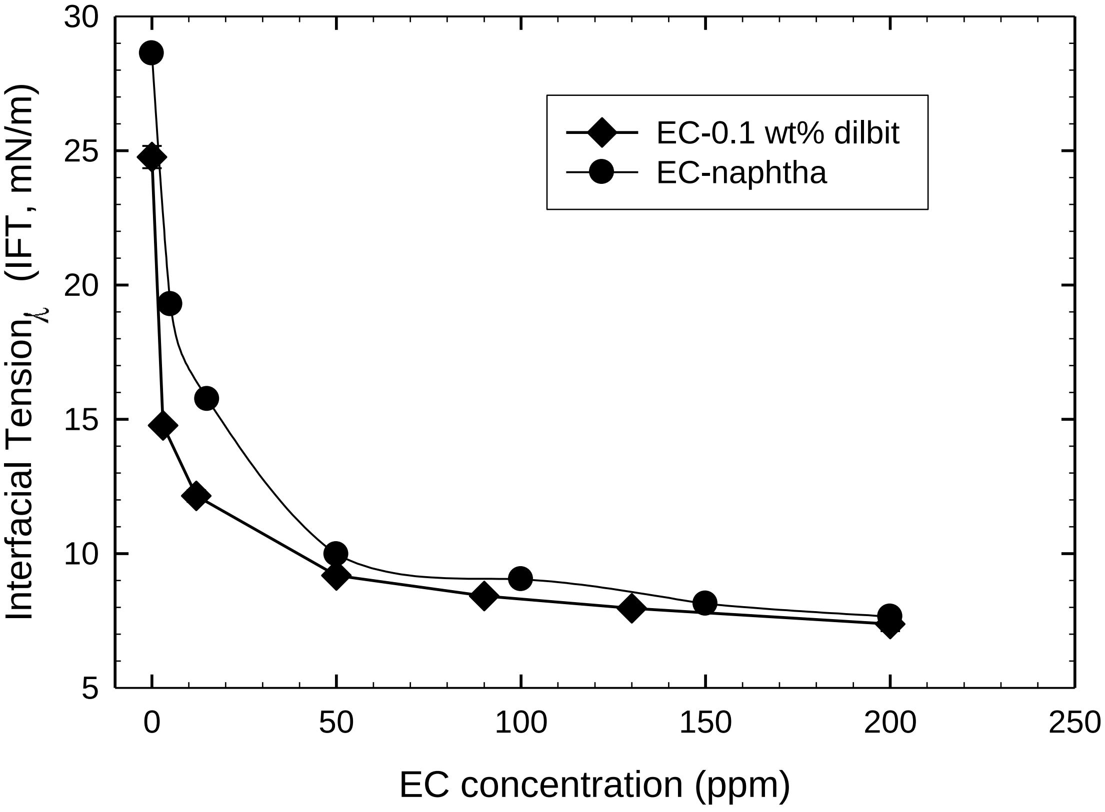

Figure 5.4. Interfacial tension isotherms of ethylcellulose (EC). EC–naphtha system (solid circles) and EC-0.1 wt% diluted bitumen in naphtha ('dilbit', solid diamonds) were measured using maximum bubble pressure method.

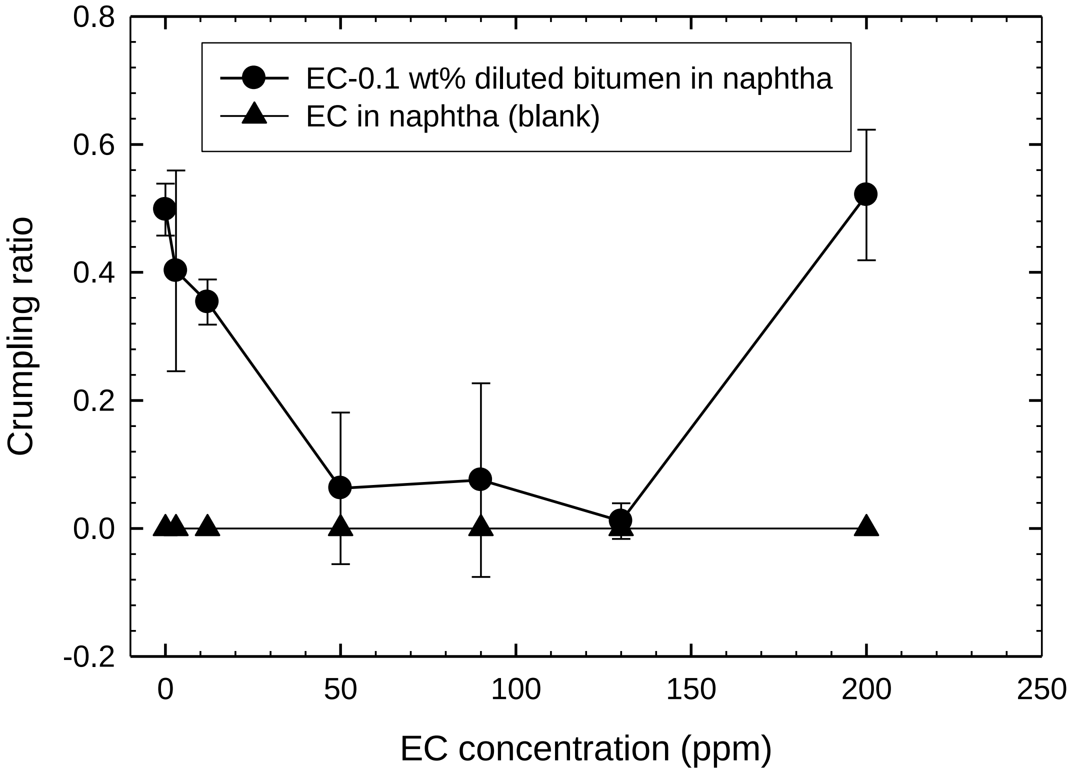

Figure 5.5. Assessment of skin formation at EC-0.1 wt% diluted bitumen in naphtha as a function of EC concentration (solid circles).

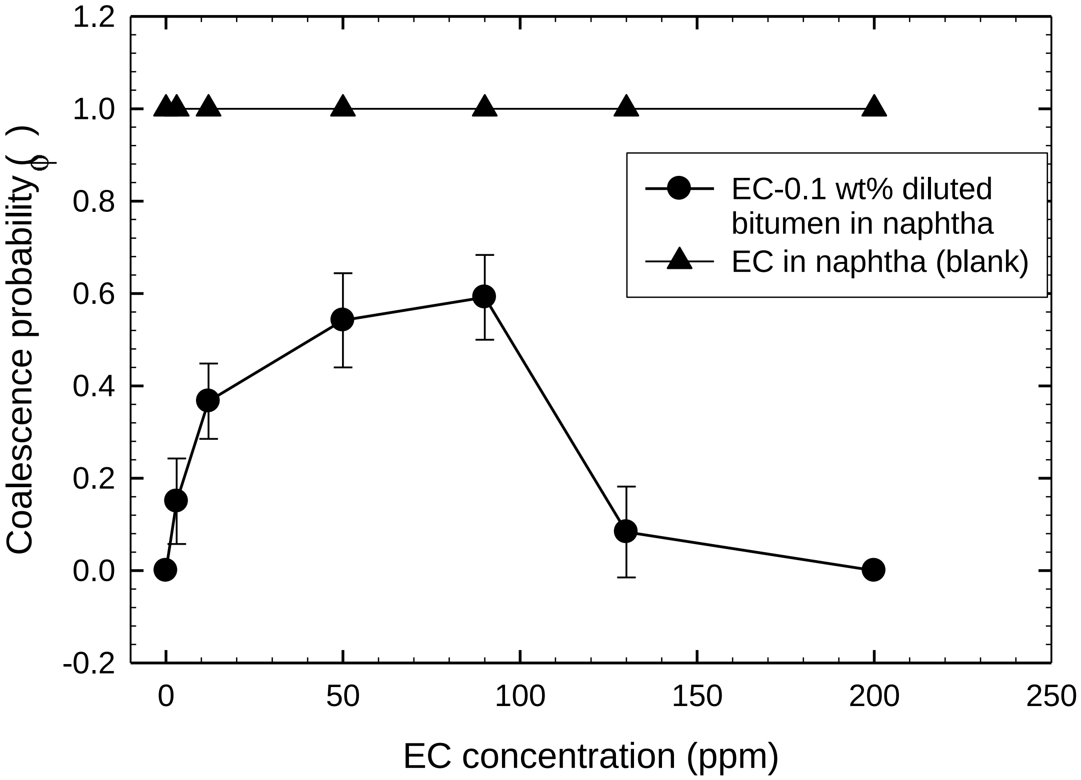

Figure 5.6. Coalescence probability of emulsified water droplets with the addition of EC in 0.1 wt% diluted bitumen in naphtha (solid circles).

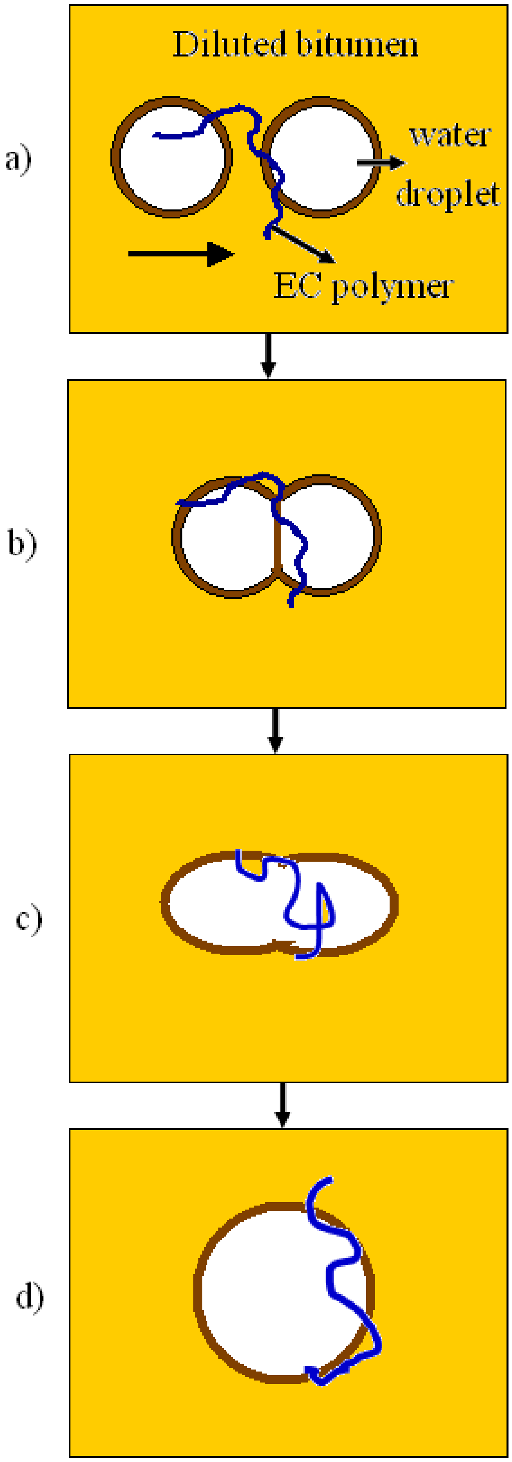

Figure 5.7. Schematic representation of coalescence for droplet-droplet interaction

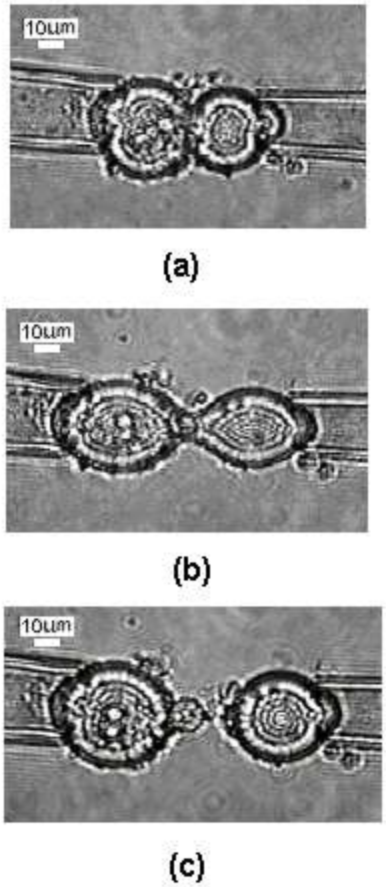

Figure 5.8. Flocculation was observed for an EC concentration of 35 ppm in diluted bitumen-naphtha system. (a): A water droplet was directed toward another static droplet; (b): One of the droplets was retracted from the second droplet after a sufficient period of direct contact under constant external force; (c): Two droplets remain intact after the removing of the external force.

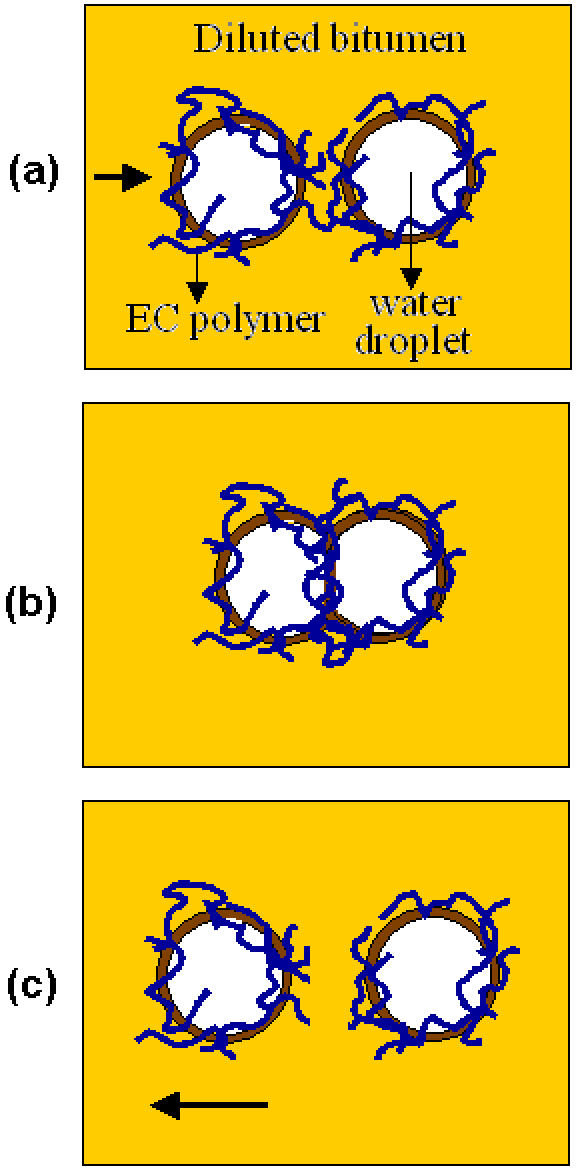

Figure 5.9. Steric repulsion due to excessive adsorption of EC polymer, the water droplets remain intact after removing the external force.

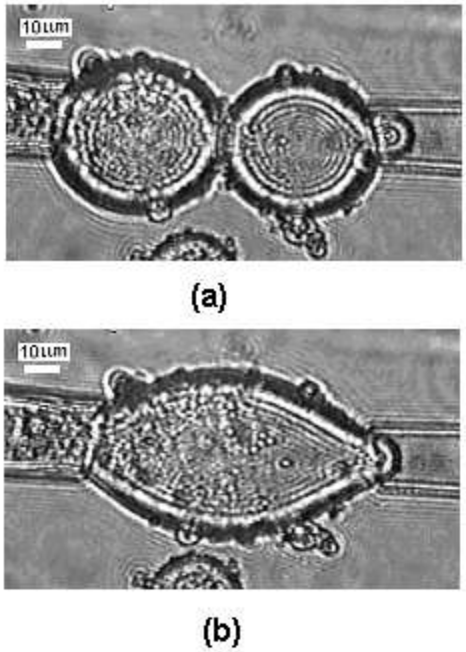

Figure 5.10. With the presence of 130ppm ethylcellulose in diluted bitumen-naphtha system, coalescence happens immediately upon the direct contact of two water droplets.

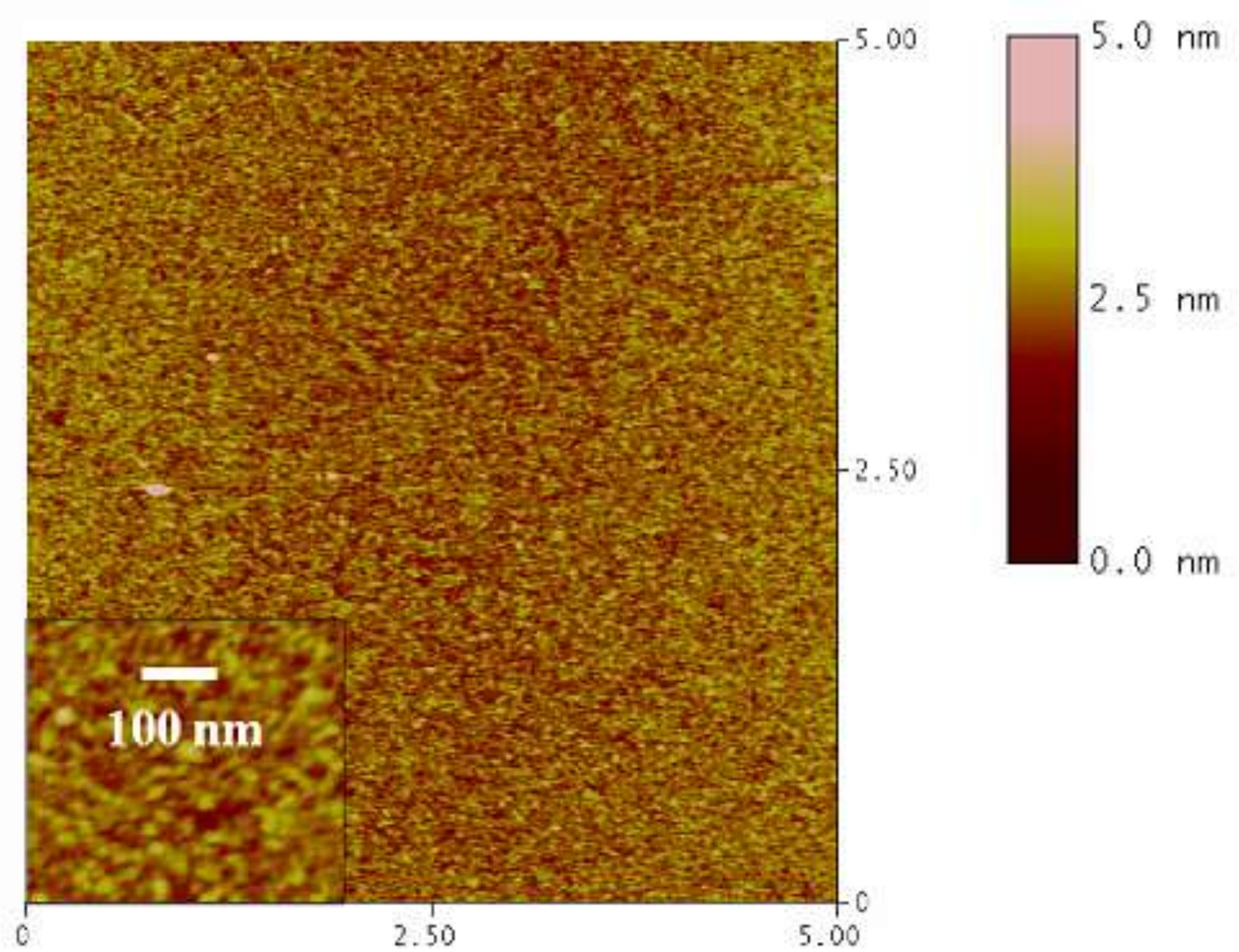

Figure 5.11. AFM image of bitumen LB interfacial film transferred at 2 mN/m interfacial pressure at naphtha−water interface. The film was prepared by spreading 20 µL of 1 mg/mL bitumen at the interface. The scale of the image on the left is 5 µm (Feng et al., 2009).

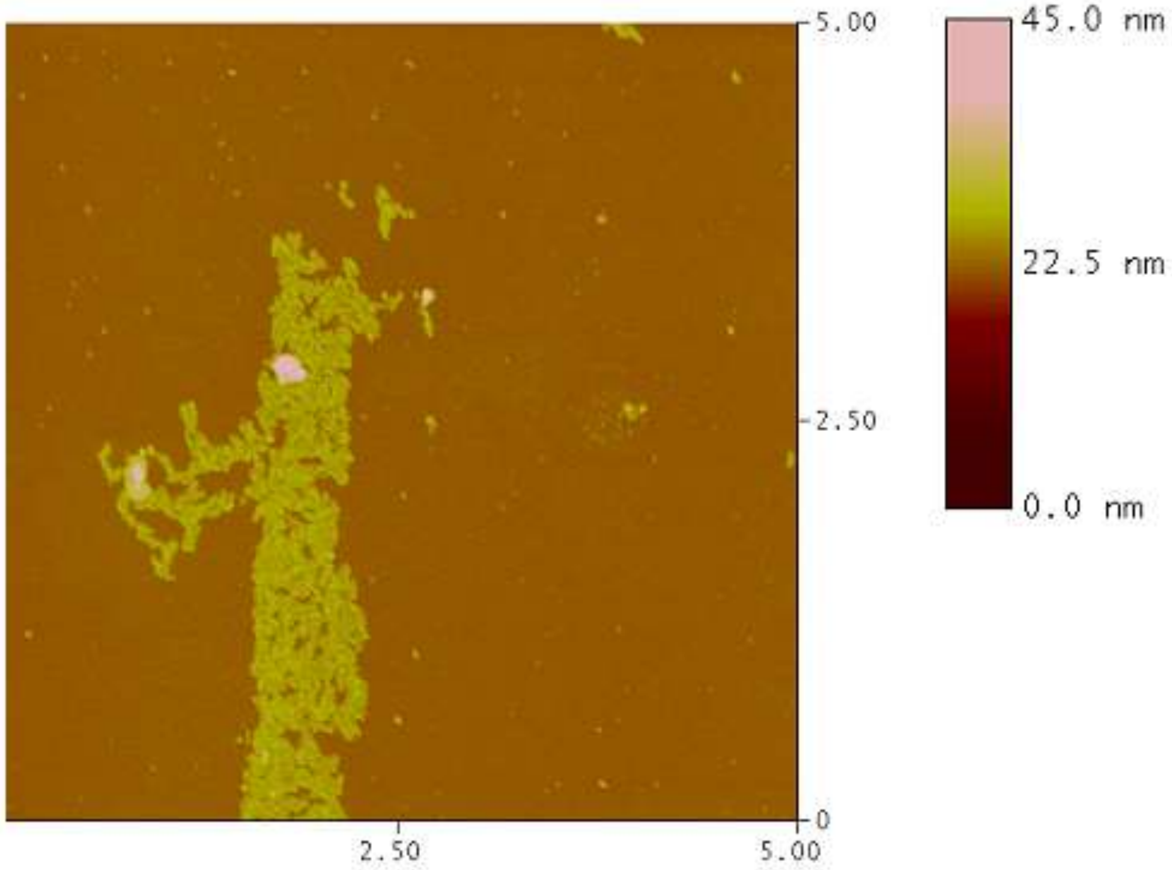

Figure 5.12. AFM image of the bitumen/EC (20 µL of 1 mg/ml EC and 20 µL of 1 mg/mL bitumen) LB interfacial film transferred at 2 mN/m interfacial pressure at naphtha−water interface. The scale of the image on the left is 5 µm (Feng et al., 2009).

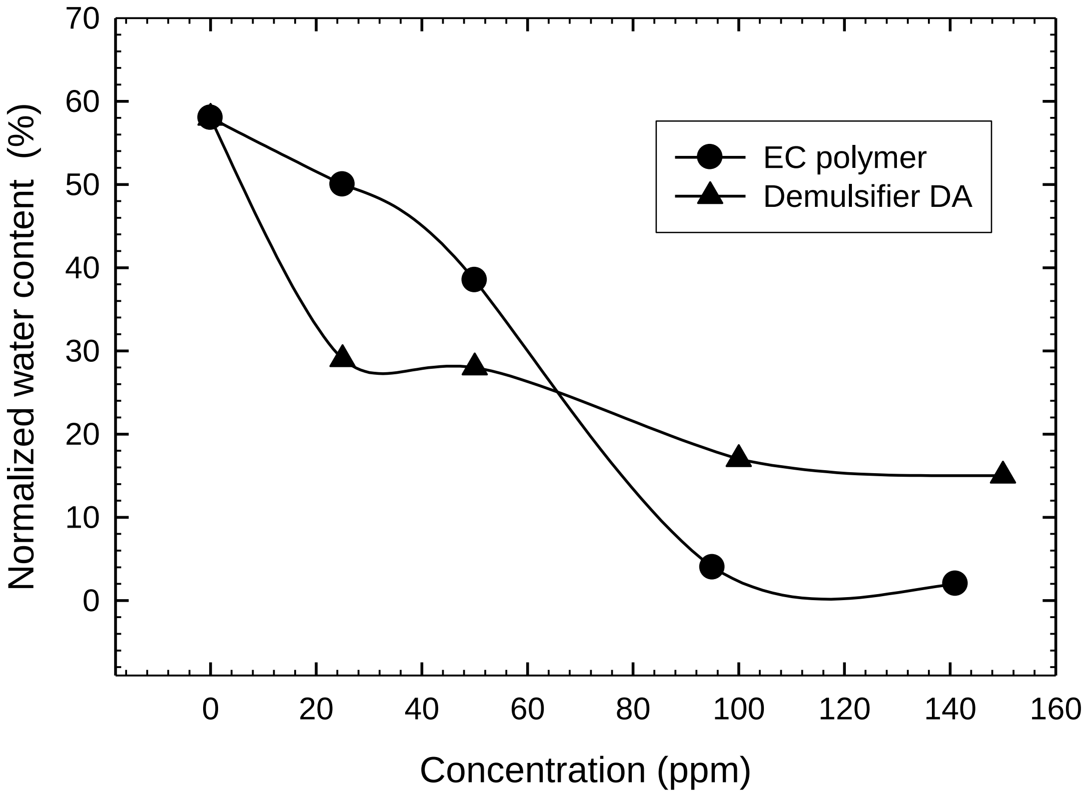

Figure 5.13. Normalized water content remaining in the emulsion as a function of demulsifier dosage.

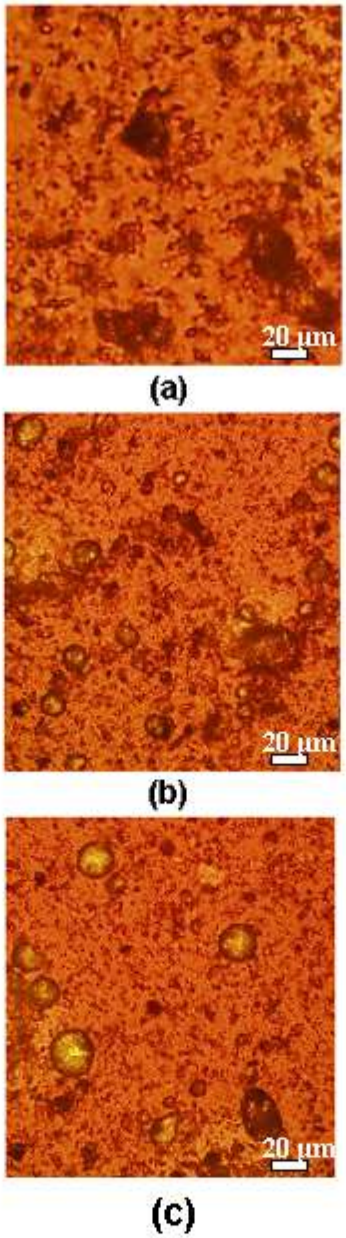

Figure 5.14. (a) Micrograph images of industrial diluted bitumen without addition of any demulsifier. (b) Micrograph images of 35 ppm EC-diluted bitumen. (c) Micrograph images of 35 ppm DA-diluted bitumen.

Chapter 6

Summary and Recommendations

Removing water from water-in-diluted bitumen emulsions remains a challenge to the oil sands industry. It is commonly believed that some indigenous surface active components in bitumen are responsible for stabilization of water-in-diluted bitumen emulsions. The objectives of this research are to understand the roles of different bitumen components in stabilizing the emulsions, to explore the stabilization mechanism by *in situ* characterization, and to clarify the roles of relevant demulsifiers. In realizing these objectives, the main contributions of this study are outlined and recommendations for future study are discussed.

6.1 Summary of contributions

The key contributions of this study can be generalized as follows:

Chapter 2: An advanced micropipette technique makes it possible to evaluate the highly concentrated and near-opaque oil systems with maintaining the surface area to volume ratio of the system. This allows for the first observance and study with the micropipette technique of relevant froth treatment emulsions.

Chapter 3: The adsorption of certain species in maltenes may contribute to the emulsion stability even without causing noticeable rigid skin at the interface. This proves that asphaltene is not the only stabilizer for water-in-oil emulsion.

Chapter 4: The presence and level of indigenous naphthenic acids was proven to be a potential indicator for optimization of bitumen production process. This is the first systematic study on the influence of indigenous naphthenic acids on water-in-oil emulsion.

Chapter 5: Ethylcellulose, a biodegradable and environmentally friendly polymer, was successfully utilized to destabilize the water-in-diluted bitumen. The implementation of this polymer has dual benefits for both technology development and environment protection.

The detailed summaries of this study were described as follows.

Micropipette technique was employed in this research since it maintains the surface area to volume ratios of the systems that are representative of industrial emulsions. The observation of water droplets in highly concentrated, near-opaque oil systems was realized by this technique. As such, the *in situ* behaviors of single emulsion drops are accurately revealed by this technique. The interfacial tension was measured by maximum bubble pressure method. The steric layer preventing the flocculation and/or coalescence of water droplets are quantified by conducting volume contraction experiments. Droplet interactions were visualized by applying external force on two water droplets to cause noticeable deformation. At the molecular level, atomic force microscope (AFM) and Brewster angle microscope (BAM) captured the morphology of different interfacial films.

The roles of asphaltenes and maltenes in stabilizing the water-in-diluted model oil were examined by measuring the interfacial tension, surface rigidity and coalescence behavior. The steric layer was found to originate from the competitive adsorption between asphaltenes and maltenes. Asphaltenes are the main stabilizer for the water-in-oil emulsion due to irreversible adsorption at the interface. Further, it was interesting to find that certain surface active materials in maltenes contribute to the stabilization of water-in-oil emulsions, without causing noticeable skin formation at the interface, provided that maltenes concentration is sufficiently high.

Further investigation focused on the influence of indigenous naphthenic acids (NAs) on the water-in-oil emulsion stability. Oil sands process water contains a complex mixture of dissolved inorganic and organic constituents. Most of the organics in the water phase are in the naphthenic acids group, a natural surfactant present in bitumen. Naphthenic acids are relatively low molecular weight saturated carboxylic acids, containing both acyclic and cyclic isomers, and are quite soluble in the aqueous digestion conditions seen in the water-based extraction processes. This study demonstrated that the presence of naphthenic acids benefits the destabilization of water-in-oil emulsions by reducing the interfacial tension, softening the rigid layer and promoting the coalescence of water droplets. This study identified the existence of an optimal level of naphthenic acids to allow for minimum rag layer development in the bitumen production process.

Ethylcellulose (EC) polymer was proven to be an effective demulsifier for water-in-diluted bitumen. The destabilization mechanism of EC, through both water droplet flocculation and coalescence, is facilitated by favorable competitive adsorption against the naturally occurring components in bitumen at the oil-water interface. Interfacial films representative of emulsified droplets in oil were disrupted in the presence of EC as revealed from the AFM images. The demulsification performance of EC was further confirmed by Karl Fisher titration measurements of residual emulsified water. Up to 90 wt% of the water in the emulsion was removed by gravity settling after ~100ppm EC addition. In general, the dewatering efficiency of EC is similar to that of DA, a commercial demulsifier currently used in oil sands industry. This study provides a sound basis for potential commercial application of EC polymer.

6.2 Recommendations for future work

In this study, all the experiments were conducted under “standard” conditions (i.e., one atmosphere and room temperature) and using “standard” products (i.e., final bitumen product, HPLC grade solvent and deionized water). Most of the industrial processes involving emulsions at temperatures different from the experimental conditions. Therefore, it is important to adapt the micropipette apparatus to study the thermo-mechanical properties of the emulsions.

The emulsions formed in bitumen froth treatment process are much more complex than the water-in-diluted model oil systems, due to many other variables/components in bitumen froth. For example, the atmospheric-topped bitumen used in this study is “clean” product ready for downstream upgrading process. Consequently, this bitumen is rather refined, only BSW trapped in bitumen is the same, relative to the indigenous bitumen found in the oil sands ore. In addition, the process water contains a variety of water-soluble species due to continuous recycling in the commercial extraction process. The deionized water used in this study can hardly reflect the presence of these species. Thus, it is imperative that samples from the industry, rather than model samples, should be used to examine the real situations in the industrial process. The influences of fines and solvent quality could also be aspects of future study.

In this study, it has been demonstrated that the level of naphthenic acids can affect the interfacial properties of water-in-oil emulsions. Current industrial practices also indicate that the level and composition of indigenous naphthenic acids depend on the oil sand ores (source and history) and the extraction conditions (pH). It is important to assess whether naphthenic acids content and composition in ore deposits can be used to reflect the processability and provide mitigation strategies, such as pH control or use of additives (natural or commercial surfactants).

References

Adamson, A. W., 1997, *Physical Chemistry of Surfaces*. 6th Ed John Wiley & Sons, New York. pp. 1-6, 47-98.

Acevedo, S., Escobar, G., Gutierrez, L. B., Rivas, H., Gutierrez, X., 1993, *Colloids Surf. A.* 71, 65-71.

Aske, N., Orr, R., Sjoblom, J., 2002, *J. Dispersion Sci. Technol*. 23 (6), 809-825.

Aveyar, R., Binks, B. P., Fletcher, P. D. I., Lu, J. R., 1990, *J. Colloid Interface Sci.* 139, 128.

Badre, S., Concalves, C. C., Norinaga, K., Gustavson, G., Mullins. O. C., 2006, *Fuel*. 85, 1-11.

Baptista, M. V.; Bowman, C. W. Proceedings, 1969, *19th Canadian Chemical Engineering Conference*, Edmonton, AB.

Bartell, F. E., Neiderhauser, D. O., 1949, Film-forming constituents of crude petroleum oils, in : *Fundamental Research on Occurrence and Recovery of Petroleum*; 1946-1947, American Institute of Petroleum, New York, p 57.

Bauget, F., Langevin, D., Lenormand, R., 2001, *J. Colloid Interface Sci*. 239, 501-508.

Berger, P. D., Hsu, C., Arendell, J. P., 1987, *Society of Petroleum Engineers of AIME*, Richardson, TX. USA. SPE 16285, pp 457-464.

Bessler, D. U., September 1983, *Demulsification of Enhanced Oil Recovery Produced Fluids*, Petrolite Corporation Research & Development.

Bhardwaj, A., Hartland, S., 1994, *Ind. Eng. Chem. Res.* 33, 1271.

Bhardwaj, A., Hartland, S., 1998, *J. Dispers. Sci. Technol*. 19, 465.

Binyon, S. J., 1984, *Oil Petroleum. Poll*. 2 (1), 57-60.

Bouriat, P., Kerri, N. El., Graciaa, A., Lachaise, A., 2004, *Langmuir*. 20 (18), 7459-7464.

Boussinesq, J. 1913, Sur l'existence d'une viscosite superficielle, dans la mince couche de transition separant un liquide d'un autre fluide contigu. *Annales de Chemie et de Physique, Huiteme Serie,* 24, 349-357.

Boussinesq, J. 1913, Application des formulas de viscosite superficielle a la surface d'une goutte liuqide spherique, tombant lentement, d'un movement devenu uniforme, au sein d'une masse fluide indefinite en repos, d'un poids specifique moindre. *Annales de Chemie et de Physique, Huiteme Series*, 24, 357-371.

Bowman, C. W., 1967, *Proc. 7th World Petroleum Congress*, 3, 583.

Bulmer, J. T., Starr, J. (Eds), 1979, " Syncrude Analytical Methods for Oil Sand and Bitumen Processing", *Alberta Oil Sands Technology and Research Authority (AOSTRA)*, Edmonton. P 121.

Canada's Oil Sands Heavy Oil: Developing the World's Largest Petroleum Resource, Petroleum Communication Foundation, Apr 2000.

Chandra, M. S., Xu, Z. H., Masliyah, J. H., 2008, *Energy & Fuels.* 22, 1784-1791.

Claesson, P. M., Blomberg, E., Poptoshev, E., 2001, in "Encylopedic Handbook of Emulsion Technology" edited by Sjöblom, J., Marcel Dekker, New York, p 305.

Cyr, T. D.; Strausz, O. P., 1983, *J. Chem. Soc. Chem. Commun*. 1028-1083.

Cyr, T. D.; Strausz, O. P., 1984, *Org. Geochem*. 7(2), 127-140.

Czarnecki, J.; Moran, K., 2005, Energy & Fuels. 19, 2074-2079.

Davis, J. T., Rideal, E. K., 1963, Interfacial Phenomena, 2nd ed.; Academic Press: New York.

Davis, K. D., 1988, Applications to the petroleum industry. In: Encyclopedia of Emulsion Technology/ Volume 3 (P. Becher, Ed). Marcel Dekker, New York, pp. 307-396.

Dicharry, C., Arla, D., Sinquin, A., Graciaa, A., Bouriat, P., 2006, *J. Colloid Interface Sci*.297, 785-791.

Djuve, J., Yang, X., Fjellanger, I. J., Sjoblom, J., Pelizzetti, E., 2001, *Colloid Polym. Sci.* 279, 232.

Drake, B., Prater, C. B., Weisenhorn, A. L., Gould, S. A. C., Albrecht, T. R., Quate, C. F., Cannell, D. S., Hansma, H. G., Hansma, P. K., 1989, Science. 243, 1586.

Eckert, W. F., Masliyah, J. H., Gray, M. R., P. M. Fedorak, 1996, Prediciton of sedimentation and consolidation of fine tails, AICHE, 42, 960-972

Eley, D. D., Hey, M. J., Lee, M. A., 1987, Colloids Surf. 24, 173-182.

Edwards, D. A., Brenner, H., Wasan, D. T., 1991, *Interfacial Transport Processes and Rheology*. Butterworth-Heinemann, Massachusetts.

ERCB ST98-2008: *Alberta's Energy Reserves 2007 and supply/Demand Outlook 2008-2017*, June 2008

Ese, M. H., Yang, X., Sjöblom, J., 1998, *Colloid Polym. Sci*. 276, 800-809.

Esmaeili, P., Moran, K., Bara, B., and Yeung, A., Novemver 12-17th, 2006, *AIChE Annual Meeting*, San Francisco, California.

Evans, E., Skalak, R., 1980, *Mechanics and Thermodynamics of Biomembranes*. CRC, Boca Raton.

Evans, E. A.; Rawicz, W., 1990, *Phys. Rev. Lett*. 64, 2094-2097.

Everett, D. H., 1988, *Basic Principles of Colloids Science*. Royal Society of Chemistry. London, pp. 30-53, 127-152.

Feng, X., Xu, Z, Masliyah, J. H., 2009, *Energy & Fuels*, 23, 451-456.

Feng, X., Mussone, P., Gao. S., Wang, S., Wu, S., Masliyah, J. H., Xu, Z., 2009, *Langmuir*, DOI: 10.1021/la9029563.

Freer, E. M., Radke, C. J., 2004, *J. Adhes*. 80, 481-496.

Freer, E. M., Svitova, T.; Radke. C. J., 2003, *J. Pet. Sci, Eng*.39, 137-158.

Gafonova, O. V., Yarranton, H. W., 2001, *J. Colloid Interface Sci*. 241 (2), 469-478.

Galopin, R., Henry, N.F.M., 1972, *A Microscopic Study of Opaque Minerals*, W. Heffer and Sons Ltd., Cambridge.

Gao, S., Moran, K., Xu, Z., Masliyah, J. H., 2009, *Energy & Fuels* 23, 2606-2612.

Gawrys, K. L., Blankenship, G. A., Kilpatrick, P. K., 2006, *Langmuir*. 22, 4487-4497.

Gray, M. R., 1994, "*Upgrading Petroleum Residues and Heavy Oils*". Marcel Dekker, New York.

Griffin, W. C., 1949, *J. Soc. Cosmetic Chem*. 1, 311-315.

Groenzin, H., Mullins, O. C., 2001, *Petrol Sci Technol*. 19, 21-230.

Gu, G.; Zhiang, Z.; Xu, Z.; Masliyah, J. H., 2003, *Colloids Surf A*. 215, 141-158.

Hansma, H. G., Gould, S. A. C., Hansma, P. K., 1991, *Langmuir*. 7, 1051-1054.

Hall, G., Herron, S. P., 1979, *Am. Chem. Soc., Div. Pet. Chem., Prepr*; American Chemical Society national meeting; Washington, DC, USA, 24 (4), 924

Heimentz, P. C., Rajagopalan, R., 1997, *Principles of Colloid and Surface Chemistry*. 3rd ed.; Marcel Dekker: New York.

Hénon, S., 1991

Horvath-Szabo, G., Masliyah, J. H., Czarnecki, J., 2001, *J. Colloids Interface Sci*. 242, 247-254.

Horvath-Szabo, G., Czarnecki, J., Masliyah, J. H., 2002, *J. Colloids Interface Sci*. 253, 427-434.

Hönig, D, 1991,

Hunter, R. J., 1986, *Foundations of Colloid Science*. Volume 1. Clarendon Press, Oxford, pp. 1-48, 55-61, 228-315, 329-398.

Hunter, R. J., 2001, *Foundations of Colloid Science*. 2nd Edition, Oxford Press.

Jestin, J., Simon, S., Zupancic, L., Barré, L., 2007, *Langmuir*. 23 (21), 10471-10478.

Jiang, T. M., Hirasaki, G., Miller, C., Moran, K., Fleury, M., 2007, *Energy & Fuels*. 21, 1325-1336.

Jones, T. J., Neustadter, E. L., Whittingham, K. P., 1978, *The Journal of Canadian Petroleum Technology*, Montreal, 17, 100-108.

Kilpatrick, P. K., Spiecker, P. M., 2001, In *Encyclopedic handbook of emulsion technology;* Sjoblom, J., Ed.; Marcel Dekker: New York, Basel, p 707.

Kim, Y. H., Wasan, D. T., 1996, *Ind. Eng. Chem. Res*. 35, 1141.

Kloet, J. V., Schramm, L. L., Shelfantook, B., 2001, *Colloids Surfaces. A*. 192, 15-24.

Krawczyk, M. A., Wasan, D. T., Shetty, C. S., 1991, *Ind. Eng. Chem. Res*. 30, 367.

Kumar, K., Nikolov, A. D., Wasan, D. T., 2001, *Ind. Eng. Chem. Res*. 40, 3009-3014.

Langmuir, I., 1917, *J. Am. Chem. Soc.* 39, 1848.

Langmuir. I., Blodgett, K. B., 1935, *Kolloid-Zeitschrift*. 73, 258.

LaPlace, P. S., 1805, *Supplément au Dixième Livre du Traité Mécanique Céleste, Tome quatriéme*. Imprimeur-Libraire pour les Mathematiques, quai des Augustins, no. 71. pp. 1-65; LaPlace, P. S., 1966, *On capillary attraction.*

Supplement to the Tenth Book of the Mécanique Céleste, Volume 4 (Translated by N. Bowditch). Chelsea Publishing Company, Bronx, New York, pp. 685-1018.
Lecomte du Noüy, P., 1919, *J. Gen. Physiol*. 1, 521.

Leja, J., Bowman, C. W., 1968, *Can. J. Chem. Eng*. 46, 479.

León, O., Contreras, E., Rogel, E., Dambakli, G., Acevedo, S., Carbognani, L., Espidel, J., 2002, *Langmuir.* 18 (13), 5106-5112.

Li, M., Xu, M., Ma, Y., Wu, Z., 2002, *Chemistry, A. Fuel*.81 (14), 1847-1853.

Liu, J., Xu, Z., Maliyah, J. H., 2004, *Role of fine clays in bitumen extraction from oil sands, AIChE Journal*. v50, n8, 1917-1927.

Makhonin, G. M., Petrov, A. A., Borisov, S. I., 1983, *Chem. Technol. Fuels Oils*, 18 (7-8), 410-413.

Masliyah, J. H., 2000, *Fundamentals of Oil Sands Extraction* (Course Notes), University of Alberta, Edmonton, Alberta.

Mason, C. W., *Handbook of Chemical Microscopy*, vol. 1, 1983, John Wiley and Sons, New York.

Márquez-Silva, R. L., Key, S., Marino, J., Guzman, C., Buitriago, S., 1997, *Proceedings SPE International Symposium on Oilfield Chemistry*, Society of Petroleum Engineers: Richardson, TX, SPE paper 37271.

Menon, V. B., Wasan, D. T., 1986, *Colloids Surf*. 19, 89-105.

Messerschmidt, R. G., Harthcock, M. A., Eds, 1988, *Infrared Microspectroscopy: Theory and Applications,* Marcel Dekker, Inc. New York.

Meyer, E., Howald, L., Overny, R. M., Heinzelmann, H., Fromer, J., Guntherode, H. J., Wager, T., Schier, H., Roth, S., 1991, *Nature*. 349, 398.

Mikula, R. J., Munoz, V. A., 2000, in Schramm, L. L. (Ed), *Surfactants, Fundamentals and Applications in the Petroleum Industry*. Cambridge Univ. Press, New York, 51-77.

Mitchell, D. L., Speight, J. G., 1973, *Fuel*. 52, 149-152.

Mohammed, R. A., Bailey, A. I., Luckham. P. F., Taylor, S. E., 1993, *Colloids Surf. A.* 80, 237-242.

Mohammed, R. A., Bailey, A. I., Luckham. P. F., Taylor, S. E., 1994, *Colloids Surf. A.* 83, 261-271.

Monson, L. T., Stenzel, R. W., 1946, *Colloid Chemistry vol. VI*, Jerome Alexander, Ed., Rheinhold Publishing Corp., New York.

Moran, K., 2007, *Langmuir*. 23, 4167-4177

Moran, K., and Czarnecki, J., June 25-29, 2006, *7th International Conference on Petroleum Phase Behaviour and Fouling, Asheville, North Carolina.*

Moran, K., Czarnecki, J., 2007, *Colloids and Surfaces A*. 292, 87-98.

Moran. K., Yeung, A., Masliyah, J. H., 2006, *Chem. Eng. Sci*. 61 (18), 6016-6028.

Mukherjee, S., Kushnick, A. P., 1989, *In Oil-Field Chemistry, Enhanced Recovery and Production Simulation*, Borchardt, J. K., Yen, T. F., Eds., American Chemical Society, Washington DC, pp 364-374.

Mussone, P., 2007, Ph.D. thesis, University of Manchester, Manchester, UK.

Pauchard, Vincent., Sjöblom, Johan., Kokal, Sunil., Bouriat, Patrick., Dicharry, Christophe., Müller, Hendrik., Al-Hajji, Adnan., 2009a, *Energy & Fuels*. 23, 1269-1279.

Pauchard, Vincent., Sjöblom, Johan., Kokal, Sunil., Bouriat, Patrick., Dicharry, Christophe., Müller, Hendrik., Al-Hajji, Adnan., 2009b, *Energy & Fuels*. 23, 1280-1288.

Pawley, J. B., Ed., 1990, *Handbook of Biological Confocal Microscopy*. Plenum Press, New York.

Pena, A. A., Hirasaki, G. J., Miller, C. A., 2005, *Ind. Eng. Chem. Res*. 44, 1139-1149.

Pintchovski, F., Price, J. B., Tobin, P. J., Peavey, J., Kobold, K., 1979, *J. Electrochem. Soc.* 126, 1428-1430.

Plateau, J. 1869, Researchés experiment et theorique sur les figures d'equilibre d'une liquide sans pesanteur, 8^e serie. *Annales de Chimie et de Physique, Quatrieme Serie*, 17, 260-276; Plateau, J. 1869, Experimental and theoretical researches into the figures of equilibrium of a liquid mass without weight, eighth series. *Phil. Mag., Fourth Series*, 38, 445-455.

Sams, G. W., Zaouk, M., 2000, Energy & Fuels. 14, 31-37.

Schramm, L. L. Marangoni, D. G., 2000, in Schramm, L. L. (Ed), *Surfactants, Fundamentals and Applications in the Petroleum Industry*. Cambridge Univ. Press, New York, 3-50.

Schramm, L. L., Stasiuk, E. N., Mackinnon, M., 2000, in Schramm, L. L. (Ed), *Surfactants, Fundamentals and Applications in the Petroleum Industry*. Cambridge Univ. Press, New York, 365-430.

Scott, Angela C., Young, Rozlyn F., Fedorak, Phillip M., 2008, *Chemosphere.* 73, 1258–1264.

Shaw, R. C., Scharmm, L. L., Cazrnecki, J., 1996, Suspensions in the hot water flotation process for Canadian oil sands, in: Schramm, L.L (Ed.), *Suspensions: Fundamentals and Applications in the Petroleum Industry;* Advances in Chemistry Series 251, American Chemical Society, Washington, D.C., p 639.

Singh, B. P., 1994, *Energy Sources*. 16, 377-385.

Sjoblom, J., Johnsen, E. E., Westvik, A., Ese, M. H., Djuve, J., Auflem, I. H., Kallevik, H., 2001, *Demulsification in the oil industry. In Encyclopedic Handbook of Emulsion Technology*. Sjoblom, J., Ed., Marcel Dekker, New York, pp 595-619.

Smith, V. H., Arnold, K. E., 1992, *In Petroleum Engineering Handbook*, Bradley, H. B., Ed., Chapter 19, pp 9-12.

Song, C. S., Ye, R. Q., Mu, B. Z., 2008, *Colloids and surfaces A*. 330(1), 49-54.

Sophie, B., 2007, *Behavior of several amphiphilic copolymers at the air-water interface*. Ph.D thesis, University of Florida.

Spiecker, P. M., Kilpatrick, P. K., 2004, *Langmuir*. 20 (10), 4022-4032.

Stalss, F., Bohm, R., Kupfer, R., 1991, *SPE Prod. Eng*. 6 (3), 334.

Strausz, O. P., 1988, in: Meyer, R. F.; Wiggins, E. J. (Eds), *44th UNITAR/UNDP International Conference on Heavy Crude and Tar Sands*, Edmonton, vol. 2, 607.

Strausz, O. P, 1989, in "*AOSTRA Technical Handbook on Oil Sands, Bitumens and Heavy Oils*", edited by Hepler, L. G., His, C., AOSTRA Technical Publication Serier #6, Edmonton.

Sztukowski, D. M., Jafari, M., Yarranton, H. W., 2003, *J. Colloid Interface Sci.* 265 (1), 179-186.

Sztukowski, D. M., Yarranton, H. W., 2004, *J. Dispersion Sci. Technol*. 25 (3), 299-310.

Sztukowski, D. M., Yarranton, H. W., 2005, *J. Colloid Interface Sci*. 285 (2), 821-833.

Takamura, K. 1985, *Physico-chemical characterization of Athabasca oil sand and its significance to bitumen recovery, AOSTRA J. Res*. 2, 1-10.

Taylor, S. D., Czarnecki, J., Masliyah, J. H., 2002, *J. Colloid Interface Sci.* 252 (1), 149-160.

Torrent-Burgues, J., Pla, M., Escriche, L., Casabo. J., Errachid, A., Sanz, F., 2006, *Journal of Colloid and Interface Science*. 301(2), 585-593.

Tsamantakis, C., Masliyah, J. H., Yeung, A., Gentzis, T., 2005, *J. Colloid Interface Sci*. 284, 176-183.

Urdahl, O., Movik, A. E., Sjoblom, J., 1993, *Colloids Surf. A*. 74, 293-302.

Van Os, N. M., Haak, J. R., Rupert, L. A. M., 1993, *Physico-Chemical Properties of Selected Anionic, Cationic and Nonionic Surfactants*, Elsevier, New York.

Wasan, D. T., Nikolov, A. 1993, Emulsion Stability Mechanisms, *Proceedings of the First World Congress on Emulsions*. Paris, France, Oct 19-22, 4, p 93.

Weisenhorn, A. L., Hansma, P. K., Albrecht, T. R., Quate, C. F., 1989, *J. Appl. Phys*. 54, 2651.

Weisenhorn, A. L., MacDougall, J. E., Gould, S. A. C., Cox, S. D., Wise, W. S., Massie, J., Maivald, P., Elings, V. B., Stucky, G. D., Hansma, P. K., 1990, *Science*. 247, 1330.

Williams, J. M., 1991, *Langmuir*, 7, 1370.

Wu. X., T. G. M., Ven, van de., Czarnecki, J., 1999, *Colloid Sruf. A*. 149, 577-583.

Yan, Z. L.; Elliott, J. A. W.; Masliyah, J. H., 1999, *J Colloid Interf Sci*. 220(2), 329-337.

Yang, X. L., Czarnecki, J., 2005, *Energy & Fuels*. 19, 2455-2459.

Yarranton, H. W., 1997, Ph.D Thesis, University of Alberta, Edmonton.

Yarranton, H. W., Hussein, H., Masliyah, J. H., 2000, *J. Colloid and Interface Sci*. 228(1), 52-63.

Yarranton, H. W., Sztukowski, D. M , Urrutia, P., 2007a, *J. Colloid Interface Sci*. 310 (1), 246-252.

Yarranton, H. W., Sztukowski, D. M , Urrutia, P., 2007b, *J. Colloid Interface Sci*. 310 (1), 253-259.

Yeung, A.; Dabros, T.; Masliyah, J. H., 1998, *J. Colloid Interface Sci*. 208, 241-247.

Yeung, A., Dabros, T., Czarnecki, J., Masliyah, J. H., 1999, *Proc. R. Soc., Lond. A*. 455, 3709-3723.

Yeung, A., Dabros, T., Masliyah, J. H., Czarnecki, J., 2000, *Colloids and Surfaces A*. 174, 169-181.

Young, T., 1805, *An essay on the cohesion of fluids. Phil. Trans. Royal Soc*. London, 95, 65-87.

Zapryanov, Z., Malhotra, K. A., Aderangi, N., Wasan, D. T., 1983, *Int. J. Multiphase Flow*. 9, 105.

Zhang, L. Y., Breen, P., Xu, Z., Masliyah, J. H., 2007, *Energy & Fuels*. 21, 274-285.

Zhang, L. Y., Lawrence, S., Xu, Z., Masliyah, J. H., 2003, *J. Colloid Interface Sci*. 264, 128-140.

Zhang. L. Y., Lopetinsky, R., Xu, Z., Masliyah, J. H., 2005, *Energy & Fuels*. 19, 1330-1336.

Zhang, L. Y., Xu, Z., Masliyah, J. H., 2003, *Langmuir.* 19 (23), 9730-9741.

Zhang, L. Y., Xu, Z., Masliyah, J. H., 2005, *Ind. Eng. Chem. Res.* 44, 1160-1174.

Zhang, Z. Q., Xu, G. Y., Fang, W., Dong, S. L., Chen, Y. J., 2005, *J Colloid Interface Sci*. 282, 1-4.